Quantized light in the presence of absorbing dielectric bodies

Dissertation

zur Erlangung des akademischen Grades
doctor rerum naturalium (Dr. rer. nat.)

vorgelegt dem Rat der Physikalisch-Astronomischen Fakultat
der Friedrich-Schiller-Universitat Jena

von Dipl.-Phys. Stefan Scheel
geboren am 31.03.1971 in Leipzig

Gutachter

1. Prof. Dr. D.-G. Welsch

2. Prof. Dr. M. Fleischhauer

3. Prof. Dr. S.M. Barnett

Tag der letzten Rigorosumsprufung: 25.09.2001

Tag der o entlichen Verteidigung: 01.11.2001

Contents

1   Introduction

Classical wave optics has strongly influenced the development of theories like relativity and quantum mechanics. In turn, quantum mechanics lead to the description of light in terms of photons as the fundamental excitations of the electromagnetic field. With the advent of the laser and the subsequent invention of a number of methods for generating and manipulating light, a new theory of optical coherence phenomena emerged, quantum optics. Quantum-statistical properties of radiation that cannot be described by a classical statistical model have lead to a definition of nonclassical light in terms of phase-space functions that cannot be regarded as classical probability distributions.

Experiments in classical as well as quantum optics require the use of optical instruments such as beam splitters, mirrors, cavities, or fibres. Their influence on the quantum statistics of radiation interacting with optical elements requires careful examination. Consider, for example, a lossless beam splitter. In classical optics, a light beam impinging on one side of the beam splitter is simply be divided into two parts. Quantum-mechanically, the second, unused input of the beam splitter introduces additional (vacuum) noise to the reflected and transmitted beams. The quantum statistics of the outgoing fields may differ significantly from that of the incoming fields. Mathematically, lossless four-port devices such as beam splitters or optical fibres act as an SU(2) group transformation on the amplitude operators of monochromatic light [1, 2, 3, 4, 5, 6].

Recent advances in the rapidly developing field of quantum information processing, in particular the fundamental experiments on quantum key distribution [7, 8, 9, 10, 11, 12] and quantum teleportation [13, 14, 15], have raised the interest in studying the quantum-statistical properties of light interacting with realistic optical instruments that show absorption. Quantum information processing exploits the quantum correlations that can exist in states of more than one subsystem. These so-called entangled states have some remarkable properties that cannot be understood classically. For example, they can violate Bell s inequalities [16] and show other nonlocal behaviour. Entanglement, being a quantum correlation effect, is subject to decoherence and therefore very fragile. In order to use entangled light beams in, for example quantum teleportation, they must be transmitted through optical channels such as fibres that necessarily show absorption. The question is then to what extent the initial entanglement can be preserved during the propagation.

These examples show, that a quantum theory of light in the presence of dielectric bodies is necessary. In principle, the matter could be treated microscopically. However, there exists

a class of dielectric media whose action can be included in the quantum theory of the electromagnetic field exactly. This class consists of dielectrics which respond linearly and locally to the electromagnetic field. The advantage of such a concept is, that it uses only very general physical properties of the dielectric material.

Quantization of the electromagnetic field in absorbing dielectric media has been subject of intensive study over a long period. The quantum theory of light in dielectric media with real and frequency-independent refractive index has been considered in a number of articles [17, 18, 19, 20, 21, 22, 23, 24, 25, 26, 27, 28, 29, 30, 31, 32, 33, 34]. Dispersion has been taken into account [35, 36, 37, 38, 39, 40, 41, 42, 43], and attempts have been made to extend the concepts also to nonlinear media [44, 45, 46, 47].

However, all these schemes are restricted to small frequency intervals where the permittivity is real and absorption can safely be disregarded. A complete quantum theory, on the other hand, requires quantization at all frequencies. For causality reasons the permittivity has to satisfy the Kramers Kronig relations which state that real and imaginary parts of the permittivity are necessarily connected to each other. Hence, in general there is always some frequency region in which absorption occurs. An immediate consequence of the existence of an imaginary part of the permittivity (and subsequently the refractive index) is that the mode expansion of the electromagnetic field operators is no longer complete since it involves non-orthogonal damped waves.

The first attempt to quantize the phenomenological Maxwell field in absorbing media was made by Lifshitz [48] in the connection of van der Waals and Casimir forces between imperfectly conducting plates. Since then, a number of works were concerned with the formulation of quantum electrodynamics in media described by a complex permittivity satisfying the Kramers Kronig relations [49, 50, 51, 52, 53, 54, 55, 56, 57, 58, 59, 60, 61, 62, 63, 64, 65]. A canonical approach that is consistent with quantum theory was developed by Huttner and Barnett [52]. It is based on the Hopfield model [66] of an isotropic, homogeneous dielectric in which a single quantum level is perturbatively coupled to a continuum of states [67]. Then explicit Fano-type diagonalization [68] of a Hamiltonian consisting of the electromagnetic field, a polarization field representing the dielectric matter, and a continuum of harmonic oscillators modelling the reservoir variables has been performed. It turned out that the vector potential could be written in terms of the Green function of the classical scattering problem [69, 70]. This observation made it possible to formulate a quantum theory of the electromagnetic field in linear, but otherwise arbitrary dielectric media. The advantage is that only experimentally accessible parameters such as permittivity and magnetic susceptibility are involved [S1, S11], without referring to specific microscopic models.

The outline of the present work is as follows. In Chapter 2, after recalling the quan-

tization scheme based on the microscopic Hop eld model, a consistent phenomenological theory of the quantized electromagnetic eld in absorbing dielectric media is presented. The source-quantity representation of the electromagnetic eld operators with the classical Green function, in terms of a continuum of harmonic-oscillator elds, is shown to lead to the correct (equal-time) commutation relations between the electromagnetic eld operators [S1]. The proof relies on general properties of the Green function and is valid for all dielectric media that respond linearly, locally, and causally to the electromagnetic eld [S1, S11].

For the interaction of quantized light with optical devices regarded as arbitrarily shaped three-dimensional dielectric bodies of nite extent the Green function can be speci ed to yield input-output relations. They are a convenient way of describing the transformation of eld operators of outgoing light from a dielectric device in terms of the eld operators of light impinging on the optical device. General expressions for arbitrarily shaped objects are given in Chapter 3 [S13]. The input-output relations are very useful for describing, for example low-order correlations in two-photon interference e ects [71, 72, 73]. In general, not only the lowest moments but the full information about the quantum state of the photon eld is needed to describe its quantum-statistical properties. Based on the operator input-output relations, the unitary transformation that relates the output quantum state to the input quantum state, including radiation and matter, is derived in Chapter 4 [S2]. Examples for the transformation of coherent states and Fock states are given.

Knowing the density operator of a bipartite quantum state allows for looking for signs of entanglement between its subsystems. Application of separability criteria for nite-dimensional states [74, 75] and in nite-dimensional Gaussian states [76, 77], together with the input-output relations, yields bounds on size and properties of optical devices that are necessary to prevent an entangled state to become separable. In Chapter 5 we compute the maximal possible length of optical bres such that a two-mode squeezed vacuum state transmitted through them stays inseparable [S7, S8, S10].

Quanti cation of entanglement is a di cult task in general. Several proposals have been made to de ne a unique measure, but there seems to be more than one quantity satisfying all requirements [78, 79] on a good entanglement measure. All of them are di cult to compute, and analytical expressions are available only for certain classes of states. In most cases it is possible to derive upper bounds on the entanglement content which is discussed in Chapter 5 [S7, S8, S10]. In particular, we introduce an upper bound on the entanglement content of Gaussian states by computing their distance to the set of separable Gaussian states. We show, that a symmetric noisy quantum channel can only transmit a certain amount of entanglement [S14]. This bound indicates the ultimate theoretical limits of continuous-variables schemes that make use of quantum information.

Entanglement degradation inhibits perfect quantum teleportation. In Chapter 6 we show how the standard teleportation scheme for qubits can be extended to yield, on average, higher teleportation delity. In particular, we concentrate on using multipartite entangled states with subsequent projection measurements and ltering [S15].

In studying quantum-state transformation by optical devices, entanglement content, or teleportation delity, the emphasis is put on the in uence of dielectric objects on the quantum state of light. On the other hand, the question is how (additional) atoms are a ected by the medium-assisted Maxwell eld. Prominent examples for such e ects are the modi ed spontaneous decay and Lamb shift of excited atoms near dielectric surfaces. Spontaneous decay is caused by ground-state uctuations of the electromagnetic eld. When the eld is coupled to dielectric matter, also its vacuum state is in uenced by the medium, which can either enhance [80] or inhibit [81, 82] spontaneous decay. The dependence on changes in the environment surrounding the radiating atom can also be used as a tool in scanning near- eld optical microscopy for detecting buried dielectric objects below planar surfaces [83].

The quantum electrodynamics in the presence of atoms is developed in Chapter 7 where the Hamiltonian describing the interaction of the medium-assisted Maxwell eld with additional atomic sources in minimal coupling and multipolar coupling is derived [S9]. In many cases the spatial extent of the atomic system is small compared to the spatial variations of the electromagnetic potentials. Then it is su cient to treat the atom eld coupling in lowest order of the multipole expansion of the electromagnetic eld. Moreover, if only two atomic levels are relevant, one can restrict to frequency components that are close to the atomic resonance frequency. Both approximations, electric-dipole and rotating-wave approximations, are used in Chapter 8 to study the spontaneous decay of an excited two-level atom in the presence of dielectric bodies. In particular, di erent models of spontaneous decay in absorbing (bulk) dielectrics [S3], absorbing microcavities [S4], and near planar interfaces [S5] are discussed. All models have in common that the leading contributions to the decay rate are proportional to the cubic inverse of the distance from the atom to the surrounding dielectric. This behaviour is due to resonant energy transfer to the absorbing dielectric material. For non-absorbing media, the calculated spontaneous decay rates of an atom inside a dielectric reproduce the classical local- eld correction factors.

A summary and future prospects are presented in Chapter 9. For the sake of transparency and readability, longer derivations have been shifted to separate Appendixes.

2 Quantization of the electromagnetic eld in causal media

The quantum theory of light in dielectric media that respond causally and linearly to an electromagnetic eld is the basis for the considerations throughout this work. We shortly review the canonical quantization scheme developed in [52] where an explicit diagonalization of a semi-microscopic model Hamiltonian for the radiation eld in isotropic, homogeneous dielectrics has been performed (Sec. 2.1). The functional form of vector potential and matter polarization, expressed in terms of polariton-type operators, presents the starting point for the development of a source-quantity representation of the electromagnetic eld operators in arbitrary inhomogeneous media [S1], which is thoroughly discussed in Sec. 2.2. Extensions to more general dielectrics such as amplifying [S1], anisotropic, and magnetic media [S11] are presented in Sec. 2.3.

2.1 Hop eld model and Fano diagonalization

In [52] a semi-microscopic Hop eld model [66] of an isotropic, homogeneous bulk dielectric is considered in which a harmonic-oscillator eld describing the polarization of the dielectric matter is linearly coupled to a continuum of harmonic-oscillator elds modelling the reservoir. In this type of coupling the energy ow is essentially only into the reservoir which is equivalent to a loss mechanism for the material polarization.

The system consisting of the electromagnetic eld, the matter polarization, and the reservoir variables is described by the Lagrangian

$$L = \quad d^3\mathbf{r}\,\mathcal{L} = \quad d^3\mathbf{r}\,(\mathcal{L}_{\mathrm{rad}} + \mathcal{L}_{\mathrm{mat}} + \mathcal{L}_{\mathrm{int}}) \tag{2.1}$$

where

$$\mathcal{L}_{\mathrm{rad}} = \frac{0}{2} \quad \mathbf{A}(\mathbf{r}) + \quad U(\mathbf{r}) \quad^2 \quad c^2\,[\quad \mathbf{A}(\mathbf{r})]^2 \tag{2.2}$$

is the free Lagrangian density of the electromagnetic eld in the Coulomb gauge, $\mathbf{A}(\mathbf{r})=0$, $\mathbf{A}(\mathbf{r})$ being the vector potential and $U(\mathbf{r})$ the scalar potential, respectively. The Lagrangian densities

$$\mathcal{L}_{\mathrm{mat}} = \frac{}{2}\quad \mathbf{X}(\mathbf{r})^2 \quad {}^2\mathbf{X}(\mathbf{r})^2 \quad + \quad d \quad \frac{}{2}\,\mathbf{Y}^2(\mathbf{r}\quad) \quad {}^2\mathbf{Y}^2(\mathbf{r}\quad) \tag{2.3}$$

densities

5

and

$$\mathcal{L}_{\text{int}} = \quad \mathbf{A}(\mathbf{r})\mathbf{X}(\mathbf{r}) + U(\mathbf{r}) \quad \mathbf{X}(\mathbf{r}) \qquad d \quad v(\ )\mathbf{X}(\mathbf{r})\mathbf{Y}(\mathbf{r} \ ) \tag{2.4}$$

describe the dielectric matter with a polarization eld $\mathbf{X}(\mathbf{r})$ and reservoir oscillators $\mathbf{Y}(\mathbf{r} \ )$, and the interaction between radiation and dielectric matter, respectively. The coupling constant is the electric polarizability, and the function $v(\ )$ is assumed to be square-integrable. After introducing canonical momenta $(\mathbf{r})$, $\mathbf{P}(\mathbf{r})$, and $\mathbf{Q}(\mathbf{r} \ )$ for the elds $\mathbf{A}(\mathbf{r})$, $\mathbf{X}(\mathbf{r})$, and $\mathbf{Y}(\mathbf{r} \ )$, respectively, the Legendre transform is performed to obtain the Hamiltonian $H = H_{\text{rad}} + H_{\text{mat}} + H_{\text{int}}$ of the overall system. In reciprocal space, after splitting the elds into their respective transverse and longitudinal parts, for example

$$\mathbf{X}(\mathbf{k}) = X \ (\mathbf{k}) \quad + \quad \sum_{=1}^{2} X \ (\mathbf{k})\mathbf{e} \ (\mathbf{k}) \tag{2.5}$$

[with unit polarization vectors $= \mathbf{k} \ \mathbf{k} \ , \mathbf{e} \ (\mathbf{k}) \quad \mathbf{k}$], new variables are de ned by

$$a \ (\mathbf{k}) \ = \quad \sqrt{\frac{0}{2\hbar k c}} \quad kcA \ (\mathbf{k}) + \frac{i}{0} \quad (\mathbf{k}) \tag{2.6}$$

$$b \ (\mathbf{k}) \ = \quad \sqrt{\frac{}{2\hbar}} \quad {}_i X \ (\mathbf{k}) + \frac{i}{} P \ (\mathbf{k}) \tag{2.7}$$

$$b \ (\mathbf{k} \ ) \ = \quad \sqrt{\frac{}{2\hbar}} \quad i \ Y \ (\mathbf{k} \ ) + \frac{1}{} Q \ (\mathbf{k} \ ) \tag{2.8}$$

for the transverse elds with the renormalized wave number k and frequency

$$k^2 = k^2 + \frac{2}{{}_0 c^2} \qquad {}^2 = \quad {}^2 + \quad d \ \frac{v^2(\ )}{2} \tag{2.9}$$

and accordingly for the longitudinal eld

$$b \ (\mathbf{k}) \ = \quad \sqrt{\frac{}{2\hbar}} \quad X \ (\mathbf{k}) + \frac{i}{} P \ (\mathbf{k}) \tag{2.10}$$

$$b \ (\mathbf{k} \ ) \ = \quad \sqrt{\frac{}{2\hbar}} \quad i \ Y \ (\mathbf{k} \ ) + \frac{1}{} Q \ (\mathbf{k} \ ) \tag{2.11}$$

[${}^2 = \quad {}^2 + \quad {}^2 (\quad {}_0)$]. Then with the variables (2.6) (2.8), (2.10), and (2.11), the Hamiltonian splits up into a transverse and a longitudinal part

$$H = H \ + H_{\text{mat}} \qquad H \ = H_{\text{rad}} + H_{\text{mat}} + H_{\text{int}} \tag{2.12}$$

Canonical quantization is performed by regarding the complex amplitudes $a \ (\mathbf{k})$, $b \ {}_{(\ )}(\mathbf{k})$, and $b \ {}_{(\ )}(\mathbf{k} \ )$ as bosonic annihilation operators $a \ (\mathbf{k})$, $b \ {}_{(\ )}(\mathbf{k})$, and $b \ {}_{(\ )}(\mathbf{k} \ )$. The Hamiltonian
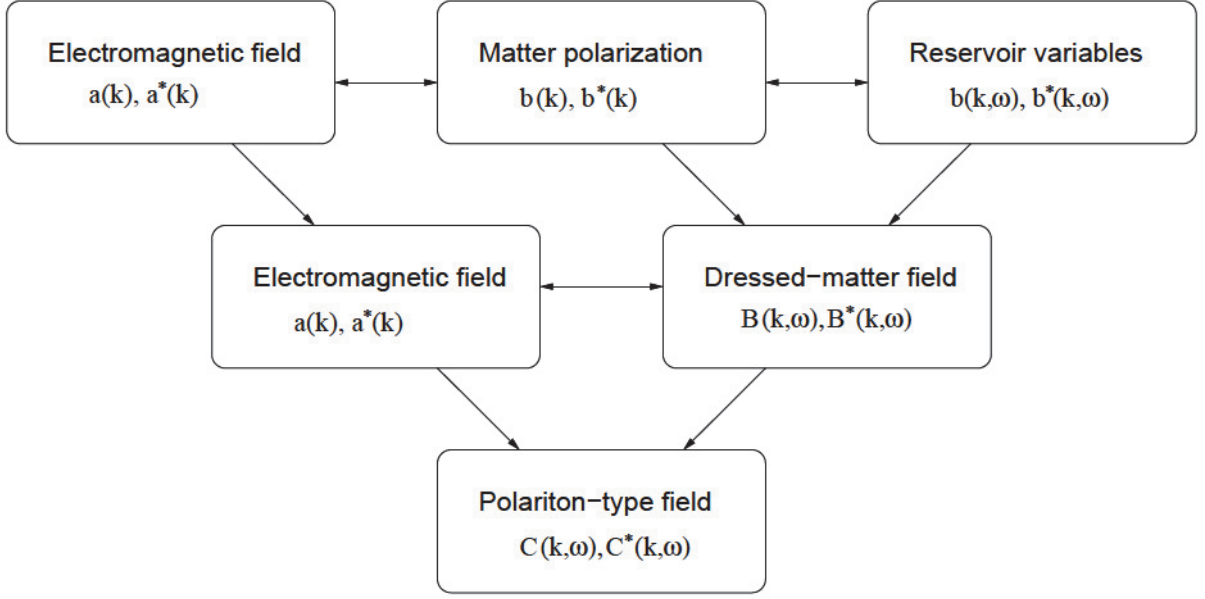
Figure 2.1: Two-step diagonalization of the overall system consisting of radiation field, dielectric matter, and reservoir.

$\hat{H}$ is bilinear in all fields and thus describes a generalized free field theory [84]. Diagonalization of the Hamiltonian is performed, following [52], by a Fano-type of technique [68] in two steps (see Fig. 2.1). First the matter Hamiltonian $\hat{H}_{\mathrm{mat}}^{\perp(\|)}$ is diagonalized by introducing the so-called dressed-matter operators $\hat{B}_{\lambda(\|)}(\mathbf{k}, \omega)$, which are linear combinations of the matter and reservoir operators $\hat{b}_{\lambda(\|)}(\mathbf{k})$ and $\hat{b}_{\lambda(\|)}(\mathbf{k}, \omega)$, such that

$$\hat{H}_{\mathrm{mat}}^{\perp} = \sum_{\lambda=1}^{2} \int d^3\mathbf{k} \int_0^\infty d\omega\, \hbar\omega\, \hat{B}_\lambda^\dagger(\mathbf{k}, \omega)\hat{B}_\lambda(\mathbf{k}, \omega)\,,$$

$$\hat{H}_{\mathrm{mat}}^{\|} = \int d^3\mathbf{k} \int_0^\infty d\omega\, \hbar\omega\, \hat{B}_\|^\dagger(\mathbf{k}, \omega)\hat{B}_\|(\mathbf{k}, \omega)\,. \tag{2.13}$$

In the second diagonalization step, the transverse dressed-matter operators are combined with the radiation-field operators $\hat{a}_\lambda(\mathbf{k})$ to the polariton operators $\hat{C}_\lambda(\mathbf{k}, \omega)$, such that

$$\hat{H}^\perp = \sum_{\lambda=1}^{2} \int d^3\mathbf{k} \int_0^\infty d\omega\, \hbar\omega\, \hat{C}_\lambda^\dagger(\mathbf{k}, \omega)\hat{C}_\lambda(\mathbf{k}, \omega)\,. \tag{2.14}$$

The vector potential and the transverse part of the material polarization can now be expressed in terms of the operators $\hat{C}_\lambda(\mathbf{k}, \omega)$ as [52, 70, 85]

$$\hat{\tilde{\mathbf{A}}}(\mathbf{k}) = -\sum_{\lambda=1}^{2} \mathbf{e}_\lambda(\mathbf{k})\sqrt{\frac{\hbar}{\pi\epsilon_0}} \int_0^\infty d\omega\, \omega\sqrt{\epsilon_I(\omega)}\tilde{G}(\mathbf{k}, \omega)\hat{C}_\lambda(\mathbf{k}, \omega) + \mathrm{H.c.} \tag{2.15}$$

and

$$\mathbf{P}(\mathbf{k}) = \sum_{\lambda=1}^{2} \mathbf{X}_\lambda(\mathbf{k}) = i \sum_{\lambda=1}^{2} \mathbf{e}_\lambda(\mathbf{k}) \overline{\frac{\hbar_0}{}}$$

$$\int_0^\infty d\omega \, \omega^2 [\varepsilon(\omega) - 1] \overline{\varepsilon_I(\omega)} G(\mathbf{k}\omega) C_\lambda(\mathbf{k}\omega) + \text{H.c.} + \mathbf{P}_N(\mathbf{k}) \tag{2.16}$$

$$\mathbf{P}_N(\mathbf{k}) = \sum_{\lambda=1}^{2} \mathbf{e}_\lambda(\mathbf{k}) \overline{\frac{\hbar_0}{}} \int_0^\infty d\omega \, i \overline{\varepsilon_I(\omega)} C_\lambda(\mathbf{k}\omega) + \text{H.c.} \tag{2.17}$$

In Eqs. (2.15) – (2.17), the complex function $\varepsilon(\omega)$ is the permittivity of the model satisfying the Kramers–Kronig relations, and $G(\mathbf{k}\omega)$ the Green function of the classical Maxwell equations

$$G(\mathbf{k}\omega) = \frac{c^2}{\omega^2 \varepsilon(\omega) - k^2 c^2} \tag{2.18}$$

The (transverse) matter polarization (2.16) consists of two contributions, the induced polarization which is proportional to $[\varepsilon(\omega) - 1]$, and a fluctuating component $\mathbf{P}_N(\mathbf{k})$ which is associated with absorption. Since the longitudinal part of the electric field operator is given by $\varepsilon_0 \mathbf{E}_\parallel(\mathbf{k}) = -\mathbf{X}_\parallel(\mathbf{k})$, there exists an analogous relation to a longitudinal noise polarization, when replacing the transverse polariton operators in Eq. (2.17) by the longitudinal dressed-matter operators $B_\parallel(\mathbf{k}\omega)$.

A major disadvantage of the explicit Fano-type diagonalization is that it is only applicable for the simplest geometries (homogeneous bulk material) and material properties (isotropic dielectrics). Even for the situation of a medium-filled half space with a planar interface to the other half space filled with vacuum, this type of quantization presented severe problems [86]. There are, however, also other ways to diagonalize the Hamiltonian (2.12). For example, path-integral quantization has been utilized in [57, 61].

2.2 Quantization of the phenomenological Maxwell field in absorbing, isotropic dielectrics

We have seen that the microscopic model has lead to a source-quantity representation of the quantized electromagnetic field operators with the Green function of the classical scattering problem, in terms of the complex permittivity $\varepsilon(\omega)$ and a continuum of harmonic-oscillator fields, which finally do not refer to the actual underlying model anymore. So far, the dielectric was assumed to be homogeneous and isotropic. Because it would be natural to start quantization at this point and to generalize the theory to arbitrary linear dielectrics, the

question is whether the (equal-time) commutation relations between electromagnetic field operators can be proved to be correct in general. The properties of the Green function and the corresponding proof of the (equal-time) commutation relations [S1, S11] are the subject of this section.

2.2.1 Classical Maxwell theory

First we shortly recapitulate the classical Maxwell theory and bring it into a form suitable for quantization. The phenomenological Maxwell equations in the presence of dielectric bodies but without external sources read

$$\nabla \cdot \mathbf{B}(\mathbf{r}) = 0 \tag{2.19}$$

$$\nabla \times \mathbf{E}(\mathbf{r}) + \dot{\mathbf{B}}(\mathbf{r}) = 0 \tag{2.20}$$

$$\nabla \cdot \mathbf{D}(\mathbf{r}) = 0 \tag{2.21}$$

$$\nabla \times \mathbf{H}(\mathbf{r}) - \dot{\mathbf{D}}(\mathbf{r}) = 0 \tag{2.22}$$

The displacement $\mathbf{D}(\mathbf{r})$ is defined by the relation

$$\mathbf{D}(\mathbf{r}) = \varepsilon_0 \mathbf{E}(\mathbf{r}) + \mathbf{P}(\mathbf{r}) \tag{2.23}$$

where $\mathbf{E}(\mathbf{r})$ is the electric field and $\mathbf{P}(\mathbf{r})$ the polarization field. Assuming non-magnetic matter, we have

$$\mathbf{H}(\mathbf{r}) = \frac{1}{\mu_0}\mathbf{B}(\mathbf{r}) \tag{2.24}$$

In the following, we consider arbitrary inhomogeneous, isotropic, non-magnetic media whose polarization responds linearly and (spatially) locally to the electric field (extensions to magnetic matter, anisotropic, and amplifying media are given in Sec. 2.3). The most general relation between the matter polarization and the electric field which is consistent with causality, hence the Kramers–Kronig relations, and the dissipation-fluctuation theorem is [87]

$$\mathbf{P}(\mathbf{r}, t) = \varepsilon_0 \int_0^\infty d\tau\, \chi(\mathbf{r}, \tau) \mathbf{E}(\mathbf{r}, t - \tau) + \mathbf{P}_{\mathrm{N}}(\mathbf{r}, t) \tag{2.25}$$

The inclusion of the noise polarization $\mathbf{P}_{\mathrm{N}}(\mathbf{r}, t)$ is necessary to fulfil the dissipation-fluctuation theorem, macroscopic electrodynamics being a statistical theory. The causal response to the electric field is thus a temporal convolution with the dielectric susceptibility $\chi(\mathbf{r}, \tau)$ as the response function. Converting Maxwell's equations (2.19)–(2.22) and the constitutive relations (2.23) and (2.24) into Fourier space by setting

$$F(t) = \int_0^\infty d\omega\, \underline{F}(\omega) e^{-i\omega t} + \text{c.c.} \tag{2.26}$$

for any real function $F(t)$, the constitutive relation (2.23) [together with (2.25)] turns into

$$\underline{D}(\mathbf{r},\omega) = \varepsilon_0\,\varepsilon(\mathbf{r},\omega)\,\underline{E}(\mathbf{r},\omega) + \underline{P}_N(\mathbf{r},\omega) \tag{2.27}$$

The matter polarization is then given by

$$\underline{P}(\mathbf{r},\omega) = \varepsilon_0[\varepsilon(\mathbf{r},\omega) - 1]\,\underline{E}(\mathbf{r},\omega) + \underline{P}_N(\mathbf{r},\omega) \tag{2.28}$$

where

$$\varepsilon(\mathbf{r},\omega) = 1 + \int_0^\infty d\tau\,\chi(\mathbf{r},\tau)e^{i\omega\tau} \tag{2.29}$$

is the relative permittivity. Being the Fourier transform of a causal response function, the real and imaginary parts of $\varepsilon(\mathbf{r},\omega)$ satisfy the Kramers–Kronig relations

$$\varepsilon_R(\mathbf{r},\omega) - 1 = \frac{\mathcal{P}}{\pi}\int d\omega'\,\frac{\varepsilon_I(\mathbf{r},\omega')}{\omega' - \omega} \tag{2.30}$$

$$\varepsilon_I(\mathbf{r},\omega) = -\frac{\mathcal{P}}{\pi}\int d\omega'\,\frac{\varepsilon_R(\mathbf{r},\omega') - 1}{\omega' - \omega} \tag{2.31}$$

[$\mathcal{P}$: principal value]. As a function of complex ω, the permittivity obeys the relation

$$\varepsilon(\mathbf{r},-\omega^*) = \varepsilon^*(\mathbf{r},\omega) \tag{2.32}$$

it is holomorphic in the upper complex half-plane without zeros and poles, and in the high-frequency limit it approaches unity, $\varepsilon(\mathbf{r},\omega) \to 1$ for $\omega \to \infty$ [87, 88]. Note that the functional form of Eq. (2.28) is similar to the form of Eq. (2.16).

With the noise polarization $\underline{P}_N(\mathbf{r},\omega)$ we define a charge density and a current density

$$\underline{\rho}_N(\mathbf{r},\omega) = -\nabla\cdot\underline{P}_N(\mathbf{r},\omega), \qquad \underline{j}_N(\mathbf{r},\omega) = -i\omega\,\underline{P}_N(\mathbf{r},\omega) \tag{2.33}$$

which, by construction, obey the usual continuity equation. With these definitions, Maxwell's equations (2.19)–(2.22) read in temporal Fourier space as

$$\nabla\cdot\underline{B}(\mathbf{r},\omega) = 0 \tag{2.34}$$

$$\nabla\times\underline{E}(\mathbf{r},\omega) - i\omega\,\underline{B}(\mathbf{r},\omega) = 0 \tag{2.35}$$

$$\varepsilon_0\nabla\cdot\varepsilon(\mathbf{r},\omega)\underline{E}(\mathbf{r},\omega) = \underline{\rho}_N(\mathbf{r},\omega) \tag{2.36}$$

$$\nabla\times\underline{B}(\mathbf{r},\omega) + i\frac{\omega}{c^2}\varepsilon(\mathbf{r},\omega)\underline{E}(\mathbf{r},\omega) = \mu_0\underline{j}_N(\mathbf{r},\omega) \tag{2.37}$$

The source terms in Eqs. (2.36) and (2.37) can be regarded as the internal (noise) sources associated with absorption processes in the dielectric medium which is consistent with the

dissipation-fluctuation theorem. Inserting Eq. (2.35) into Eq. (2.37) yields a partial differential equation for the electric field

$$\nabla\times\nabla\times\underline{\mathbf{E}}(\mathbf{r},\omega) - \frac{\omega^2}{c^2}\varepsilon(\mathbf{r},\omega)\underline{\mathbf{E}}(\mathbf{r},\omega) = i\mu_0\omega\,\underline{\mathbf{j}}_N(\mathbf{r},\omega) \qquad (2.38)$$

which can be solved by writing

$$\underline{\mathbf{E}}(\mathbf{r},\omega) = i\mu_0\omega\int d^3r'\,\mathbf{G}(\mathbf{r},\mathbf{r}',\omega)\underline{\mathbf{j}}_N(\mathbf{r}',\omega) \qquad (2.39)$$

where the Green function $\mathbf{G}(\mathbf{r},\mathbf{r}',\omega)$ (actually a second-rank tensor) obeys the partial differential equation

$$\nabla\times\nabla\times\mathbf{G}(\mathbf{r},\mathbf{r}',\omega) - \frac{\omega^2}{c^2}\varepsilon(\mathbf{r},\omega)\mathbf{G}(\mathbf{r},\mathbf{r}',\omega) = \delta(\mathbf{r}-\mathbf{r}') \qquad (2.40)$$

Together with the boundary conditions at infinity, Eq. (2.40) has a unique solution.

2.2.2 Properties of Green functions

The Green function $\mathbf{G}(\mathbf{r},\mathbf{r}',\omega)$ has some very useful properties. Having been constructed from the permittivity function $\varepsilon(\mathbf{r},\omega)$ with the property (2.32), the Green function satisfies an analogous relation,

$$\mathbf{G}(\mathbf{r},\mathbf{r}',\omega) = \mathbf{G}^*(\mathbf{r},\mathbf{r}',-\omega^*) \qquad (2.41)$$

Moreover, one can show that also the reciprocity relation

$$\mathbf{G}(\mathbf{r},\mathbf{r}',\omega) = \mathbf{G}^T(\mathbf{r}',\mathbf{r},\omega) \qquad (2.42)$$

holds generally [S11]. It means physically that the electric field at point $\mathbf{r}$ of a (point-like) source at point $\mathbf{r}'$ is the same as the field electric field at point $\mathbf{r}'$ produced by a (point-like) source at $\mathbf{r}$ [89]. Both relations (2.41) and (2.42) are necessary to derive the integral relation (see Appendix A with $\mu(\mathbf{r},\omega)=1$)

$$\int d^3s\,\frac{\omega^2}{c^2}\varepsilon_I(\mathbf{s},\omega)\,\mathbf{G}(\mathbf{r},\mathbf{s},\omega)\,\mathbf{G}^+(\mathbf{s},\mathbf{r}',\omega) = \operatorname{Im}\mathbf{G}(\mathbf{r},\mathbf{r}',\omega) \qquad (2.43)$$

which reads in Cartesian coordinates as

$$\int d^3s\,\frac{\omega^2}{c^2}\varepsilon_I(\mathbf{s},\omega)\,G_{ik}(\mathbf{r},\mathbf{s},\omega)G_{jk}^*(\mathbf{r}',\mathbf{s},\omega) = \operatorname{Im}G_{ij}(\mathbf{r},\mathbf{r}',\omega) \qquad (2.44)$$

2.2.3 Quantization and equal-time commutation relations

As it can be read off from Eqs. (2.39) and (2.33), the noise polarization $\underline{\mathbf{P}}_N(\mathbf{r})$ plays the fundamental role in determining the electric field. For the following it is convenient to split off some factor and define the fundamental dynamical variables $\mathbf{f}(\mathbf{r})$ by

$$\underline{\mathbf{P}}_N(\mathbf{r}) = i\,\sqrt{\frac{\hbar\,_0}{\pi}}\,_I(\mathbf{r})\,\mathbf{f}(\mathbf{r}) \tag{2.45}$$

Upon quantization, we replace the classical fields $\mathbf{f}(\mathbf{r})$ and $\mathbf{f}^*(\mathbf{r})$ by the operator-valued bosonic fields $\mathbf{f}(\mathbf{r})$ and $\mathbf{f}^\dagger(\mathbf{r})$ which are associated with the elementary excitations of the system composed of the electromagnetic field and the absorbing dielectric matter. Their commutation relations are

$$\big[\,f_i(\mathbf{r})\,,\,f_j^\dagger(\mathbf{r}')\,\big] = \delta_{ij}\,\delta(\mathbf{r}-\mathbf{r}')\,\delta(\omega-\omega') \tag{2.46}$$

$$\big[\,f_i(\mathbf{r})\,,\,f_j(\mathbf{r}')\,\big] = 0 \tag{2.47}$$

The normally-ordered Hamiltonian of the composed system is

$$H = \int d^3\mathbf{r} \int_0^\infty d\omega\,\hbar\omega\,\mathbf{f}^\dagger(\mathbf{r})\mathbf{f}(\mathbf{r}) \tag{2.48}$$

showing that the time-dependence of $\mathbf{f}(\mathbf{r})$ induced by the Hamiltonian (2.48) in the Heisenberg picture is given by

$$\dot{\mathbf{f}}(\mathbf{r}) = (i\hbar)^{-1}\big[\mathbf{f}(\mathbf{r})\,,\,H\big] = -i\omega\,\mathbf{f}(\mathbf{r}) \tag{2.49}$$

hence they represent a continuous set of harmonic oscillators. Since the operators in the Hamiltonian (2.48) are normally-ordered, an infinite constant term, the ground-state energy, has been discarded.

The operator-valued equivalents of the fields $\underline{\mathbf{E}}(\mathbf{r})$, $\underline{\mathbf{B}}(\mathbf{r})$, and $\underline{\mathbf{D}}(\mathbf{r})$ are obtained by rewriting Eq. (2.39) as

$$\underline{\mathbf{E}}(\mathbf{r}) = i\,\sqrt{\frac{\hbar}{\pi\,_0}}\frac{\omega^2}{c^2}\int d^3\mathbf{r}'\,\,_I(\mathbf{r}')\mathbf{G}(\mathbf{r},\mathbf{r}',\omega)\,\mathbf{f}(\mathbf{r}') \tag{2.50}$$

and using Maxwell's equation (2.35) to obtain the magnetic induction

$$\underline{\mathbf{B}}(\mathbf{r}) = (i\omega)^{-1}\nabla\times\underline{\mathbf{E}}(\mathbf{r}) \tag{2.51}$$

Finally, the displacement field reads, by Eq. (2.27), as

$$\begin{aligned}\underline{\mathbf{D}}(\mathbf{r}) &= \,_0\,(\mathbf{r})\underline{\mathbf{E}}(\mathbf{r}) + \underline{\mathbf{P}}_N(\mathbf{r})\\ &= (\,_0\,\omega^2)^{-1}\nabla\times\nabla\times\underline{\mathbf{E}}(\mathbf{r}) \end{aligned} \tag{2.52}$$

The electromagnetic field operators in the Schrödinger picture are obtained by integration over ω:

$$\mathbf{E}(\mathbf{r}) = \int_0^\infty d\omega \, \underline{\mathbf{E}}(\mathbf{r}, \omega) + \text{H.c.} \tag{2.53}$$

and all other fields analogously.

The representation of the electric-field operator (2.53) [together with Eq. (2.50)] generalizes the usual mode expansion, which fails when losses are taken into account. In the limit of vanishing absorption and dispersion, $\varepsilon(\mathbf{r}, \omega) \to 1 + i0_+$, the source-quantity representation with the Green function in terms of the fundamental basic fields (2.50) reduces to the familiar mode expansion with (linear combinations of) the basic fields $\mathbf{f}(\mathbf{r}, \omega)$ becoming annihilation operators of the electromagnetic field. This becomes clear when reminding the Lagrangian formalism in Sec. 2.1. The couplings between the electromagnetic field and the harmonic oscillators modelling dielectric matter and reservoir vanish in that limit, leaving behind vacuum quantum electrodynamics.

In view of the general solution to the inhomogeneous Helmholtz equation (2.38), Eq. (2.50) would represent the (particular) inhomogeneous solution, and a general solution should be constructed by Eq. (2.50) and a solution of the homogeneous Helmholtz equation. The physical interpretation of the latter is usually done in terms of radiation that propagates freely in the vacuum region. So far nothing has been said where this radiation was created. The integration region in (2.50) extends over the whole space. Thus, every possible source of radiation is already included in that particular solution, that is, also those sources which are located in the far distance giving rise to an (approximately) homogeneous solution. In the case when no dielectric is present, that is $\varepsilon(\mathbf{r}, \omega) \to 1 + i0_+$, by the discussion above, the (homogeneous) free-space solution is recovered. There cannot be any additional sources which are not included in (2.50). We therefore conclude that an additional homogeneous solution does not exist physically.

In order to prove the consistency of the quantization scheme with standard quantum electrodynamics, we compute the equal-time commutation relations between the field operators and show their equivalence with standard QED commutation relations. From the integral representation of the Fourier components of the electric field (2.50) and the magnetic induction (2.51), one derives, using the properties (2.41) and (2.42) of the Green function as well as the integral relation (2.43) [or equivalently Eq. (2.44)],

$$\left[E_i(\mathbf{r}), E_k(\mathbf{r}') \right] = \left[B_i(\mathbf{r}), B_k(\mathbf{r}') \right] = 0 \tag{2.54}$$

and

$$\left[E_i(\mathbf{r}),\, B_k(\mathbf{r}')\right] = \frac{\hbar}{\varepsilon_0}\, \epsilon_{kmj}\, \partial^r_m \int d\omega\, \frac{\omega}{c^2} \Im G_{ij}(\mathbf{r},\mathbf{r}',\omega) \tag{2.55}$$

Equation (2.55) has to be shown to lead to the standard QED relation

$$\left[E_i(\mathbf{r}),\, B_k(\mathbf{r}')\right] = \frac{i\hbar}{\varepsilon_0}\, \epsilon_{ikm}\, \partial^r_m\, \delta(\mathbf{r}-\mathbf{r}') \tag{2.56}$$

which is fulfilled only if in Eq. (2.55) the ω integral yields

$$\epsilon_{kmj}\, \partial^r_m \int d\omega\, \frac{\omega}{c^2} \Im G_{ij}(\mathbf{r},\mathbf{r}',\omega) = i\, \epsilon_{kmj}\, \partial^r_m\, \delta_{ij}\, \delta(\mathbf{r}-\mathbf{r}') \tag{2.57}$$

Apart from scalar electrodynamics for slab-like systems [54, 56, 71], Eq. (2.57) has proved to be correct for bulk material [70] and for two infinite half-spaces with a common planar interface [60] by direct computation using the explicit form of the Green function. For arbitrary inhomogeneous dielectrics for which the Green function is not explicitly known, we now prove the validity of Eq. (2.57) by converting the partial differential equation (2.44), satisfied by the Green function, into an integral equation and performing a suitable decomposition of the Green function [S1].

Proof of the commutation relation for inhomogeneous dielectrics

From the theory of partial differential equations it is known (see, e.g., [90]) that there exists an equivalent formulation of the problem in terms of an integral equation. Rewriting the partial differential equation satisfied by the Green function (2.40) which reads in Cartesian components as

$$\left[\partial^r_i \partial^r_k - \delta_{ik}\, \Delta^r + \frac{\omega^2}{c^2} \varepsilon(\mathbf{r},\omega)\right] G_{kj}(\mathbf{r},\mathbf{s},\omega) = \delta_{ij}\, \delta(\mathbf{r}-\mathbf{s}) \tag{2.58}$$

with the formal definition $\varepsilon(\mathbf{r},\omega) = \varepsilon(\mathbf{r},\omega) + \varepsilon_0(\omega) - \varepsilon_0(\omega)$, where $\varepsilon_0(\omega) \equiv \overline{\varepsilon(\mathbf{r},\omega)}^{\,\mathbf{r}}$ is an appropriately space-averaged reference permittivity, we obtain

$$\left[\Delta^r + q_0^2(\omega)\right] G_{ij}(\mathbf{r},\mathbf{s},\omega) = \left[q_0^2(\omega) - q^2(\mathbf{r},\omega)\right] G_{ij}(\mathbf{r},\mathbf{s},\omega) + \partial^r_i \partial^r_k G_{kj}(\mathbf{r},\mathbf{s},\omega) - \delta_{ij}\, \delta(\mathbf{r}-\mathbf{s}) \tag{2.59}$$

Here, the abbreviations

$$q^2(\mathbf{r},\omega) = \frac{\omega^2}{c^2} \varepsilon(\mathbf{r},\omega) \qquad q_0^2(\omega) = \frac{\omega^2}{c^2} \varepsilon_0(\omega) \tag{2.60}$$

have been used. Now we introduce the scalar Green function

$$g(\mathbf{r},\omega) = \frac{e^{iq_0(\omega)r}}{4\pi r} = \int \frac{d^3\mathbf{k}}{(2\pi)^3} \frac{e^{i\mathbf{k}\cdot\mathbf{r}}}{k^2 - q_0^2(\omega)} \tag{2.61}$$

which satisfies the differential equation

$$\nabla^r + q_0^2(\omega) \; g(\mathbf{r}, \omega) = \delta(\mathbf{r}) \tag{2.62}$$

The Green function $g(\mathbf{r}, \omega)$ enables us to convert Eq. (2.59) into the integral equation

$$G_{ij}(\mathbf{r}, \mathbf{s}, \omega) = G_{ij}^{(0)}(\mathbf{r}, \mathbf{s}, \omega) + \int d^3\mathbf{v} \, K_{ik}(\mathbf{r}, \mathbf{v}, \omega) G_{kj}(\mathbf{v}, \mathbf{s}, \omega) \tag{2.63}$$

where

$$G_{ij}^{(0)}(\mathbf{r}, \mathbf{s}, \omega) = \left[\delta_{ij} + \partial_i^r \partial_j^s q^{-2}(\mathbf{s}, \omega) \right] g(\mathbf{r}, \mathbf{s}, \omega) \tag{2.64}$$

and

$$K_{ik}(\mathbf{r}, \mathbf{v}, \omega) = \left\{ \partial_k^v \ln q^2(\mathbf{v}, \omega) \left[\partial_i^r g(\mathbf{r}, \mathbf{v}, \omega) \right] + \left[q^2(\mathbf{v}, \omega) - q_0^2(\omega) \right] g(\mathbf{r}, \mathbf{v}, \omega) \delta_{ik} \right\} \tag{2.65}$$

Obviously, $G_{ij}^{(0)}(\mathbf{r}, \mathbf{s}, \omega)$ is the Green function for a homogeneous medium with permittivity $\varepsilon(\mathbf{r}, \omega) \to \varepsilon_0(\omega)$. The second term on the right-hand side in Eq. (2.63) essentially arises from the inhomogeneities. Note that, according to the Fredholm alternative, the solution of the integral equation (2.63) is unique, because of the non-existence of non-trivial solutions of the homogeneous problem. From Eqs. (2.61), (2.62), and the analyticity properties of the Green function it follows that the integral kernel $K_{ik}(\mathbf{r}, \mathbf{v}, \omega)$, Eq. (2.65), is a holomorphic function of ω in the upper complex half-plane, with $K_{ik}(\mathbf{r}, \mathbf{v}, \omega) \to 0$ for $\omega \to \infty$, where $K_{ik}(\mathbf{r}, \mathbf{v}, \omega)$ decreases as does $\varepsilon(\mathbf{r}, \omega) - 1$.

Let us write the integral equation (2.63) in the compact form

$$G = G^{(0)} + \mathcal{K} G \tag{2.66}$$

where

$$\mathcal{K} G \equiv (\mathcal{K} G)_{ij}(\mathbf{r}, \mathbf{s}, \omega) = \int d^3\mathbf{v} \, K_{ik}(\mathbf{r}, \mathbf{v}, \omega) G_{kj}(\mathbf{v}, \mathbf{s}, \omega) \tag{2.67}$$

Assuming that G can be found by iteration, we may write

$$G = G^{(0)} + \sum_{n=1}^{\infty} \mathcal{K}^n G^{(0)} \tag{2.68}$$

From Eq. (2.64) it is seen that $G_{ij}^{(0)}(\mathbf{r}, \mathbf{s}, \omega)$ has a cubic singularity $|\mathbf{r} - \mathbf{s}|^{-3}$ for $\mathbf{r} \to \mathbf{s}$, and Eq. (2.65) reveals that the kernel $K_{ik}(\mathbf{r}, \mathbf{v}, \omega)$ is only weakly singular (the singularity is weaker than the spatial dimension). Hence, at least after the third iteration step the result is perfectly regular at $\mathbf{r} = \mathbf{s}$.

In order to compute the ω integral (2.57), we first decompose the Green function into two parts,

$$G_{ij}(\mathbf{r}, \mathbf{s}, \omega) = (G_1)_{ij}(\mathbf{r}, \mathbf{s}, \omega) + (G_2)_{ij}(\mathbf{r}, \mathbf{s}, \omega) \tag{2.69}$$

where $(G_1)_{ij}(\mathbf{r}\,\mathbf{s}\,)$ and $(G_2)_{ij}(\mathbf{r}\,\mathbf{s}\,)$ satisfy the integral equations

$$G_\nu = G_\nu^{(0)} + \mathcal{K}\,G_\nu \qquad (\nu = 1,2) \tag{2.70}$$

with

$$(G_1)_{ij}^{(0)}(\mathbf{r}\,\mathbf{s}\,) = \delta_{ij}\, g(\mathbf{r}\,\mathbf{s}\,) \tag{2.71}$$

and

$$(G_2)_{ij}^{(0)}(\mathbf{r}\,\mathbf{s}\,) = \partial_j^s \partial_i^r q^2(\mathbf{s}\,)g(\mathbf{r}\,\mathbf{s}\,) \tag{2.72}$$

Now, $(G_2)_{ij}(\mathbf{r}\,\mathbf{s}\,)$ can be given by

$$(G_2)_{ij}(\mathbf{r}\,\mathbf{s}\,) = \partial_j^s \Gamma_i(\mathbf{r}\,\mathbf{s}\,) \tag{2.73}$$

where Γ is the solution of the integral equation

$$\Gamma = \Gamma^{(0)} + \mathcal{K}\,\Gamma \tag{2.74}$$

with

$$\Gamma_i^{(0)}(\mathbf{r}\,\mathbf{s}\,) = \partial_i^r q^2(\mathbf{s}\,)g(\mathbf{r}\,\mathbf{s}\,) \tag{2.75}$$

Both $(G_1)_{ij}(\mathbf{r}\,\mathbf{s}\,)$ and $(G_2)_{ij}(\mathbf{r}\,\mathbf{s}\,)$ are holomorphic functions of ω in the upper complex half-plane, with $(G_\nu)_{ij}(\mathbf{r}\,\mathbf{s}\,) \to 0$ if $\omega \to \infty$. Note that $(G_2)_{ij}(\mathbf{r}\,\mathbf{s}\,)$ may be singular at $\omega = 0$. Nevertheless, when substituting $G_{ij}(\mathbf{r}\,\mathbf{s}\,)$ from Eq. (2.69) [together with Eq. (2.73)] back into the expression of the electric eld in terms of the Green function (2.50), we can integrate by parts and use the equation of continuity to obtain

$$\underline{E}_i(\mathbf{r}\,) = i\mu_0\omega \int d^3s\, (G_1)_{ik}(\mathbf{r}\,\mathbf{s}\,)\underline{j}_k(\mathbf{s}\,) + \mu_0 \int d^3s\, \omega^2 \Gamma_i(\mathbf{r}\,\mathbf{s}\,)\underline{\rho}(\mathbf{s}\,) \tag{2.76}$$

Hence, $i\mu_0\omega\,(G_1)_{ik}(\mathbf{r}\,\mathbf{s}\,)$ and $\mu_0\omega^2\Gamma_i(\mathbf{r}\,\mathbf{s}\,)$ are the Fourier transforms of the response functions relating the electric- eld strength to the (noise) current density $\underline{j}_k(\mathbf{s}\,)$ and the (noise) charge density $\underline{\rho}(\mathbf{s}\,)$ separately. Obviously, $\omega^2\Gamma_i(\mathbf{r}\,\mathbf{s}\,)$ is not singular at $\omega = 0$.

Combining Eqs. (2.69) and (2.73), we easily see that the ν integral over the Green function (2.57) can be rewritten as, on recalling that $\epsilon_{kmj}\partial_m^r \partial_j^r(\cdots) = 0$,

$$\epsilon_{kmj}\partial_m^r \int_{-\infty}^{+\infty} d\omega\, \frac{\omega^2}{c^2}G_{ij}(\mathbf{r}\,\mathbf{r}'\,) = \epsilon_{kmj}\partial_m^r \int_{-\infty}^{+\infty} d\omega\, \frac{\omega^2}{c^2}(G_1)_{ij}(\mathbf{r}\,\mathbf{r}'\,) \tag{2.77}$$

Thus, only the noise-current response function $(G_1)_{ij}(\mathbf{r}\,\mathbf{r}'\,)$ contributes to the commutator. We now substitute in Eq. (2.77) for $(G_1)_{ij}(\mathbf{r}\,\mathbf{r}'\,)$ the integral equation (2.70) $(\nu = 1)$ to obtain

$$\int_{-\infty}^{+\infty} d\omega\, \frac{\omega^2}{c^2}(G_1)_{ij}(\mathbf{r}\,\mathbf{r}'\,) = i\omega\,\delta_{ij}\,\delta(\mathbf{r}-\mathbf{r}')\, + \int_{-\infty}^{+\infty} d\omega \int d^3v\, \frac{\omega^2}{c^2} K_{ik}(\mathbf{r}\,\mathbf{v}\,)(G_1)_{kj}(\mathbf{v}\,\mathbf{r}'\,)$$

$$\tag{2.78}$$

where the (bulk-material) relation [70]

$$\omega^+ \frac{\omega}{c^2}(G_1)_{ij}^{(0)}(\mathbf{r},\mathbf{r}',\omega)=i\omega\delta_{ij}(\mathbf{r}-\mathbf{r}') \tag{2.79}$$

has been used. Hence it remains to prove that the second term on the right-hand side in Eq. (2.78) vanishes.

Since $K_{ik}(\mathbf{r},\mathbf{v},\omega)$ and $(G_1)_{kj}(\mathbf{v},\mathbf{s},\omega)$ are holomorphic functions of ω in the upper complex half-plane, the ω integral can be calculated by contour integration along a large half-circle (with $|\omega|=R$, $R\to\infty$). To calculate this integral, we recall that for $\omega\to\infty$ both $K_{ik}(\mathbf{r},\mathbf{v},\omega)$ and $(G_1)_{kj}(\mathbf{v},\mathbf{s},\omega)$ approach zero at least as ω^{-1}, and $K_{ik}(\mathbf{r},\mathbf{v},\omega)$ $(G_1)_{kj}(\mathbf{v},\mathbf{s},\omega)$ approaches zero at least as ω^{-2}. Hence, for $R\to\infty$ the contour integral vanishes at least as R^{-1}, and the second term on the right-hand side in Eq. (2.78) indeed equals zero, i.e.,

$$\omega^+ \frac{\omega}{c^2}(G_1)_{ij}(\mathbf{r},\mathbf{r}',\omega)=i\omega\delta_{ij}(\mathbf{r}-\mathbf{r}') \tag{2.80}$$

This completes the proof of the correct (equal-time) commutation relations between electric field and magnetic induction. Other commutation relations can be derived accordingly. For example, because the polarization $\mathbf{P}(\mathbf{r})$ is related to the matter degrees of freedom, we immediately get

$$[P_i(\mathbf{r}),E_j(\mathbf{r}')]=0 \tag{2.81}$$

An equivalent, but conceptually different proof of the commutation relations based on the Feshbach formula [91] can be found in [S11].

The representation of the electric-field operator (2.50) also implies that the ground-state expectation value of $\underline{\mathbf{E}}(\mathbf{r})$ is zero whereas the fluctuation of $\underline{\mathbf{E}}(\mathbf{r})$ is not. The ground state $|0\rangle$ for the basic-field operators $\mathbf{f}(\mathbf{r},\omega)$ is defined as the ground state of the electromagnetic field and the ground state of matter and reservoir, and will henceforth be called the vacuum state. Using the commutation relations (2.46) and (2.47) of the basic fields $\mathbf{f}(\mathbf{r},\omega)$ and the integral relation (2.43) yields

$$\langle 0|\underline{E}_i(\mathbf{r})\underline{E}_j(\mathbf{r}')|0\rangle=\frac{\hbar\omega^2}{\varepsilon_0 c^2}\,\mathrm{Im}\,G_{ij}(\mathbf{r},\mathbf{r}',\omega)\,(\quad) \tag{2.82}$$

Thus, the fluctuation of the electromagnetic field is determined by the imaginary part of the Green function. This result is consistent with the dissipation-fluctuation theorem [92], noting that the Green function plays the role of the response function of the electromagnetic field to an external perturbation.

Instead of using the electromagnetic field strengths, scalar and vector potentials can be introduced and expressed in terms of the basic fields $\mathbf{f}(\mathbf{r})$. For example, in the Coulomb gauge the potentials are defined as

$$\varphi(\mathbf{r}) = \mathbf{E}_\parallel(\mathbf{r}) \tag{2.83}$$

and

$$\mathbf{A}(\mathbf{r}) = \int_0^\infty d\omega\, \underline{\mathbf{A}}(\mathbf{r},\omega) + \text{H.c.} \tag{2.84}$$

where

$$\underline{\mathbf{A}}(\mathbf{r},\omega) = (i\omega)^{-1}\underline{\mathbf{E}}_\perp(\mathbf{r},\omega) \tag{2.85}$$

For bulk material, this representation of the vector potential, together with Eq. (2.50), exactly corresponds to Eq. (2.15) in the canonical quantization of a Hopfield dielectric.

An equivalent formalism developed in [58, 59] also starts off from the phenomenological Maxwell equations. Here, a set of auxiliary fields, instead of the noise current, is introduced. The auxiliary fields allow for replacing Maxwell's equations, which feature a time convolution relating the polarization to the electric field [Eq. (2.25) without the noise polarization], by a new set of equations for the combined electromagnetic and auxiliary fields. Although this method looks quite different from our approach, both methods are equivalent since we have shown [S12] that one can construct the operator noise current from the auxiliary fields.

2.3 Extensions to other media

The quantization scheme has so far been restricted to absorbing, isotropic, nonmagnetic, linear media. Once the outline is clear, we can extend the scheme to more general situations [S1, S11]. Starting point is always the representation of the electric field strength operator (2.50) in terms of the fundamental dynamical variables of the system composed of electromagnetic field and the medium. Recalling Eqs. (2.33) and (2.45), we can write

$$\underline{\mathbf{E}}(\mathbf{r},\omega) = i\mu_0\omega^2 \int d^3s\, G(\mathbf{r},\mathbf{s},\omega)\,\underline{\mathbf{j}}_N(\mathbf{s},\omega) \tag{2.86}$$

with

$$\underline{\mathbf{j}}_N(\mathbf{r},\omega) = \sqrt{\frac{\hbar\varepsilon_0}{\pi}}\,\omega\,\varepsilon_I(\mathbf{r},\omega)\,\mathbf{f}(\mathbf{r},\omega) \tag{2.87}$$

In the following possible extensions are briefly described.

Amplifying media

As the first example we consider a dielectric medium which is amplifying in some finite region of space and frequency, and absorbing in all other regions. Amplification can also be described by a complex permittivity function $\varepsilon(\mathbf{r}, \omega)$ which still satisfies the Kramers–Kronig relations but has a negative imaginary part. Quantization is performed by setting [S1]

$$\underline{\mathbf{j}}_{N}(\mathbf{r}, \omega) = \sqrt{\frac{\hbar \varepsilon_0 \omega^2}{\pi}} \sqrt{|\varepsilon_I(\mathbf{r}, \omega)|} \left[\Theta(\varepsilon_I)\mathbf{f}(\mathbf{r}, \omega) + \Theta(-\varepsilon_I)\mathbf{f}^\dagger(\mathbf{r}, \omega) \right] \tag{2.88}$$

[$\Theta(x)$: Heaviside step function], which reflects the fact that amplification requires the roles of (noise) creation and annihilation operators to be exchanged [93, 94, 95, 96, 97]. Inserting (2.88) into (2.86), one can prove the correctness of the fundamental QED commutation relations if the spatial and frequency region in which amplification occurs, extends only over a finite region. Especially, we require $\lim_{\mathbf{r}\to\infty} [\varepsilon(\mathbf{r}, \omega) - 1] \to i0_+$.

Anisotropic media

In anisotropic media the scalar permittivity function $\varepsilon(\mathbf{r}, \omega)$ has to be replaced by a second-rank tensor $\boldsymbol{\varepsilon}(\mathbf{r}, \omega)$. The Green function has to be determined from the equation

$$\nabla \times \nabla \times \mathbf{G}(\mathbf{r}, \mathbf{s}, \omega) - \frac{\omega^2}{c^2} \boldsymbol{\varepsilon}(\mathbf{r}, \omega) \mathbf{G}(\mathbf{r}, \mathbf{s}, \omega) = \delta(\mathbf{r} - \mathbf{s}) \tag{2.89}$$

The reciprocity relation (2.42) for the Green function is ensured if $\boldsymbol{\varepsilon}(\mathbf{r}, \omega)$ is a symmetric tensor. In analogy to the integral relation derived in Appendix A [cf. Eq. (2.44)] we obtain [S11]

$$\int d^3\mathbf{r} \, \frac{\omega^2}{c^2} \varepsilon_{I\,kl}(\mathbf{r}, \omega) G_{ik}(\mathbf{r}, \mathbf{s}, \omega) G_{jl}^*(\mathbf{r}, \mathbf{s}', \omega) = \mathrm{Im} G_{ij}(\mathbf{s}, \mathbf{s}', \omega) \tag{2.90}$$

The operator noise current density is now defined as

$$\underline{\mathbf{j}}_{N}(\mathbf{r}, \omega) = \sqrt{\frac{\hbar \varepsilon_0 \omega^2}{\pi}} \, \varepsilon_I^{1/2}(\mathbf{r}, \omega) \mathbf{f}(\mathbf{r}, \omega) \tag{2.91}$$

where the square-root of the imaginary part of the permittivity tensor is given by the eigen-value problem

$$\varepsilon_I^{1/2}(\mathbf{r}, \omega) = \mathbf{O}(\mathbf{r}, \omega) \, \epsilon_I^{1/2}(\mathbf{r}, \omega) \mathbf{O}^{-1}(\mathbf{r}, \omega) \tag{2.92}$$

with the (positive) diagonal matrix $\epsilon_I^{1/2}(\mathbf{r}, \omega)$ and an orthogonal matrix $\mathbf{O}(\mathbf{r}, \omega)$.

Magnetic media

In all previous cases the response of the matter was solely of electric type giving rise to an (electric) polarization. We now include also a magnetic response into the theory, restricted

to isotropic media with a scalar magnetic susceptibility $(\mathbf{r})$ [S11]. From the preceding section it is clear that anisotropy presents no additional difficulty but lengthens notation. We start from constitutive relations in non-standard form,

$$\underline{\mathbf{D}}(\mathbf{r}) = {}_0\underline{\mathbf{E}}(\mathbf{r}) + \underline{\mathbf{P}}(\mathbf{r}) \tag{2.93}$$

$$\underline{\mathbf{H}}(\mathbf{r}) = {}_0\underline{\mathbf{B}}(\mathbf{r}) + \underline{\mathbf{M}}(\mathbf{r}) \tag{2.94}$$

which can be justified from a relativistic point of view [98]. They have the advantage of preserving the interpretation of the fields **E** and **B** as the fundamental electromagnetic fields. As before, the (electric) polarization is defined as

$$\underline{\mathbf{P}}(\mathbf{r}) = {}_0\left[(\mathbf{r}) \quad 1\right]\underline{\mathbf{E}}(\mathbf{r}) + \underline{\mathbf{P}}_{\mathrm{N}}(\mathbf{r}) \tag{2.95}$$

whereas the equivalent expression for the magnetization reads $[{}_0 = {}_0{}^1, \ (\mathbf{r}) = {}^1(\mathbf{r})]$

$$\underline{\mathbf{M}}(\mathbf{r}) = {}_0\left[(\mathbf{r}) \quad 1\right]\underline{\mathbf{B}}(\mathbf{r}) + \underline{\mathbf{M}}_{\mathrm{N}}(\mathbf{r}) \tag{2.96}$$

The magnetic susceptibility $(\mathbf{r})$ [as well as $(\mathbf{r})$] satisfies analogous causality relations as the dielectric permittivity. The Green function obeys the partial differential equation

$$(\mathbf{r}) \quad G(\mathbf{r}\,\mathbf{s}) \quad \frac{2}{c^2}(\mathbf{r})G(\mathbf{r}\,\mathbf{s}) = (\mathbf{r}\quad\mathbf{s}) \tag{2.97}$$

The generalization of the integral relation (2.44) reads now

$$d^3\mathbf{s} \ _I(\mathbf{s}) \ {}^s_k G_{in}(\mathbf{r}\,\mathbf{s}) \ {}^s_n G_{jk}(\mathbf{r}\,\mathbf{s}) \ {}^s_k G_{jn}(\mathbf{r}\,\mathbf{s})$$

$$+ \quad d^3\mathbf{s}\frac{2}{c^2} \ _I(\mathbf{s})G_{in}(\mathbf{r}\,\mathbf{s})G_{jn}(\mathbf{r}\,\mathbf{s}) = \operatorname{Im}G_{ij}(\mathbf{r}\,\mathbf{r}) \tag{2.98}$$

which is proved in Appendix A.

Since, by Eq. (2.96), there exists also a noise contribution from the magnetization, we have to define the operator noise current as

$$\underline{\mathbf{j}}_{\mathrm{N}}(\mathbf{r}) = i \ \underline{\mathbf{P}}_{\mathrm{N}}(\mathbf{r}) \qquad \underline{\mathbf{M}}_{\mathrm{N}}(\mathbf{r})$$

$$= \quad \frac{\hbar \ _0}{} \ _I(\mathbf{r})\,\mathbf{f}(\mathbf{r}) \quad i \quad \frac{\hbar \ _0}{} \ _I(\mathbf{r})\,\mathbf{f}(\mathbf{r}) \tag{2.99}$$

In Eq. (2.99) we have assumed an absorbing medium for which $_I(\mathbf{r}) > 0$ [87] such that $_I(\mathbf{r}) = \ _I(\mathbf{r}) \ (\mathbf{r})^2 < 0$. The ($ $-components of the) electric field strength is obtained by substituting Eq. (2.99) into Eq. (2.86), all other fields accordingly. Note that, although electric and magnetic noise contributions are present, Maxwell's equations have only (for each frequency and each spatial component) three degrees of freedom. Thus, it is sufficient to introduce a single bosonic vector field $\mathbf{f}(\mathbf{r})$.

The above examples show that the quantization scheme is valid in all situations in which the matter responds linearly and locally to an externally applied electric or magnetic field.

3 Quantum-optical input-output relations at dielectric plates

Input-output relations for the mode operators of the electromagnetic field at dielectric objects, relating the photonic operators of the incoming fields to those of the outgoing fields, represent a powerful tool for describing the influence of material bodies on light impinging on some dielectric device such as a beam splitter, a mirror, or an optical fibre. The general theory of quantizing the electromagnetic field developed in Sec. 2.2 can directly be applied to input-output coupling at arbitrary three-dimensional dielectric objects. Based on the source-quantity representation with the Green function, the theory presented in Sec. 3.1 [S13] is rather general and not restricted to special geometries. The question is only whether one is able to derive some analytical expression for the Green function. Certainly, this can be done only in some special (usually highly symmetric) cases, an example being a planar multilayer structure which is treated in Sec. 3.2. In all other situations, there is the possibility to apply Dyson expansion around some explicitly known function, as it is done in the case of scattering at rough surfaces [83, 99, 100, 101].

Let us shortly review the input-output theory for propagation of linearly polarized light in the z direction [69, 70]. Starting from the Green-function representation (2.50) of the electric-field operator and correspondingly the operator of the vector potential (2.84) [together with Eq. (2.85)], quasi-mode operators $a_\pm(z,\omega)$ associated with the amplitudes of damped plane waves propagating to the left (-) and right (+) are introduced by writing

$$A(z) = \sqrt{\frac{\hbar}{\varepsilon_0 \mathcal{A}}} \int_0^\infty d\omega \left[c_+(z,\omega) a_+(z,\omega) + c_-(z,\omega) a_-(z,\omega) \right] + \text{H.c.} \tag{3.1}$$

where

$$c_+(z,\omega) a_+(z,\omega) = \int_{-\infty}^{z} dz'\, \frac{\omega^2}{c^2} \sqrt{\varepsilon_I(z',\omega)}\, G(z,z',\omega) f(z',\omega) \tag{3.2}$$

$$c_-(z,\omega) a_-(z,\omega) = \int_{z}^{\infty} dz'\, \frac{\omega^2}{c^2} \sqrt{\varepsilon_I(z',\omega)}\, G(z,z',\omega) f(z',\omega) \tag{3.3}$$

The (scalar) Green function of a medium with piecewise constant permittivity $\varepsilon_j(\omega)$ can always be decomposed into [89, 102]

$$G(z,z',\omega) = \vartheta_j(z,z')\, G_j^{(0)}(z,z',\omega) + R(z,z',\omega) \tag{3.4}$$

where the symbol $\Theta_j(z, z')$ is one if both z and z' are in the region j and zero otherwise. The function $G_j^{(0)}(z, z', \omega)$ is the Green function of a bulk material with permittivity $\varepsilon_j(\omega)$, and $R(x, x', \omega)$ is a solution to homogeneous wave equation that ensures the correct boundary conditions at the interfaces between the different regions. Assuming a dielectric plate sur-
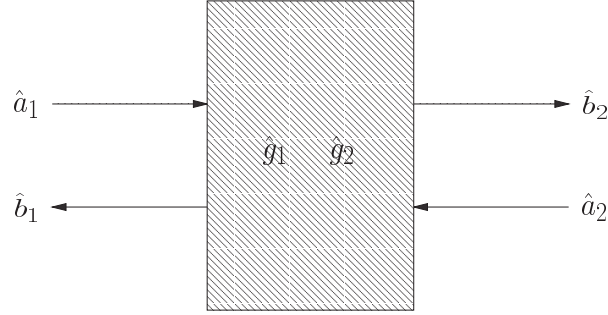

Figure 3.1: Scheme of a four-port device. The incoming fields described by operators $a_i(\omega)$ produce outgoing fields described by operators $b_i(\omega)$, the $g_i(\omega)$ being operators of device excitations.

rounded by vacuum (Fig. 3.1), the input-output relations between the amplitude operators of the incoming light $a_i(\omega)$ and the outgoing light $b_i(\omega)$ at the surfaces of the slab have been derived as [71]

$$\mathbf{b}(\omega) = \mathbf{T}(\omega)\mathbf{a}(\omega) + \mathbf{A}(\omega)\mathbf{g}(\omega) \tag{3.5}$$

with the notation

$$\mathbf{a}(\omega) = \begin{pmatrix} a_1(\omega) \\ a_2(\omega) \end{pmatrix} \qquad \mathbf{b}(\omega) = \begin{pmatrix} b_1(\omega) \\ b_2(\omega) \end{pmatrix} \qquad \mathbf{g}(\omega) = \begin{pmatrix} g_1(\omega) \\ g_2(\omega) \end{pmatrix} \tag{3.6}$$

Transmission and reflection coefficients are scalar functions of ω which have been combined to the characteristic transmission matrix $\mathbf{T}(\omega)$. The operators of device excitations $g_i(\omega)$ have been normalized to be bosonic, with the associated prefactors being collected in the characteristic absorption matrix $\mathbf{A}(\omega)$. Additionally, the characteristic transmission and absorption matrices satisfy

$$\mathbf{T}(\omega)\mathbf{T}^+(\omega) + \mathbf{A}(\omega)\mathbf{A}^+(\omega) = \mathbf{I} \tag{3.7}$$

For single- and multilayer dielectric slabs these matrices have been computed explicitly in [71], the only ingredients being the scalar Green function of the associated scattering problem that depends on the dielectric permittivity of the material and the slab thickness.

3.1   General Green function approach

Let us start from the representation of the electric-field operator in terms of the classical Green function (2.50). We now assume that the space $\mathbb{R}^3$ can be subdivided into three

spatially separated regions I, II, and III, where region II represents an arbitrarily shaped dielectric body (Fig. 3.2). Regions I and III are assumed to contain vacuum.
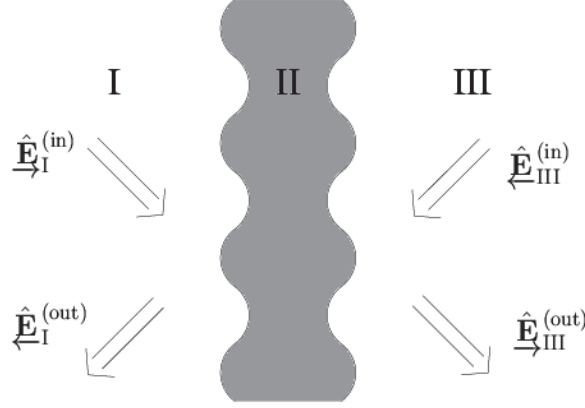

Figure 3.2: Dielectric object in region II surrounded by vacuum in regions I and III.

The electric-field operator in region I is given by

$$\underline{\mathbf{E}}^{(\mathrm{I})}(\mathbf{r}) = i\mu_0 \int_{\mathbb{R}^3} d^3s\, \boldsymbol{G}^{(\mathrm{I})}(\mathbf{r}, \mathbf{s})\, \underline{\mathbf{j}}_N(\mathbf{s}) \tag{3.8}$$

where the Green function can be split into four parts [89, 102, 103]:

$$
\begin{aligned}
\boldsymbol{G}^{(\mathrm{I})}(\mathbf{r}, \mathbf{s}) = \quad & \boldsymbol{G}^{(10)}(\mathbf{r}, \mathbf{s}) && (\mathbf{s} \in \mathrm{I}) \\
& + \boldsymbol{G}^{(11)}(\mathbf{r}, \mathbf{s}) && (\mathbf{s} \in \mathrm{I}) \\
& + \boldsymbol{G}^{(12)}(\mathbf{r}, \mathbf{s}) && (\mathbf{s} \in \mathrm{II}) \\
& + \boldsymbol{G}^{(13)}(\mathbf{r}, \mathbf{s}) && (\mathbf{s} \in \mathrm{III})
\end{aligned}
\tag{3.9}
$$

Here, $\boldsymbol{G}^{(10)}(\mathbf{r}, \mathbf{s})$ is the solution of the inhomogeneous Helmholtz equation for the case in which region I would extend over the whole space to infinity, and the $\boldsymbol{G}^{(1i)}(\mathbf{r}, \mathbf{s})$ are solutions of the homogeneous Helmholtz equation that ensure the correct boundary conditions at the surfaces of discontinuity. The electric-field operator in III is given accordingly by

$$\underline{\mathbf{E}}^{(\mathrm{III})}(\mathbf{r}) = i\mu_0 \int_{\mathbb{R}^3} d^3s\, \boldsymbol{G}^{(\mathrm{III})}(\mathbf{r}, \mathbf{s})\, \underline{\mathbf{j}}_N(\mathbf{s}) \tag{3.10}$$

with the Green function

$$
\begin{aligned}
\boldsymbol{G}^{(\mathrm{III})}(\mathbf{r}, \mathbf{s}) = \quad & \boldsymbol{G}^{(30)}(\mathbf{r}, \mathbf{s}) && (\mathbf{s} \in \mathrm{III}) \\
& + \boldsymbol{G}^{(31)}(\mathbf{r}, \mathbf{s}) && (\mathbf{s} \in \mathrm{III}) \\
& + \boldsymbol{G}^{(32)}(\mathbf{r}, \mathbf{s}) && (\mathbf{s} \in \mathrm{II}) \\
& + \boldsymbol{G}^{(33)}(\mathbf{r}, \mathbf{s}) && (\mathbf{s} \in \mathrm{I})
\end{aligned}
\tag{3.11}
$$

Consider now the field at the interface between regions I and II. The identification of the contributions of incoming and outgoing fields in Eq. (3.8) with the Green function (3.9) is unique. The contribution determined by the (free) Green function $G^{(10)}(\mathbf{r},\mathbf{s},\omega)$ represents the input field, since it describes free propagation from a point $\mathbf{s}$ in region I to the point $\mathbf{r}$ in region I (which we take to be at the surface). The term associated with $G^{(11)}(\mathbf{r},\mathbf{s},\omega)$ describes the part of the field which is reflected at the left surface, whereas the term associated with $G^{(13)}(\mathbf{r},\mathbf{s},\omega)$ is the transmitted field through the dielectric from the right (region III). The remaining term is the contribution of noise inside the dielectric. We now divide the field at the left surface (with the notation $\mathbf{r}_{\text{left}} \equiv \mathbf{r}^-$) into input and output fields as

$$\underline{\mathbf{E}}(\mathbf{r}^-) = \mathbf{E}_I^{(\text{in})}(\mathbf{r}^-) + \mathbf{E}_I^{(\text{out})}(\mathbf{r}^-) \tag{3.12}$$

with

$$\mathbf{E}_I^{(\text{in})}(\mathbf{r}^-) = i\omega\mu_0 \int_I d^3s\, G^{(10)}(\mathbf{r}^-,\mathbf{s},\omega)\underline{\mathbf{j}}_N(\mathbf{s},\omega) \tag{3.13}$$

$$\begin{aligned}
\mathbf{E}_I^{(\text{out})}(\mathbf{r}^-) &= i\omega\mu_0 \int_I d^3s\, G^{(11)}(\mathbf{r}^-,\mathbf{s},\omega)\underline{\mathbf{j}}_N(\mathbf{s},\omega) \\
&\quad + i\omega\mu_0 \int_{II} d^3s\, G^{(12)}(\mathbf{r}^-,\mathbf{s},\omega)\underline{\mathbf{j}}_N(\mathbf{s},\omega) \\
&\quad + i\omega\mu_0 \int_{III} d^3s\, G^{(13)}(\mathbf{r}^-,\mathbf{s},\omega)\underline{\mathbf{j}}_N(\mathbf{s},\omega)
\end{aligned} \tag{3.14}$$

Analogously, for the field at the interface between regions II and III ($\mathbf{r}_{\text{right}} \equiv \mathbf{r}^+$) we have

$$\underline{\mathbf{E}}(\mathbf{r}^+) = \mathbf{E}_{III}^{(\text{in})}(\mathbf{r}^+) + \mathbf{E}_{III}^{(\text{out})}(\mathbf{r}^+) \tag{3.15}$$

with

$$\mathbf{E}_{III}^{(\text{in})}(\mathbf{r}^+) = i\omega\mu_0 \int_{III} d^3s\, G^{(30)}(\mathbf{r}^+,\mathbf{s},\omega)\underline{\mathbf{j}}_N(\mathbf{s},\omega) \tag{3.16}$$

$$\begin{aligned}
\mathbf{E}_{III}^{(\text{out})}(\mathbf{r}^+) &= i\omega\mu_0 \int_{III} d^3s\, G^{(31)}(\mathbf{r}^+,\mathbf{s},\omega)\underline{\mathbf{j}}_N(\mathbf{s},\omega) \\
&\quad + i\omega\mu_0 \int_{II} d^3s\, G^{(32)}(\mathbf{r}^+,\mathbf{s},\omega)\underline{\mathbf{j}}_N(\mathbf{s},\omega) \\
&\quad + i\omega\mu_0 \int_I d^3s\, G^{(33)}(\mathbf{r}^+,\mathbf{s},\omega)\underline{\mathbf{j}}_N(\mathbf{s},\omega)
\end{aligned} \tag{3.17}$$

The arrows indicate the direction of propagation in Fig. 3.2. The first terms in Eqs. (3.14) and (3.17) are the reflected fields in the respective regions, the last terms are the transmitted

fields from the respective other sides of the dielectric body, whereas the second terms arise from noise contributions inside the device.

Input-output relations are derived by rewriting Eqs. (3.14) and (3.17) in terms of the input fields (3.13) and (3.16). In a linear theory, which we are considering here, this is always possible since the superposition principle holds. Thus, we write (formally)

$$\mathbf{E}_{\mathrm{I}}^{(\mathrm{out})}(\mathbf{r}) = \int d^2\mathbf{s}\; R_{\mathrm{I}}(\mathbf{r},\mathbf{s})\, \mathbf{E}_{\mathrm{I}}^{(\mathrm{in})}(\mathbf{s})$$
$$+ \int d^2\mathbf{s}^+\, T_{\mathrm{I,III}}(\mathbf{r},\mathbf{s}^+)\, \mathbf{E}_{\mathrm{III}}^{(\mathrm{in})}(\mathbf{s}^+)$$
$$+ \underline{\mathbf{G}}_{\mathrm{I}\,1}(\mathbf{r}) + \underline{\mathbf{G}}_{\mathrm{I}\,2}(\mathbf{r}) \tag{3.18}$$

$$\mathbf{E}_{\mathrm{III}}^{(\mathrm{out})}(\mathbf{r}^+) = \int d^2\mathbf{s}^+\, R_{\mathrm{III}}(\mathbf{r}^+,\mathbf{s}^+)\, \mathbf{E}_{\mathrm{I}}^{(\mathrm{in})}(\mathbf{s}^+)$$
$$+ \int d^2\mathbf{s}\; T_{\mathrm{III,I}}(\mathbf{r}^+,\mathbf{s})\, \mathbf{E}_{\mathrm{I}}^{(\mathrm{in})}(\mathbf{s})$$
$$+ \underline{\mathbf{G}}_{\mathrm{III}\,1}(\mathbf{r}^+) + \underline{\mathbf{G}}_{\mathrm{III}\,2}(\mathbf{r}^+) \tag{3.19}$$

with the reflection coefficients R and transmission coefficients T which are actually second-rank tensors. The integrations run over the respective surfaces of the body. For example, the field at a point $\mathbf{r}$ at the left surface is created by the input field from the left impinging at the surface at points $\mathbf{s}$ leading to the first term in Eq. (3.18), and by the input field from the right at points $\mathbf{s}^+$ producing the second term in Eq. (3.18). The operators $\underline{\mathbf{G}}_{(\mathrm{I,III})\,(1\,2)}$ are related to left and right propagating noise excitations inside the body.

Comparing Eqs. (3.14) and (3.18), we obtain, for example for the reflection coefficient $R_{\mathrm{I}}(\mathbf{r},\mathbf{s})$, the Fredholm integral equation of the first kind

$$\int d^2\mathbf{s}\; R_{\mathrm{I}}(\mathbf{r},\mathbf{s})\, G^{(10)}(\mathbf{s},\mathbf{s}) = G^{(11)}(\mathbf{r},\mathbf{s}) \tag{3.20}$$

which has to be inverted to find the reflection coefficient $R_{\mathrm{I}}(\mathbf{r},\mathbf{s})$. This can be done by using the relation

$$\int_{\mathrm{I}} d^3\mathbf{s}\, G^{(10)}(\mathbf{r},\mathbf{s})\, G^{(10)}(\mathbf{s},\mathbf{s})^{-1} = (\mathbf{r},\mathbf{s}) \tag{3.21}$$

Thus, we obtain the reflection coefficient by changing the order of integration as

$$R_{\mathrm{I}}(\mathbf{r},\mathbf{s}) = \int_{\mathrm{I}} d^3\mathbf{s}\, G^{(11)}(\mathbf{r},\mathbf{s})\, G^{(10)}(\mathbf{s},\mathbf{s})^{-1} \tag{3.22}$$

Similarly, the transmission coefficient reads

$$T_{\mathrm{I,III}}(\mathbf{r},\mathbf{s}^+) = \int_{\mathrm{III}} d^3\mathbf{s}\, G^{(13)}(\mathbf{r},\mathbf{s})\, G^{(10)}(\mathbf{s}^+,\mathbf{s})^{-1} \tag{3.23}$$

Re ection and transmission coe cients for region III are derived analogously as

$$\boldsymbol{R}_{\mathrm{III}}(\mathbf{r}^+ \ \mathbf{s}^+ \ ) = \ _{\mathrm{III}} d^3\mathbf{s} \, \boldsymbol{G}^{(33)}(\mathbf{r}^+ \ \mathbf{s} \ ) \ \boldsymbol{G}^{(30)}(\mathbf{s}^+ \ \mathbf{s} \ )^{ \ 1} \qquad (3.24)$$

$$\boldsymbol{T}_{\mathrm{III,I}}(\mathbf{r}^+ \ \mathbf{s} \ ) = \ _{\mathrm{I}} d^3\mathbf{s} \, \boldsymbol{G}^{(31)}(\mathbf{r}^+ \ \mathbf{s} \ ) \ \boldsymbol{G}^{(30)}(\mathbf{s} \ \mathbf{s} \ )^{ \ 1} \qquad (3.25)$$

Note that the re ection and transmission coe cients depend on the polarization. The remaining task is to invert the free Green functions $\boldsymbol{G}^{(10)}(\mathbf{s} \ \mathbf{s} \ )$ and $\boldsymbol{G}^{(30)}(\mathbf{s} \ \mathbf{s} \ )$. This can be done by expanding them in terms of a complete set of orthogonal solutions of the Helmholtz equation and using their respective orthogonality relations.

3.2 Planar multilayer structures

An important application of the general description developed above is a planar multilayer structure (Fig. 3.3). Beam splitters and other passive optical devices consist of layers with di erent dielectric properties, for example anti-re ection coatings. The input-output relations of light at such a device can be given e ectively by specifying the Green function and using the general theory described above. The Green function for a planar multilayer structure can be found in the literature [89, 102, 103, 104] and is presented in Appendix C.1. Since it is given in terms of TE and TM vector potentials the distinction between di erent polarizations is rather straightforward.
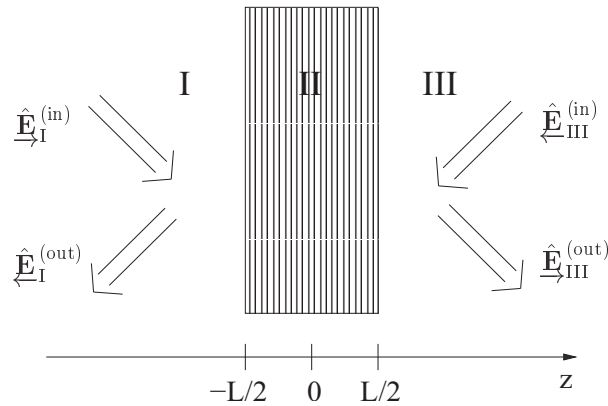

Figure 3.3: Dielectric slab located in region II ($L \ 2 \ z \ L \ 2$) surrounded by vacuum in regions I and III.

Let us suppose the plate of thickness L would consist of N dielectric layers. Thus, region II is subdivided into N subregions IIi, $i = 1 \ \ N$. The input elds are given by Eqs. (3.13)

and (3.16) where we identify the contributions from the plate with

$$\int_{\mathrm{II}} d^3s\, G^{(12)}(\mathbf{r}\quad \mathbf{s}\quad) \qquad \sum_{i=1}^{N} \int_{\mathrm{II}i} d^3s\, G^{(12i)}(\mathbf{r}\quad \mathbf{s}\quad) \tag{3.26}$$

$$\int_{\mathrm{II}} d^3s\, G^{(32)}(\mathbf{r}^+\ \mathbf{s}\quad) \qquad \sum_{i=1}^{N} \int_{\mathrm{II}i} d^3s\, G^{(32i)}(\mathbf{r}^+\ \mathbf{s}\quad) \tag{3.27}$$

This leads to the re ection and transmission coe cients according to Eqs. (3.22) (3.25), with the representation of the Green function as described in Appendix C.1. A special feature for planar structures is that di erent polarizations do not mix. That is, an incident eld with polarization solely described by TE vector wave functions (s-polarization) does not contain contribution from elds described by TM vector wave functions (p-polarization) and *vice versa*. The reason for this behaviour is that the Green function consists only of dyadic products of vector wave functions of one type. For roughened surfaces this need not be the case [99, 100, 101].

The identi cation of the noise terms in Eqs. (3.18) and (3.19) is not di cult remembering the Green function representation in Appendix C.1. We subdivide it into contributions of waves with positive and negative (real parts of the) wave vectors in z-direction h, hence

$$\underline{\mathbf{G}}_{\mathrm{I}\,1}(\mathbf{r}\quad) = \quad\frac{0}{4}\sum_{i=1}^{N}\int_{\mathrm{II}i}d^3s\quad d\quad \sum_{n=0}^{\infty}\frac{2\quad_{0n}}{h_{2i}}$$

$$A_M^{12i}\mathbf{M}_{\substack{e\\o}n}\,(\mathbf{r}\quad h_1)\quad \mathbf{M}_{\substack{e\\o}n}\,(\mathbf{s}\quad h_{2i}) + A_N^{12i}\mathbf{N}_{\substack{e\\o}n}\,(\mathbf{r}\quad h_1)\quad \mathbf{N}_{\substack{e\\o}n}\,(\mathbf{s}\quad h_{2i})\ \underline{\mathbf{j}}_{\mathrm{N}}(\mathbf{s}\quad)$$

$$\tag{3.28}$$

$$\underline{\mathbf{G}}_{\mathrm{I}\,2}(\mathbf{r}\quad) = \quad\frac{0}{4}\sum_{i=1}^{N}\int_{\mathrm{II}i}d^3s\quad d\quad \sum_{n=0}^{\infty}\frac{2\quad_{0n}}{h_{2i}}$$

$$B_M^{12i}\mathbf{M}_{\substack{e\\o}n}\,(\mathbf{r}\quad h_1)\quad \mathbf{M}_{\substack{e\\o}n}\,(\mathbf{s}\ h_{2i}) + B_N^{12i}\mathbf{N}_{\substack{e\\o}n}\,(\mathbf{r}\quad h_1)\quad \mathbf{N}_{\substack{e\\o}n}\,(\mathbf{s}\ h_{2i})\ \underline{\mathbf{j}}_{\mathrm{N}}(\mathbf{s}\quad)$$

$$\tag{3.29}$$

$$\underline{\mathbf{G}}_{\mathrm{III}\,1}(\mathbf{r}^+\quad) = \quad\frac{0}{4}\sum_{i=1}^{N}\int_{\mathrm{II}i}d^3s\quad d\quad \sum_{n=0}^{\infty}\frac{2\quad_{0n}}{h_{2i}}$$

$$C_M^{12i}\mathbf{M}_{\substack{e\\o}n}\,(\mathbf{r}^+\ h_1)\quad \mathbf{M}_{\substack{e\\o}n}\,(\mathbf{s}\quad h_{2i}) + C_N^{12i}\mathbf{N}_{\substack{e\\o}n}\,(\mathbf{r}^+\ h_1)\quad \mathbf{N}_{\substack{e\\o}n}\,(\mathbf{s}\quad h_{2i})\ \underline{\mathbf{j}}_{\mathrm{N}}(\mathbf{s}\quad)$$

$$\tag{3.30}$$

$$\underline{\mathbf{G}}_{\mathrm{III}\,2}(\mathbf{r}^+\ ) = \ \ \frac{0}{4} \sum_{i=1}^{N} \int_{\mathrm{II}i} d^3\mathbf{s} \int_0 d\ \sum_{n=0} \frac{2\ \ _{0n}}{h_{2i}}$$

$$D_M^{12i}\mathbf{M}_{o\ n}^{e}\ (\mathbf{r}^+\ h_1)\quad \mathbf{M}_{o\ n}^{e}\ (\mathbf{s}\ h_{2i}) + D_N^{12i}\mathbf{N}_{o\ n}^{e}\ (\mathbf{r}^+\ h_1)\quad \mathbf{N}_{o\ n}^{e}\ (\mathbf{s}\ h_{2i})\ \underline{\mathbf{j}}_{\mathrm{N}}(\mathbf{s}\ )$$

$$(3.31)$$

Equations (3.18) and (3.19), together with the re ection and transmission coe cients (3.22) (3.25) and the noise contributions from the multilayer (3.28) (3.31) constitute the three-dimensional input-output relations at planar multilayer dielectric devices. They allow for computing the outgoing eld from a dielectric object that is characterized by measurable quantities such as dielectric permittivity and geometrical dimensions.

Analogously, we can rewrite the frequency components of the electric- eld operators with amplitude operators $a_i(\ )$ and $b_i(\ )$ $(i = 1\ 2)$ of photonic modes with polarization ,

$$\mathbf{E}_{\mathrm{I}}^{(\mathrm{in})}(\mathbf{r}\ ) = i\ \sqrt{\frac{\hbar}{4\ _0 c\mathcal{A}}} e^{i\mathbf{k}_1\mathbf{r}}\ \mathbf{e}\ (\mathbf{k}_1)\,a_1(\ ) \tag{3.32}$$

$$\mathbf{E}_{\mathrm{I}}^{(\mathrm{out})}(\mathbf{r}\ ) = i\ \sqrt{\frac{\hbar}{4\ _0 c\mathcal{A}}} e^{\ i\mathbf{k}_1\mathbf{r}}\ \mathbf{e}\ (\mathbf{k}_1)\,b_1(\ ) \tag{3.33}$$

$$\mathbf{E}_{\mathrm{III}}^{(\mathrm{in})}(\mathbf{r}^+\ ) = i\ \sqrt{\frac{\hbar}{4\ _0 c\mathcal{A}}} e^{\ i\mathbf{k}_2\mathbf{r}^+}\ \mathbf{e}\ (\mathbf{k}_2)\,a_2(\ ) \tag{3.34}$$

$$\mathbf{E}_{\mathrm{III}}^{(\mathrm{out})}(\mathbf{r}^+\ ) = i\ \sqrt{\frac{\hbar}{4\ _0 c\mathcal{A}}} e^{i\mathbf{k}_2\mathbf{r}^+}\ \mathbf{e}\ (\mathbf{k}_2)\,b_2(\ ) \tag{3.35}$$

with $\mathbf{k}_i = \mathbf{k}_i = \ c$. The amplitude operators are superpositions of basic- eld operators with the corresponding Green function [cf. Eqs. (3.2) and (3.3)]. An analogous decomposition can be done for the operators of device excitations, $\underline{\mathbf{G}}_{(\mathrm{I},\mathrm{III})\ (1\ 2)}$. Then for each frequency , the amplitude operators $a_i(\ )$ and $b_i(\ )$ are related by an input-output relations of the type (3.5), with re ection and transmission coe cients that must be derived from the general coe cients (3.22) (3.25).

4 Quantum-state transformation by passive optical devices

The formalism of input-output coupling developed in Chapter 3 is best suited to study moments and (low-order) correlations of field operators [71, 72, 73, 105]. In many situations, knowledge about the whole quantum state in terms of its density matrix is desired. For example, measures of entanglement are usually functions of the density matrix and cannot be expressed in terms of moments in a simple way. The input-output relations enable us to construct a unitary operator [S2] that allows us to study the transformation of quantum states by passive optical elements such as beam splitters or optical fibres. Because all these devices have, for each polarization and each frequency, two input channels and two output channels, they are usually called four-ports in order to abstract from their specific physical realization. In Sec. 4.1 the general theory of quantum-state transformation by absorbing four-ports is developed and applied to the transformation of coherent states and Fock states in Sec. 4.2. The extension to amplifying devices is discussed in Sec. 4.3.

4.1 Transformation by absorbing four-port devices

Consider linearly polarized light of polarization λ impinging on a multilayer dielectric plate surrounded by vacuum (Sec. 3.2). For each frequency ω, the amplitude operators of incoming and outgoing light at the surface of the plate are related to each other by an input-output relation of the type (3.5). In what follows, we restrict our attention to one-dimensional light propagation along the z direction (as in Fig. 3.1). We look for an operator U that transforms the amplitude operators of the incoming fields $a_i(\omega)$ to those of the outgoing fields $b_i(\omega)$. That is, we seek a relation of the type

$$b_i(\omega) = U^\dagger a_i(\omega) U \tag{4.1}$$

Requiring the photonic operators to be bosonic, U must be unitary. Because of the coupling to the noisy environment, we will not be able to construct a unitary transformation that acts on the electromagnetic field operators alone. Recalling, that the original formulation of electromagnetic-field quantization in absorbing dielectrics was based on a Lagrangian formalism (Sec. 2.1) that introduces a unitary time evolution with the associated Hamiltonian (2.48), we have to look for a unitary operator acting in a larger Hilbert space corresponding to field operators *and* device operators.

4.1.1 Unitary matrix transformation

We supply the input-output relations (3.5), which are written for the electromagnetic-field operators, by equivalent relations for the device operators

$$\mathbf{h}(\omega) = \mathbf{F}(\omega)\mathbf{a}(\omega) + \mathbf{G}(\omega)\mathbf{g}(\omega) \tag{4.2}$$

with $\mathbf{h}(\omega)$ being the corresponding output device operators and $\mathbf{F}(\omega)$ and $\mathbf{G}(\omega)$ (2×2)-matrices which are to be determined. Introducing four-dimensional vectors

$$\boldsymbol{\alpha}(\omega) = \begin{pmatrix} \mathbf{a}(\omega) \\ \mathbf{g}(\omega) \end{pmatrix} = \begin{pmatrix} a_1(\omega) \\ a_2(\omega) \\ g_1(\omega) \\ g_2(\omega) \end{pmatrix} \qquad \boldsymbol{\beta}(\omega) = \begin{pmatrix} \mathbf{b}(\omega) \\ \mathbf{h}(\omega) \end{pmatrix} = \begin{pmatrix} b_1(\omega) \\ b_2(\omega) \\ h_1(\omega) \\ h_2(\omega) \end{pmatrix} \tag{4.3}$$

we define a unitary (4×4)-matrix $\Lambda(\omega)$ as [S2, S11]

$$\boldsymbol{\beta}(\omega) = \Lambda(\omega)\boldsymbol{\alpha}(\omega) \tag{4.4}$$

hence, $\Lambda(\omega)\Lambda^+(\omega) = \boldsymbol{I}$. We show in Appendix D that $\Lambda(\omega)$ can be written in terms of the characteristic transmission and absorption matrices $\mathbf{T}(\omega)$ and $\mathbf{A}(\omega)$, respectively, as

$$\Lambda(\omega) = \begin{pmatrix} \mathbf{T}(\omega) & \mathbf{A}(\omega) \\ -\mathbf{S}(\omega)\mathbf{C}^{-1}(\omega)\mathbf{T}(\omega) & \mathbf{C}(\omega)\mathbf{S}^{-1}(\omega)\mathbf{A}(\omega) \end{pmatrix} \tag{4.5}$$

with the positive commuting Hermitian matrices

$$\mathbf{C}(\omega) = \sqrt{\mathbf{T}(\omega)\mathbf{T}^+(\omega)} \qquad \mathbf{S}(\omega) = \sqrt{\mathbf{A}(\omega)\mathbf{A}^+(\omega)} \tag{4.6}$$

Analogously to Eq. (3.7), the relation $\mathbf{C}^2(\omega) + \mathbf{S}^2(\omega) = \mathbf{I}$ is valid. After inclusion of common phase factors into the input operators, $\Lambda(\omega)$ can be regarded, for each frequency ω, as an element of the group SU(4). To the unitary matrix transformation (4.4) corresponds a unitary operator transformation

$$\boldsymbol{\beta}(\omega) = U^\dagger \boldsymbol{\alpha}(\omega)U \tag{4.7}$$

where the operator U is given by

$$U = \exp\left[i \int_0^\infty d\omega\, \boldsymbol{\alpha}^\dagger(\omega)^T \, \Theta(\omega)\, \boldsymbol{\alpha}(\omega) \right] \tag{4.8}$$

The Hermitian (4×4)-matrix $\Theta(\omega)$ is related to $\Lambda(\omega)$ by $\exp[-i\Theta(\omega)] = \Lambda(\omega)$, noting that the exponential is uniquely defined for all linear groups [106]. By Eq. (4.8), the operator U realizing the unitary transformation between the input and output operators solely depends on material and geometrical properties of the device, that is, on experimentally accessible data.

Lossless devices

For narrow-bandwidth radiation in a frequency region Ω where absorption can be disregarded, $\mathbf{A}(\omega) \approx 0$, the ω integral in Eq. (4.8) can be restricted to a small interval Ω with

$$\mathbf{\Lambda}(\omega) = \begin{pmatrix} \mathbf{T}(\omega) & \mathbf{0} \\ \mathbf{0} & \mathbf{I} \end{pmatrix} \tag{4.9}$$

hence

$$\mathbf{\Phi}(\omega) = \begin{pmatrix} \mathbf{V}(\omega) & \mathbf{0} \\ \mathbf{0} & \mathbf{0} \end{pmatrix} \qquad \exp[-i\mathbf{V}(\omega)] = \mathbf{T}(\omega) \tag{4.10}$$

The unitary operator U from Eq. (4.8) now simplifies to

$$U = \exp\left[-i \int_\Omega d\omega\, \mathbf{a}^\dagger(\omega)^T \mathbf{V}(\omega)\mathbf{a}(\omega)\right] \tag{4.11}$$

As expected, it does not depend on the device operators since the electromagnetic field does not couple to the reservoir variables anymore. Hence, quantum-state transformation occurs in the subspace of electromagnetic field operators only. In that way we recover the well-known SU(2) group transformation for lossless devices [1, 2, 3, 4, 5, 6]. Since the characteristic absorption matrix was assumed to vanish, the matrix transformation (4.4) as well as the input-output relations (3.5) reduce to

$$\mathbf{b}(\omega) = \mathbf{T}(\omega)\mathbf{a}(\omega) \tag{4.12}$$

with $\mathbf{T}(\omega)\mathbf{T}^+(\omega) = \mathbf{I}$, hence the characteristic transmission matrix $\mathbf{T}(\omega)$ becomes, after inclusion of an overall phase factor into the input operators, an element of the group SU(2).

4.1.2 Decomposition into products of U(2) matrices

As it is well-known from linear algebra, every U(N)-matrix can be decomposed into products of matrices with exponential phases on the main diagonal and all other entries being zero, and (2×2)-matrices of the form

$$\begin{pmatrix} \cos\vartheta & \sin\vartheta \\ -\sin\vartheta & \cos\vartheta \end{pmatrix} \tag{4.13}$$

In view of the matrix transformation (4.4) it means to split up the matrix $\mathbf{\Lambda}(\omega)$ into products of several modular matrices $\mathbf{\Lambda}_i(\omega), i = 1 \ldots n$. An experimental proposal realizing a U(N) transformation with $n = N(N-1)/2$ lossless beam splitters as well as mirrors and phase

shifters has been made in [107]. To each of the $\Lambda_i(\ )$ corresponds, according to Eq. (4.8), a unitary operator U_i. The input-output relation (4.4) can then be written as

$$
\begin{aligned}
(\ ) &= \quad_n(\ ) \qquad _2(\ )\ _1(\ )\ (\ ) \\
&= U_1 U_2 \quad U_n\ (\ )U_n \quad U_2 U_1 \\
&= U\ (\ )U \tag{4.14}
\end{aligned}
$$

where $U_i = U[\ _i\ ]$. Since each of the matrices $\ _i(\ )$ is, by Eq. (4.13), a U(2) group element, it can be realized physically by a lossless beam splitter. The action of arbitrary U(N) [or SU(N)] transformations, like for example the SU(4) of an absorbing beam splitter, can therefore be visualized by a network of lossless beam splitters with properly adjusted reection and transmission coecients.

According to the results presented in Appendix E, the matrix $(\ )$ can be factorized into a product of eight U(2)-matrices, leading to the network of ideal four-ports depicted in Fig. 4.1. The U(2) beam splitters are labeled by their respective U(2)-matrices, with $\mathbf{Y}$
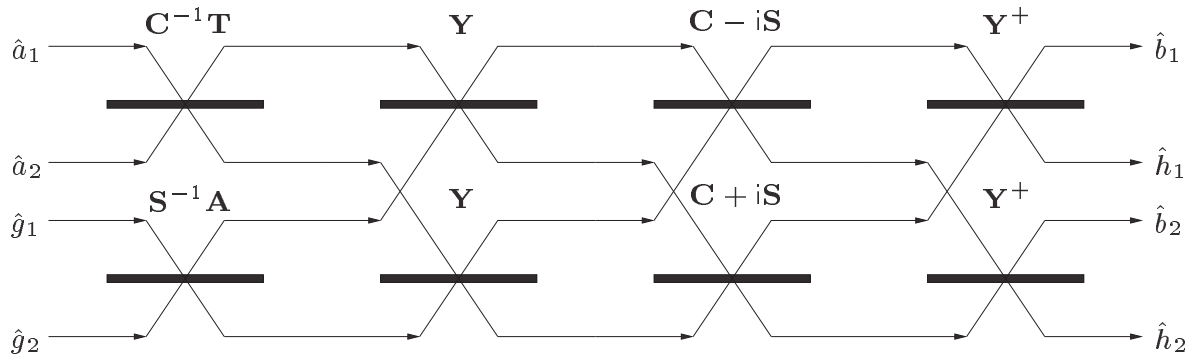
Figure 4.1: Lossless beam splitter network building up a single absorbing beam splitter.

being a symmetric beam splitter matrix of the form

$$
\mathbf{Y} = \frac{1}{\sqrt{2}} \begin{pmatrix} 1 & i \\ i & 1 \end{pmatrix} \tag{4.15}
$$

It should be stressed that this picture is to be understood as a visualization only, and has little to do with an experimental modelling. Any realistic beam splitter realizes all eight U(2) transformations at once.

In practical situations, it is often useful to describe the losses caused by optical elements (mirrors or optical bres) by introducing auxiliary beam splitters that take away some portion of the electromagnetic eld. The decomposition of $(\ )$ into products of U(2)-matrices and the construction of the corresponding network allows to determine the parameters of these auxiliary beam splitters.

4.1.3 Transformation of density operators

The effect of the device cannot only be described by transforming the photonic operators $\hat{a}_i(\omega)$, but equivalently by transforming the density operator $\hat{\rho}_{in}$. Suppose the operators of the incoming photon fields and the device operators transform according to Eq. (4.7). Then the input-state density operator $\hat{\rho}_{in}$ transforms into the output-state density operator $\hat{\rho}_{out}$ as

$$\hat{\rho}_{out} = \hat{U}\,\hat{\rho}_{in}\,\hat{U}^\dagger \tag{4.16}$$

Since the input-state density operator can be written as a functional of the input operators, $\hat{\rho}_{in} = \hat{\rho}_{in}[\hat{\alpha}(\omega), \hat{\alpha}^\dagger(\omega)]$, Eq. (4.16) reads

$$\hat{\rho}_{out} = \hat{\rho}_{in}\big[\hat{U}\hat{\alpha}(\omega)\hat{U}^\dagger, \hat{U}\hat{\alpha}^\dagger(\omega)\hat{U}^\dagger\big] \tag{4.17}$$

Observing, that

$$\hat{U}\hat{\alpha}(\omega)\hat{U}^\dagger = \Lambda^+(\omega)\hat{\alpha}(\omega) \tag{4.18}$$

$$\hat{U}\hat{\alpha}^\dagger(\omega)\hat{U}^\dagger = \Lambda^T(\omega)\hat{\alpha}^\dagger(\omega) \tag{4.19}$$

the output state is obtained by transforming the input state with the inverse matrix $\Lambda^{-1}(\omega) = \Lambda^+(\omega)$,

$$\hat{\rho}_{out} = \hat{\rho}_{in}\big[\Lambda^+(\omega)\hat{\alpha}(\omega), \Lambda^T(\omega)\hat{\alpha}^\dagger(\omega)\big] \tag{4.20}$$

Finally, tracing over the device variables leads to the quantum state of the outgoing field

$$\hat{\rho}_{out}^{(F)} = \mathrm{Tr}^{(D)}\,\hat{\rho}_{in}\big[\Lambda^+(\omega)\hat{\alpha}(\omega), \Lambda^T(\omega)\hat{\alpha}^\dagger(\omega)\big] \tag{4.21}$$

From the theory described in Sec. 3 and [71], the characteristic transmission and absorption matrices $\mathbf{T}(\omega)$ and $\mathbf{A}(\omega)$ of a dielectric four-port device are explicitly known for any frequency, given the (complex) refractive-index profile $n(\omega)$. Knowledge of $\mathbf{T}(\omega)$ and $\mathbf{A}(\omega)$ then enables us to construct the unitary operator $\hat{U}$ (4.8) and the matrix $\Lambda(\omega)$ (4.5). They enable us to derive closed formulas for the output quantum state given arbitrarily chosen input quantum states of electromagnetic field and dielectric device. Our approach to quantum-state transformation is similar to the usual open-systems approach to dissipation [108]. In both cases, unitary transformations in an extended Hilbert space are constructed, and then the device variables are traced out. Mathematically, the partial trace is an example of a (global) completely positive (CP) map [109]. However, master equations, to which an open-systems theory would lead, are not required here because the action of the environment is explicitly known from the underlying quantization scheme and the input-output relations.

The transformation formula (4.21) is in general difficult to handle. Practically, a description of the incoming and outgoing radiation in terms of discrete quasi-monochromatic modes

is desired. For this, the frequency axis is subdivided into small intervals with mid-frequencies ω_m and widths $\Delta\omega_m$, over which the transmission and absorption matrices $\mathbf{T}(\omega)$ and $\mathbf{A}(\omega)$ are approximately constants, and define the discrete photonic input and output operators

$$\alpha_m = \frac{1}{\sqrt{\Delta\omega_m}} \int_{\Delta\omega_m} d\omega\, \hat{\alpha}(\omega) \qquad \beta_m = \frac{1}{\sqrt{\Delta\omega_m}} \int_{\Delta\omega_m} d\omega\, \hat{\beta}(\omega) \tag{4.22}$$

To each pair of operators α_m, β_m, we assign an input-output relation (4.4) with a (4 × 4)-matrix $\Lambda_m \equiv \Lambda(\omega_m)$. With this, we define unitary operators U_m with

$$U_m = \exp\left(i\, \alpha_m^T \Lambda_m \beta_m\right) \tag{4.23}$$

such that the unitary operator U in Eq. (4.8) can be written as a product $U = \prod_m U_m$.

4.1.4 Phase-space functions

In quantum optics it is often useful to describe quantum states in terms of phase-space functions [110, 111, 112], prominent examples being the Glauber-Sudarshan P representation [113, 114], the Husimi Q function [115, 116] or the Wigner function W introduced by Wigner as early as 1932 [117].

Phase-space functions of that type are defined as expectation values of the operator delta function in a given operator order, for example normal, anti-normal, or symmetrical order,

$$P(\alpha) = \langle : \delta(\alpha - a) : \rangle \tag{4.24}$$
$$Q(\alpha) = \langle \# \delta(\alpha - a) \# \rangle \tag{4.25}$$
$$W(\alpha) = \langle \delta(\alpha - a) \rangle \tag{4.26}$$

where the symbols $::$ and $\#\#$ denote normal and anti-normal operator ordering, respectively. More generally, s-ordering of operators can be defined [110, 111, 118], special cases being $s = +1$ (normal ordering), $s = -1$ (anti-normal ordering), and $s = 0$ (symmetrical ordering). Given an operator $O(a\, a^\dagger)$ in s-order, the associated c-number function $O(\alpha; s)$ is introduced by replacing the operators a and $a^\dagger$ by the c numbers α and α^*, respectively. The expectation value of the operator $O(a\, a^\dagger)$ is obtained by integrating $O(\alpha; s)$ over the phase space with a weight function, the s-parametrized phase-space function, $P(\alpha; s)$,

$$\langle O(a\, a^\dagger) \rangle = \int d^2\alpha\, P(\alpha; s) O(\alpha; s) \tag{4.27}$$

The quantum-state transformation by absorbing devices does not change a previously fixed operator ordering. Hence, by Eq. (4.20), the s-parametrized phase-space function

$P_{\text{out}}[\quad(\quad);s]$ (since $\quad$ is continuous, it is actually a functional rather than an ordinary function) corresponding to the density operator $\quad_{\text{out}}$ is

$$P_{\text{out}}[\quad(\quad);s] = P_{\text{in}}[\quad^{+}(\quad)\quad(\quad);s] \tag{4.28}$$

Comparing this result with the unitary operator transformation (4.4), we see that phase-space functions are transformed with the corresponding inverse matrix $\quad^{1}(\quad) = \quad^{+}(\quad)$ [6]. The phase-space functional of the outgoing radiation is then derived by integration over the complex phase-space variables $g_1(\quad)$ and $g_2(\quad)$ of the dielectric device,

$$P^{(\text{F})}_{\text{out}}[\mathbf{a}(\quad);s] = \quad \mathcal{D}\mathbf{g}\, P_{\text{out}}[\quad(\quad);s] = \quad \mathcal{D}\mathbf{g}\, P_{\text{in}}[\quad^{+}(\quad)\quad(\quad);s] \tag{4.29}$$

For discrete quasi-monochromatic modes defined in frequency intervals with mid-frequencies $\quad_m$ and widths $\quad_m$, the functional integral (4.29) reduces to an ordinary multiple integral. Especially, for single-mode fields the phase-space function of the outgoing radiation field reads

$$P^{(\text{F})}_{\text{out}}(\mathbf{a};s) = \quad d^2\mathbf{g}\, P_{\text{out}}(\quad;s) = \quad d^2\mathbf{g}\, P_{\text{in}}(\quad^{+}\quad;s) \tag{4.30}$$

Changing the integration variables from $\mathbf{g}$ to $\mathbf{g}$, $\mathbf{g} = \mathbf{S}^{1}\quad\mathbf{C}\mathbf{a}\quad\mathbf{C}^{1}\mathbf{g}$, and correspondingly the integration measure $d^2\mathbf{g} = \quad\det(\mathbf{C}\mathbf{S})^{1\,2} d^2\mathbf{g}$, Eq. (4.30) can be rewritten as

$$P^{(\text{F})}_{\text{out}}(\mathbf{a};s) = \quad \frac{d^2\mathbf{g}}{\det\mathbf{T}\det\mathbf{A}^2}\, P_{\text{in}}\left(\quad \begin{matrix}\mathbf{T}^{1}\mathbf{g}\\ \mathbf{A}^{1}(\mathbf{a}\quad\mathbf{g})\end{matrix}\quad;s\right) \tag{4.31}$$

which is the most general relation for phase-space functions of quasi-monochromatic light at linear, absorbing four-port devices. Usually, the incoming radiation and the device are not entangled. Then the phase-space function P_{in} factorizes as $P_{\text{in}}(\quad;s) = P^{(\text{F})}_{\text{in}}(\mathbf{a};s)\, P^{(\text{D})}_{\text{in}}(\mathbf{g};s)$, and Eq. (4.31) reduces to

$$P^{(\text{F})}_{\text{out}}(\mathbf{a};s) = \quad \frac{d^2\mathbf{g}}{\det\mathbf{T}\det\mathbf{A}^2}\, P^{(\text{F})}_{\text{in}}(\mathbf{T}^{1}\mathbf{g}\;;s)\, P^{(\text{D})}_{\text{in}}[\mathbf{A}^{1}(\mathbf{a}\quad\mathbf{g});s] \tag{4.32}$$

The phase-space function of the outgoing radiation is thus a convolution of the phase-space functions of incoming radiation and the device.

4.2   Applications to coherent states and Fock states

In the following examples we restrict ourselves to (quasi-)monochromatic radiation with the single frequency component $\quad$.

4.2.1 Coherent states

Suppose the incoming eld and the device are prepared in a pure coherent state with complex amplitudes $\alpha = \binom{c}{d}$,

$$|\alpha\rangle_{in} = |\alpha\rangle = \exp[\alpha^T \hat{a}^\dagger - \alpha^\dagger \hat{a}]|0000\rangle \qquad (4.33)$$

Application of Eq. (4.20) shows that the quantum state after the transformation by a dielectric device is again a pure coherent state with

$$|\alpha\rangle_{out} = |\beta\rangle_{out}|\gamma\rangle_{out} = \qquad (4.34)$$

Tracing over the device variables leads to

$$\hat{\rho}^{(F)}_{out} = |\mathbf{T}c + \mathbf{A}d\rangle\langle \mathbf{T}c + \mathbf{A}d| \qquad (4.35)$$

which shows explicitly that the resulting coherent amplitude depends both on the characteristic transmission and absorption matrices and on the quantum state the device was initially prepared in. The Wigner function that corresponds to the density operator (4.35) is

$$W^{(F)}_{out}(\mathbf{a}) = \left(\frac{2}{\pi}\right)^2 \exp\left[-2|\mathbf{a} - \mathbf{T}c - \mathbf{A}d|^2\right] \qquad (4.36)$$

The result is easily generalized to superpositions of coherent states, for example

$$|\psi\rangle_{in} = 2[1 + e^{-2\alpha^2}]^{-1}(|\alpha\rangle + |-\alpha\rangle)|000\rangle \qquad (4.37)$$

The Wigner function of the Schrodinger cat in the rst mode is

$$W_{in}(a_1) = \left(\frac{2}{\pi}\right)\left[1 + e^{-2\alpha^2}\right]^{-1}\left[e^{-2|\alpha - a_1|^2} + e^{-2|\alpha + a_1|^2} + 2e^{-2|a_1|^2}\cos[4(\alpha a_1)]\right] \qquad (4.38)$$

The rst two terms in Eq. (4.38) correspond to the two peaks at $a_1 = \pm\alpha$, whereas the last term describes the interference pattern due to the coherent superposition. Applying the quantum-state transformation formula (4.20), the density matrix of the quantum state in the ith output channel is

$$\hat{\rho}^{(F)}_{out i} = 2[1 + \exp(-2\alpha^2)]^{-1}\left[|T_{i1}\alpha\rangle\langle T_{i1}\alpha| + |-T_{i1}\alpha\rangle\langle -T_{i1}\alpha|\right.$$
$$\left. + (|T_{i1}\alpha\rangle\langle -T_{i1}\alpha| + |-T_{i1}\alpha\rangle\langle T_{i1}\alpha|)\exp\left[-2\alpha^2(1 - T_{i1}^2)\right]\right] \qquad (4.39)$$

The two peaks at $\pm T_{i1}\alpha$ decay as T_{i1}^2, whereas the quantum interference terms [second line in Eq. (4.39)] decay exponentially fast as $T_{i1}^2 \exp[-2\alpha^2(1 - T_{i1}^2)]$. That is, the larger the mean number of photons $n = \alpha^2 \tanh \alpha^2$ becomes, the faster the decay of the

interferences will be. Let us turn to the transmitted Schrödinger cat ($i = 2$). By the current conservation formula (3.7) we have the relation $1 - |T_{21}|^2 = |T_{11}|^2 + |A_{11}|^2 + |A_{21}|^2$. That is, the exponential decay of the interference terms after transmission through a dielectric four-port device is both due to reflection $\exp[-2|\epsilon|^2 |T_{11}|^2]$ and due to absorption $\exp[-2|\epsilon|^2(|A_{11}|^2 + |A_{21}|^2)]$. In beam splitter replacement schemes that model absorption it is therefore not correct to specify the reflectivity T_{11} of the beam splitter because that would only account for the destruction of the interference pattern due to reflection. Instead, the value of $1 - |T_{21}|^2$ has to be used.
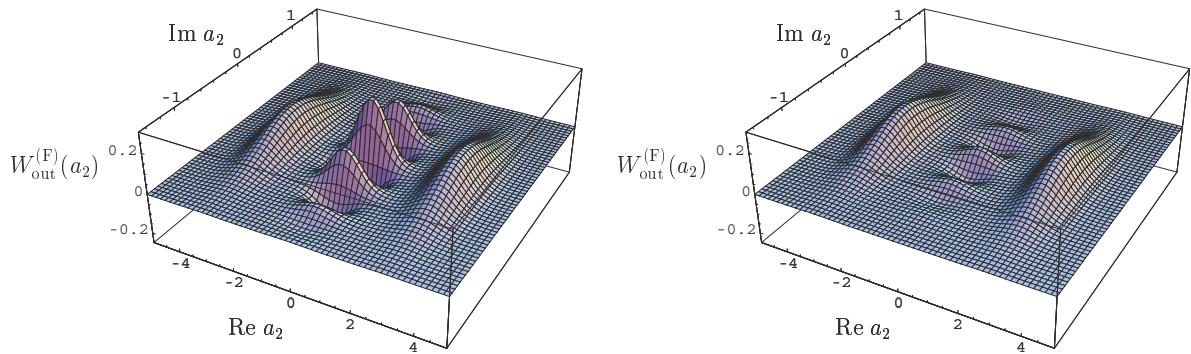

Figure 4.2: Wigner function of a Schrödinger cat with $\epsilon = 3$ before (left figure) and after transmission through a beam splitter with $T_{21} = 0.95$ (right figure).

From the density operator (4.39), we calculate the Wigner function of the transmitted state as

$$W_{\text{out}}^{(\text{F})}(a_2) = \frac{2}{\pi}\left[1 + e^{-2|\epsilon|^2}\right]^{-1}\left[e^{-2|T_{21}\epsilon - a_2|^2} + e^{-2|T_{21}\epsilon + a_2|^2}\right.$$

$$\left. + 2e^{-2|\epsilon|^2(1 - |T_{21}|^2) - 2|a_2|^2} \cos\left[4\,\Im(T_{21}\epsilon\, a_2^*)\right]\right] \tag{4.40}$$

The first two terms in Eq. (4.40) are the two peaks of the coherent states at $a_2 = \pm T_{21}\epsilon$, and the last term are the remains of the interference pattern. In order to illustrate this effect, in Fig. 4.2 we have plotted the Wigner function of the Schrödinger cat (4.38) and compared it with the Wigner function (4.40) of the Schrödinger cat after transmission through a beam splitter with $T_{21} = 0.95$. The interference pattern which are clearly visible in the left figure are due to the quantum coherence in the superposition (4.37). This pattern dies out very rapidly (right figure) leaving behind a statistical mixture of two coherent states that are shifted towards the origin. Neglecting reflection losses from the beam splitter, the exponential decay of the interference pattern is solely due to absorption, hence due to interaction with the noisy environment. This is the well-known phenomenon of decoherence [108].

4.2.2 Fock states

Suppose one of the modes of the impinging photon eld is prepared in a Fock state containing n quanta, all other modes are left in their respective ground states,

$$|\psi_{\text{in}}\rangle = |n\ 0\ 0\ 0\rangle \tag{4.41}$$

The Wigner function of the input state (4.41) reads (see for example [119])

$$W_{\text{in}}(\alpha) = (-1)^n \left(\frac{2}{\pi}\right)^4 L_n(4|\alpha_1|^2)\exp(-2|\alpha|^2) \tag{4.42}$$

[$L_n(x)$: Laguerre polynomial]. Integrating over the device variables and the unused output channel, we obtain the Wigner function of the mode in the ith output channel as

$$W_{\text{out}i}^{(\text{F})}(\alpha_i) = \sum_{k=0}^{n} \binom{n}{k} |T_{i1}|^{2k}(1-|T_{i1}|^2)^{n-k} W_k(\alpha_i) \tag{4.43}$$

$W_k(x)$ being the Wigner function of a k-photon Fock state. Since transformation by absorbing devices does not change a previously xed operator ordering, Eq. (4.43) holds for any phase-space function. Equivalently, we obtain for the density matrix of the ith output

$$\hat{\rho}_{\text{out}i}^{(\text{F})} = \sum_{k=0}^{n} \binom{n}{k} |T_{i1}|^{2k}(1-|T_{i1}|^2)^{n-k} |k\rangle\langle k| \tag{4.44}$$

that is, a binomial distribution of Fock states up to photon number n. This is a rather general result. Since the quantum-state transformation (4.21) is described by a matrix $\Lambda(\omega)$ which is an element of the compact group SU(4), the total photon number in all output channels (here the single channel i) must not exceed the total number of initially existing quanta.

Finally, we consider the situation where both incoming eld modes are excited with a single quantum. The input state then has the form

$$|\psi_{\text{in}}\rangle = |1\ 1\ 0\ 0\rangle \tag{4.45}$$

Tracing over the device and one output channel we arrive at

$$\hat{\rho}_{\text{out}i} = \left[1-|T_{i1}|^2(1-|T_{i2}|^2)-|T_{i2}|^2(1-|T_{i1}|^2)\right]|0\rangle\langle 0| \\ +(|T_{i1}|^2+|T_{i2}|^2-4|T_{i1}|^2|T_{i2}|^2)|1\rangle\langle 1| + 2|T_{i1}|^2|T_{i2}|^2|2\rangle\langle 2| \tag{4.46}$$

In the special case of a lossless 50%:50% beam splitter Eq. (4.46) reduces to $\hat{\rho}_{\text{out}i}=\frac{1}{2}(|0\rangle\langle 0|+|2\rangle\langle 2|)$ and the e ect of photon correlation is observed.

To illustrate the theory, we consider a single dielectric plate in its ground state and assume a single-resonance medium with the model permittivity

$$\varepsilon(\omega) = 1+\frac{\omega_{\text{s}}^2}{1-(\omega-\omega_0)^2-2i\omega\gamma-\omega_0^2} \tag{4.47}$$

From the formulas given in [71] one can calculate the reﬂection coeﬃcient $|T_{11}|^2$, the transmission coeﬃcient $|T_{21}|^2$, and the absorption coeﬃcient $(1 - |T_{11}|^2 - |T_{21}|^2)$, whose dependencies on frequency ω are shown in Fig. 4.3 [$\omega_s = 1.5$, $\gamma_0 = 0.01$, plate thickness $2c/\omega_0$]. With these data, the (radial-symmetric) Wigner function $W^{(F)}_{\text{out}}(a_1)$ of the quantum state in
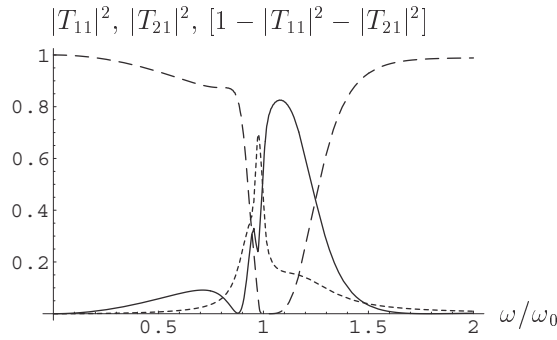
Figure 4.3: Reﬂection coeﬃcient (solid line), transmission coeﬃcient (dashed line), and absorption coeﬃcient (dotted line) of a dielectric plate as a function of frequency ω.

the ﬁrst output channel is shown in Fig. 4.4 for an input state $|1\,0\,0\,0\rangle$, and for an input state $|1\,1\,0\,0\rangle$, respectively. Suﬃciently far oﬀ resonance, $\omega_0 \ll 1$, the plate acts as a
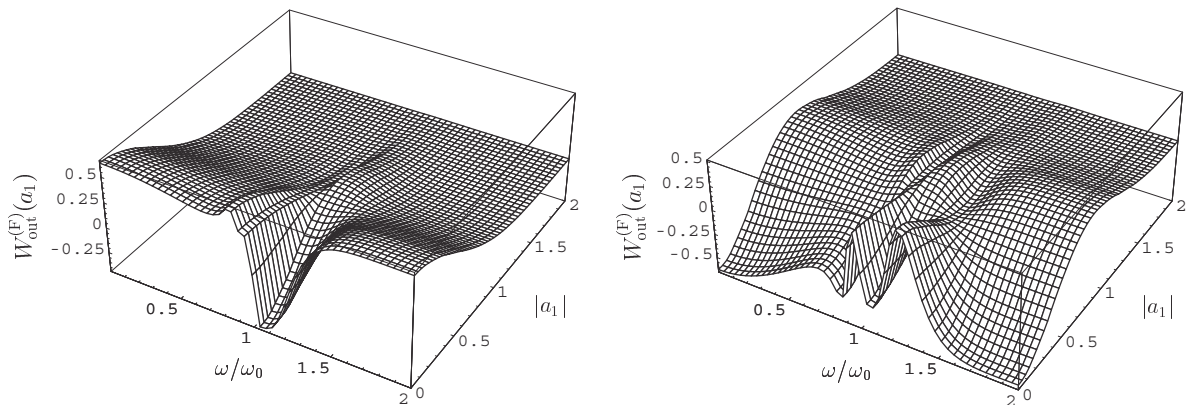
Figure 4.4: (Radial-symmetric) Wigner function of the quantum state in the ﬁrst output channel for an input state $|1\,0\,0\,0\rangle$ (left ﬁgure) and for $|1\,1\,0\,0\rangle$ (right ﬁgure).

lossless beam splitter with $|T_{11}|^2 \approx 0$ and $|T_{21}|^2 \approx 1$. That is, the reﬂected ﬁeld is found to be in a quantum state close to the vacuum (left ﬁgure in Fig. 4.4) or in a single-photon Fock state (right ﬁgure in Fig. 4.4). Just below the resonance frequency, $\omega \lesssim \omega_0$, where absorption is strongest, in both cases the resulting quantum state is almost the vacuum state.

4.3 Extension to amplifying devices

The situation is different if there exists a frequency region in which the dielectric four-port device under consideration is linearly amplifying. As we have seen in Sec. 2.3 we can quantize the electromagnetic field accordingly, replacing the annihilation operators $\mathbf{f}(\mathbf{r}, \omega)$ by their corresponding creation operators $\mathbf{f}^\dagger(\mathbf{r}, \omega)$ in the frequency region where amplification occurs. Introducing a parameter σ which takes values of $+1$ in case absorption is present and -1 whenever there is amplification, the input-output relations can be generalized to

$$\mathbf{b}(\omega) = \mathbf{T}(\omega)\mathbf{a}(\omega) + \mathbf{A}(\omega)\mathbf{d}(\omega) \tag{4.48}$$

with $\mathbf{d}(\omega) = \mathbf{g}(\omega)$ for $\sigma = +1$ and $\mathbf{d}(\omega) = \mathbf{g}^\dagger(\omega)$ for $\sigma = -1$. The characteristic matrices $\mathbf{T}(\omega)$ and $\mathbf{A}(\omega)$ satisfy the relation

$$\mathbf{T}(\omega)\mathbf{T}^+(\omega) + \sigma\,\mathbf{A}(\omega)\mathbf{A}^+(\omega) = \mathbf{I} \tag{4.49}$$

In case of amplification the matrix $\mathbf{A}(\omega)$ must be considered as a gain matrix instead of an absorption matrix. As in Sec. 4.1.3 we define four-dimensional operators

$$\alpha(\omega) = \begin{pmatrix} \mathbf{a}(\omega) \\ \mathbf{d}(\omega) \end{pmatrix} \qquad \beta(\omega) = \begin{pmatrix} \mathbf{b}(\omega) \\ \mathbf{f}(\omega) \end{pmatrix} \tag{4.50}$$

$[\mathbf{f}(\omega) = \mathbf{h}(\omega)$ for $\sigma = +1$ and $\mathbf{f}(\omega) = \mathbf{h}^\dagger(\omega)$ for $\sigma = -1]$ which are related to each other by

$$\beta(\omega) = \Lambda(\omega)\alpha(\omega) \tag{4.51}$$

with

$$\Lambda(\omega)\mathbf{J}\Lambda^+(\omega) = \mathbf{J} \qquad \mathbf{J} = \begin{pmatrix} \mathbf{I} & 0 \\ 0 & \sigma\mathbf{I} \end{pmatrix} \tag{4.52}$$

Depending on the value of σ, the (4×4)-matrix $\Lambda(\omega)$ is either an element of SU(4) ($\sigma = +1$) or, for $\sigma = -1$, an element of the non-compact group SU(2,2) (once an overall phase factor has been included in the input operators) which has important consequences. Introducing again the positive Hermitian matrices $\mathbf{C}(\omega)$ and $\mathbf{S}(\omega)$ as in Eq. (4.6) which now, by Eq. (4.49), obey the relation $\mathbf{C}^2(\omega) + \sigma\mathbf{S}^2(\omega) = \mathbf{I}$, the unitary matrix $\Lambda(\omega)$ can be represented as

$$\Lambda(\omega) = \begin{pmatrix} \mathbf{T}(\omega) & \mathbf{A}(\omega) \\ \mathbf{S}(\omega)\mathbf{C}^{-1}(\omega)\mathbf{T}(\omega) & \mathbf{C}(\omega)\mathbf{S}^{-1}(\omega)\mathbf{A}(\omega) \end{pmatrix} \tag{4.53}$$

It is generated by a matrix $\Omega(\omega)$ with

$$\Lambda(\omega) = e^{i\Omega(\omega)} \qquad \Omega^+(\omega) = \mathbf{J}\Omega(\omega)\mathbf{J} \tag{4.54}$$

from which the unitary operator transformation analogous to Eq. (4.8) can be constructed, where

$$U = \exp\left[i \int_0 d \quad ( )^T \boldsymbol{J} ( ) ( ) \right] \tag{4.55}$$

Following the line given in Sec. 4.1.3 the density operator of the outgoing fields is given by

$$\begin{array}{c}{{\mathrm{(F)}}}\\{{\mathrm{out}}}\end{array} = \mathrm{Tr}^{\mathrm{(D)}}\left[U \begin{array}{c}{{}}\\{{\mathrm{in}}}\end{array}U \right] = \mathrm{Tr}^{\mathrm{(D)}}\left[\begin{array}{c}{{}}\\{{\mathrm{in}}}\end{array} \boldsymbol{J} ^{+}( )\boldsymbol{J} ( ) \boldsymbol{J} ^{T}( )\boldsymbol{J} ( ) \right] \tag{4.56}$$

Since the SU(2,2) group transformation for amplifying devices mixes creation and annihilation operators, an arbitrarily given operator order is not preserved by the transformation. That means, that an equation for the transformation of phase-space functions of the type (4.28) cannot be valid for amplifying four-port devices. An exception is the Wigner function corresponding to symmetrical operator ordering before *and* after the transformation,

$$W_{\mathrm{out}}[( )] = W_{\mathrm{in}}[\boldsymbol{J} ( )\boldsymbol{J} ( )] \tag{4.57}$$

Formulas for Fock-state transformation based on Eq. (4.57) are presented in Appendix F. Here the non-compactness of the SU(2,2) group transformation shows up explicitly. In contrast to the case of absorbing four-port devices with compact group transformation where the total photon number in the output channels does not exceed the total photon number of the input states, in the case of amplification arbitrarily high photon-number states are excited.

Equations (4.53) and (4.56) represent the general form of a quantum-state transformation by absorbing *and* amplifying four-port devices. They enable us to compute the density operator of the outgoing radiation from the density operator of incoming radiation and dielectric device.

5 Entanglement degradation

Quantum information processing such as quantum cryptography [7] and quantum teleportation [120, 121] is based on entanglement or quantum correlations. As entanglement is a quantum-mechanical property, we expect it to be very fragile. The theory of quantum-state transformation allows us to discuss decoherence effects and entanglement degradation of bipartite quantum states where each part is transmitted through an optical device.

After shortly reviewing the basic notations and results on separability and entanglement measures in Sec. 5.1, we apply the theory of quantum-state transformation developed in Chapter 4 to the entanglement degradation of Bell-type states in Sec. 5.2 [S7, S8, S11]. In Sec. 5.3 the separability criterion for Gaussian quantum states, together with the input-output relations, is used to derive bounds on the length of optical fibres for which entanglement of a two-mode squeezed vacuum state transmitted through them can be retained [S7, S10, S11]. Moreover, a measure for entanglement degradation of Gaussian quantum states based on the distance to the set of separable Gaussian states is defined [S14] and applied to the transmission of a two-mode squeezed vacuum state through optical fibres.

5.1 Separability and entanglement

Given an arbitrary bipartite quantum state that shows correlations between its subsystems, one is interested whether these correlations are of classical or quantum nature. If quantum correlations exist, the state is called entangled. A rigorous definition of an entangled state is the following: A bipartite state is called separable if it can be written in the form

$$\rho = \sum_i p_i\, \rho_1^i \otimes \rho_2^i, \qquad 0 \le p_i \le 1, \qquad \sum_i p_i = 1 \tag{5.1}$$

where the indices $1,2$ label its subsystems. Otherwise it is said to be entangled. For example, the pure bipartite state

$$\psi = \frac{1}{\sqrt{2}}\left(|0_1 1_2\rangle - |1_1 0_2\rangle\right) \tag{5.2}$$

cannot be written in the form (5.1) and therefore represents an entangled state. In order to distinguish between separable and entangled states, a necessary criterion has been developed [74]. It says that if a state is separable, the partial transpose (P.T.) of its density operator in any given basis is again a well-defined density operator, hence positive semi-definite:

$$\rho \text{ separable} \Rightarrow \rho^{PT} \ge 0 \tag{5.3}$$

The converse is true only in certain low dimensions of the Hilbert spaces of the subsystems (2×2 and 2×3) [75]. Note that one can establish a whole class of such criteria by applying any positive partial operator, partial transposition being just one example.

Let us turn to quantification of entanglement, and consider first the pure state (5.2). The amount of correlations, both quantum and classical, in a quantum state ρ are measured by the correlation index (or mutual information) [122]

$$I_c = S_1 + S_2 - S_{12} \tag{5.4}$$

The quantity S_{12} is the von Neumann entropy of ρ, $S_{12} = -\mathrm{Tr}\,\rho \ln \rho$, and S_1 and S_2 are the von Neumann entropies of its subsystems, $S_{2(1)} = -\mathrm{Tr}\,\rho_{2(1)} \ln \rho_{2(1)}$, where $\rho_{2(1)} = \mathrm{Tr}_{1(2)}\,\rho$. By the Araki–Lieb inequality [123]

$$|S_1 - S_2| \le S \le S_1 + S_2 \tag{5.5}$$

the correlation index is positive semi-definite, $I_c \ge 0$. For the pure state (5.2) the von Neumann entropy S_{12} vanishes, but its mutual information does not. Since from the Araki–Lieb inequality (5.5) it follows that $S_1 = S_2$, we have

$$I_c = S_1 + S_2 = 2S_1 = 2S_2 \tag{5.6}$$

Hence, both subsystems are correlated, and a measurement on one subsystem yields information about the other. These correlations solely have their origin in the coherent superposition (5.2). Therefore, they are of quantum nature and can be associated with entanglement. Neglecting the numerical factor 2, the amount of entanglement in a pure state is defined as the von Neumann entropy of one subsystem, $E(\rho) = S_1 = S_2$.

The quantification of entanglement for mixed quantum states has been subject of long discussions in the literature [78, 124, 125, 126, 127, 128, 129], and so far no unique measure has been found. However, one has agreed that there are some properties an entanglement measure E for bipartite quantum states should fulfil [78, 79]:

1. $E(\rho) \ge 0$, and $E(\rho) = 0$ if and only if ρ is separable.

2. $E(\rho)$ does not change under local unitary transformations on the subsystems, i.e. $E(\rho) = E(U_1 \otimes U_2\, \rho\, U_1^\dagger \otimes U_2^\dagger)$.

3. $E(\rho)$ does not increase by applying local operations $A_i \otimes B_i$, and classical communication, i.e. $\sum_i \mathrm{Tr}\,\rho_i E(\rho_i / \mathrm{Tr}\,\rho_i) \le E(\rho)$, where $\rho_i = A_i \otimes B_i\, \rho\, A_i^\dagger \otimes B_i^\dagger$ and $\sum_i A_i^\dagger A_i B_i^\dagger B_i = \mathbb{I}$.

4. $E(\rho)$ reduces to the von Neumann entropy of one subsystem for pure states.

What does these requirements mean physically? The first is obvious saying that the entanglement measure should be zero for states that are not entangled. The second means that a local change of basis does not change the correlations between the subsystems. The third requirement means that it is impossible to increase entanglement by local measurements aided by classical communication. Local manipulations of this type are described mathematically by local completely positive (CP) maps. The last property is a normalization in order to establish the contact to the pure-state entanglement described above.

Apart from other measures it has been shown [78] that the distance to the set of separable states $\mathcal{S}$, measured by the relative entropy [109, 130, 131],

$$E(\varrho) = \min_{\mathcal{S}} S(\varrho) = \min_{\mathcal{S}} \mathrm{Tr}\left[\varrho(\ln\varrho - \ln\sigma)\right] \tag{5.7}$$

fulfils all the requirements. It is, however, difficult to compute. So far there is no analytical expression known for an arbitrary given quantum state. There are few exceptions. Some examples for binary systems, the dimensions of the corresponding Hilbert spaces being just 2, have been given [78]. An important property of the relative entropy of entanglement (5.7) is convexity, that is,

$$E[p\varrho_1 + (1-p)\varrho_2] \leq pE(\varrho_1) + (1-p)E(\varrho_2) \tag{5.8}$$

which follows directly from the joint convexity of the relative entropy [132],

$$S[p\varrho_1 + (1-p)\varrho_2 \| p\sigma_1 + (1-p)\sigma_2] \leq pS(\varrho_1\|\sigma_1) + (1-p)S(\varrho_1\|\sigma_1) \tag{5.9}$$

Note that the relative entropy of entanglement, the quantum analog of the classical Kullback Leibler distance frequently used in information theory [133], is not a proper metric.

5.2 Entanglement degradation of Bell-type states

We now apply the theory of quantum-state transformation developed in Chapter 4 and the preliminaries about entanglement measures in Sec. 5.1 to degradation of entanglement at dielectric four-port devices [S7, S8]. It is clear from Eqs. (4.17) (4.21) that the transmission of a bipartite state through separate dielectric devices (Fig. 5.1), each representing a unitary operation in an extended Hilbert space, corresponds to the action of local CP maps [109, 134]. The entanglement content of a bipartite quantum state interacting with two dielectric four-port devices is therefore decreased in general.

Since we are now dealing with two-mode (bipartite) quantum states where each mode is transmitted through its respective dielectric system, we have to consider the quantum-state
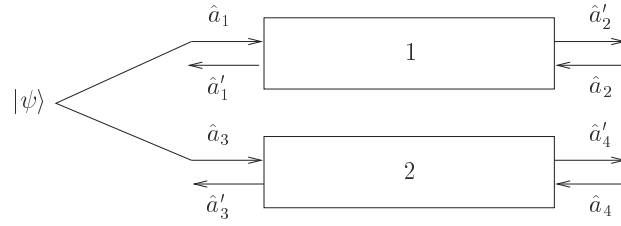
Figure 5.1: A two-mode input field prepared in the bipartite quantum state $|\psi\rangle$ is transmitted through two dielectric four-port devices.

transformation developed in Chapter 4 for both devices separately. That is, to each dielectric device acting on the amplitude operators of (quasi-) monochromatic modes $\hat{a}_i$ ($\hat{a}'_i$) ($i = 1, 3$) of the bipartite quantum state there exists a unitary (4×4)-matrix Λ_i (Λ'_i).

For example, let the incoming radiation field (described by the amplitude operators $\hat{a}_1$ and $\hat{a}_3$ in Fig. 5.1) be prepared in a Bell-type state

$$|\psi_n\rangle = \frac{1}{\sqrt{2}}\left(|0n\rangle \pm |n0\rangle\right) \tag{5.10}$$

Setting $n = 1$ in Eq. (5.10), the ordinary Bell-basis states are recovered. The state (5.10) is to be transmitted through dielectric four-port devices with transmission coefficients $T_i \equiv T_{21}^{(i)}$ and reflection coefficients $R_i \equiv T_{11}^{(i)}$. We assume that both devices are left in their respective ground states $|0_i^{(D)}\rangle$, and the input ports corresponding to the photonic operators $\hat{a}_2$ and $\hat{a}_4$ are unused. The total input state we are considering is therefore

$$|\Psi_{\text{in}}\rangle = |\psi_n\rangle|0_2 0_4\rangle|0_1^{(D)}\rangle|0_2^{(D)}\rangle \tag{5.11}$$

Then we apply the quantum-state transformation formula (4.21) to both sets of input operators $\{\hat{a}_1, \hat{a}_2\}$ and $\{\hat{a}_3, \hat{a}_4\}$ together with their corresponding device operators. After tracing out the degrees of freedom of the devices as well as the modes described by $\hat{a}_1$ and $\hat{a}_3$, we obtain the density operator of the transmitted modes $\hat{a}_2$ and $\hat{a}_4$, which we again denote by $\hat{\rho}_{\text{out}}^{(F)}$, as

$$\hat{\rho}_{\text{out}}^{(F)} = \frac{1}{2}\sum_{k=0}^{n-1}\binom{n}{k}\left[|T_1|^{2k}\left(1-|T_1|^2\right)^{n-k}|k0\rangle\langle k0| + |T_2|^{2k}\left(1-|T_2|^2\right)^{n-k}|0k\rangle\langle 0k|\right]$$
$$+\frac{1}{2}\left(|T_1|^{2n}+|T_2|^{2n}\right)|\chi_n\rangle\langle\chi_n| \tag{5.12}$$

with

$$|\chi_n\rangle = \left(|T_1|^{2n}+|T_2|^{2n}\right)^{-1/2}\left(T_1^n|n0\rangle \pm T_2^n|0n\rangle\right) \tag{5.13}$$

Note that, although only the transmission coefficients T_i appear explicitly in Eqs. (5.12) and (5.13), by the matrix relation (3.7) for the characteristic transmission and absorption

matrices, reflection and absorption coefficients are implicitly present in the terms $(1 - T_i^2)$ in Eq. (5.12).

The density operator (5.12) has been written as a convex sum of separable states and a single pure state ψ_n for which we can apply the convexity property of the relative entropy (5.8) to derive an upper bound on the entanglement content. By definition, a separable state contains no entanglement at all, and the entanglement content of a pure state is uniquely measured by the von Neumann entropy of one of its subsystems. Thus, by convexity,

$$E_{\text{out}}^{(\text{F})} \leq \frac{1}{2} \left[\left(T_1^{2n} + T_2^{2n} \right) \ln \left(T_1^{2n} + T_2^{2n} \right) - T_1^{2n} \ln T_1^{2n} - T_2^{2n} \ln T_2^{2n} \right] \tag{5.14}$$

In particular, when the transmission coefficients of the devices are equal, $T_1 = T_2 = T$, Eq. (5.14) reduces to

$$E_{\text{out}}^{(\text{F})} \leq T^{2n} \ln 2 \tag{5.15}$$

Assuming perfect input coupling, hence $R_1 = R_2 = 0$, each four-port device essentially reduces to a two-port. In that case the transmission coefficients can be assumed to follow the Lambert Beer law of extinction, $T = e^{-l/l_A}$, l_A being the absorption length. Then we have

$$E_{\text{out}}^{(\text{F})} \leq e^{-2nl/l_A} \ln 2 \tag{5.16}$$

showing that the characteristic length of entanglement degradation decreases at least as $1/(2n)$. That is, with increasing number of photons the quantum correlations of a bipartite quantum state decrease faster than exponentially. This behaviour is typical for quantum decoherence phenomena and not restricted to Fock states. It should be noted that for bipartite states in Hilbert spaces of dimension 2×2 the decomposition of the density operator into a sum of separable states ρ_{sep} and a single pure state

$$\rho = p \, \rho_{\text{sep}} + (1 - p) \rho \tag{5.17}$$

is always possible [129]. Moreover, there exists a unique maximal p in the convex sum (5.17) such that the inequality (5.8) reduces to an equality and thus defines an entanglement measure. That is, once $p_{\max}$ is found, $E(\rho) = (1 - p_{\max})S(\rho)$ [$S(\rho)$ being the reduced von Neumann entropy of the state ρ] is the amount of entanglement in ρ.

Another class of Bell-type states is defined by

$$\psi_n = \frac{1}{\sqrt{2}} \left(|00\rangle - |nn\rangle \right) \tag{5.18}$$

which can be obtained from a more general class of states

$$\psi_n^q = \frac{1}{\sqrt{1 + q^2}} \left(|00\rangle + q |nn\rangle \right) \tag{5.19}$$

with $q = 1$. For $n = 1$ and small values of q, $|\Psi_n^q\rangle$ is the first-order approximation of the two-mode squeezed vacuum state that is considered in Sec. 5.3. If the state $|\Psi_n^q\rangle$ is transmitted through dielectric devices, the quantum-state transformation (4.21) results in an output density operator

$$\hat{\varrho}_{out}^{(F)} =$$

$$\frac{q^2}{1+q^2} \sum_{k_1,k_2=0}^{n} \binom{n}{k_1}\binom{n}{k_2} T_1^{2k_1} T_2^{2k_2} (1-T_1^2)^{n-k_1}(1-T_2^2)^{n-k_2} |k_1 k_2\rangle\langle k_1 k_2|$$

$$+ T_1^{2n} T_2^{2n} |nn\rangle\langle nn| + \frac{1}{1+q^2}\Big(|00\rangle + qT_1T_2|nn\rangle\Big)\Big(\langle 00| + (qT_1T_2)^*\langle nn|\Big) \quad (5.20)$$

Again, using the convexity property (5.8), an upper bound of the entanglement can be derived as

$$E\big(\hat{\varrho}_{out}^{(F)}\big) \leq \frac{1}{1+\tilde{q}^2}\Big[(1+\tilde{q}^2)\ln(1+\tilde{q}^2) - \tilde{q}^2 \ln \tilde{q}^2\Big] \quad (5.21)$$

$[\tilde{q} = qT_1^n T_2^n]$. For small values of q we find by Taylor expansion that the entanglement decreases roughly as $\tilde{q}^2$.
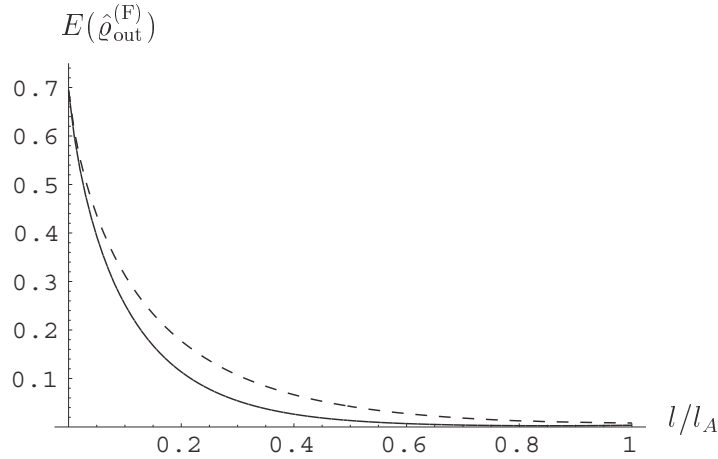

$E(\hat{\varrho}_{out}^{(F)})$

Figure 5.2: Entanglement degradation of Bell-type states $|\Phi_1\rangle$ (full curve) and $|\Psi_1\rangle$ (dashed curve) transmitted through equal optical fibres with absorption length l_A.

Comparison between entanglement degradation of the states $|\Phi_n\rangle$ and the states $|\Psi_n\rangle$ [obtained from Eq. (5.21) setting $q = 1$] shows that the $|\Psi_n\rangle$-states are more robust against decoherence than the $|\Phi_n\rangle$-states. This behaviour can be understood by observing that the probability of finding n photons in one output channel decreases as T_i^n for $|\Psi_n\rangle$ but decreases as $T_1T_2^n$ for $|\Phi_n\rangle$. In fact, since for states of the type $|n0\rangle$ or $|0n\rangle$ only one mode feels the effect of decoherence, in states of the type $|nn\rangle$ both modes interact simultaneously with the environment. Numerical calculations for $n = 1$ support this result [see Fig. (5.2)].

Note that the states ρ_1 and σ_1 are inseparable whenever $T > 0$ which is easily checked by applying the criterion (5.3).

5.3 Entanglement degradation of Gaussian states

In contrast to the finite-dimensional Fock states above, here we consider Gaussian states living in infinite-dimensional Hilbert spaces. A quantum state is called Gaussian if its density operator, or equivalently its characteristic function, can be written in exponential quadratic form. Since phase-space functions, such as the Wigner function, are defined by Fourier transforms of characteristic functions, they are also exponential quadratic forms. A typical example is the two-mode squeezed vacuum (TMSV) state

$$|\text{TMSV}\rangle = e^{\xi a_1 a_2 - \xi^* a_1^\dagger a_2^\dagger}|00\rangle = \sqrt{1 - |q|^2}\sum_{n=0}^{\infty}(-q)^n |nn\rangle \qquad (5.22)$$

[$\xi = \zeta e^{i\phi}$, $q = \tanh\zeta\, e^{i\phi}$]. The second equality follows from general exponential-operator disentangling theorems [135, 136]. The TMSV is of wide theoretical interest and has been used in the first experimental demonstration of teleportation of continuous quantum variables [137].

5.3.1 Application of the separability criterion

For Gaussian states there exists a necessary and sufficient criterion for separability [76, 77]. The Wigner function of a Gaussian quantum state with zero mean can be written in exponential quadratic form

$$W(\xi) = \frac{1}{4\pi^2\sqrt{\det \mathbf{V}}}\exp\left(-\frac{1}{2}\xi^T \mathbf{V}^{-1}\xi\right) \qquad (5.23)$$

with the symmetric (4×4) variance matrix $\mathbf{V}$ and the vector of the quadrature components $\xi = (x_1\ p_1\ x_2\ p_2)$. Writing the variance matrix in block matrix form

$$\mathbf{V} = \begin{pmatrix} \mathbf{X} & \mathbf{Z} \\ \mathbf{Z}^T & \mathbf{Y} \end{pmatrix} \qquad (5.24)$$

the bipartite Gaussian quantum state defined by this variance matrix is separable if and only if the following inequality holds [76, 77]:

$$\det \mathbf{X}\det \mathbf{Y} + \left(\frac{1}{4} - |\det \mathbf{Z}|\right)^2 - \text{Tr}\,\mathbf{XJZJYJZ}^T\mathbf{J} \geq \frac{1}{4}(\det \mathbf{X} + \det \mathbf{Y}) \qquad (5.25)$$

where **J** is the symplectic matrix

$$\mathbf{J} = \begin{pmatrix} 0 & 1 \\ 1 & 0 \end{pmatrix} \tag{5.26}$$

Any variance matrix can be brought to the generic form, diagonalizing the matrices **X**, **Y**, and **Z**,

$$\mathbf{V}_0 = \begin{pmatrix} x & 0 & z_1 & 0 \\ 0 & x & 0 & z_2 \\ z_1 & 0 & y & 0 \\ 0 & z_2 & 0 & y \end{pmatrix} \tag{5.27}$$

by local operations, i.e. by the action of an element of the symplectic group $\text{Sp}(2,\mathbb{R}) \otimes \text{Sp}(2,\mathbb{R})$, which leaves the separability criterion (5.25) unaltered [77]. Then, if the inequality

$$4(xy - z_1^2)(xy - z_2^2) - (y^2 + z^2 + 2\,z_1 z_2) \geq \frac{1}{4} \tag{5.28}$$

is satisﬁed, the Gaussian state is separable. Once the variance matrix is in the form (5.27), there are only four real parameters determining whether a Gaussian state is separable or entangled.

Now we apply the separability criterion for Gaussian quantum states [Eq. (5.25)] to the state (5.22). The variance matrix of the TMSV reads

$$\mathbf{V} = \begin{pmatrix} c/2 & 0 & s_1/2 & s_2/2 \\ 0 & c/2 & s_2/2 & s_1/2 \\ s_1/2 & s_2/2 & c/2 & 0 \\ s_2/2 & s_1/2 & 0 & c/2 \end{pmatrix} \tag{5.29}$$

$[c = \cosh 2\chi, \; s_1 = \sinh 2\chi \cos \vartheta, \; s_2 = \sinh 2\chi \sin \vartheta]$. We assume that the input ports corresponding to the photonic operators a_2 and a_4 in Fig. 5.1 are unused, and the devices, say optical ﬁbres, are prepared in thermal states with mean thermal photon numbers $n_{\text{th}i}$. Applying the input-output relations for absorbing and amplifying devices [Eq. (4.48) together with Eq. (4.49)], we transform the second-order moments in the variance matrix into $[s = \sinh 2\chi]$:

$$X_{11} = X_{22} = \frac{c}{2} |T_1|^2 + \frac{1}{2} |R_1|^2 + \left(n_{\text{th}1} + \frac{1}{2} \right) \left| 1 - |T_1|^2 - |R_1|^2 \right| \tag{5.30}$$

$$Y_{11} = Y_{22} = \frac{c}{2} |T_2|^2 + \frac{1}{2} |R_2|^2 + \left(n_{\text{th}2} + \frac{1}{2} \right) \left| 1 - |T_2|^2 - |R_2|^2 \right| \tag{5.31}$$

$$Z_{11} = -Z_{22} = \frac{s}{2} \text{Re}\left\{ T_1 T_2 \, e^{i\vartheta} \right\} \tag{5.32}$$

$$Z_{12} = Z_{21} = \frac{s}{2} \text{Im}\left\{ T_1 T_2 \, e^{i\vartheta} \right\} \tag{5.33}$$

where $\sigma = +(-)1$ for absorbing (amplifying) devices, and T_i and R_i are their respective transmission and reflection coefficients. Inserting the output variance matrix into the separability criterion (5.25), we obtain (for equal devices) the inequality [S10, S11]

$$n_{\text{th}} \leq \frac{(1-\sigma)(1-R^2)+T^2(\sigma-e^{-2\zeta})}{2\sigma(1-R^2-\sigma T^2)} \tag{5.34}$$

Thus, there exists for each squeezing parameter ζ and given material properties of the fibres a maximal excitation number of thermal photons in the fibres such that the initial TMSV state is still inseparable.

In case of absorbing fibres ($\sigma = +1$) without reflection losses ($R = 0$) we find, using the Lambert Beer law of extinction $T = e^{-l/l_A}$, that separability occurs when

$$l \geq l_{\text{S}} = \frac{l_A}{2}\ln\left[1+\frac{1}{2n_{\text{th}}}\left(1-e^{-2\zeta}\right)\right] \tag{5.35}$$

This result agrees with that in [76, 138] obtained by solving Fokker Planck equations for the Wigner function of the photon field. The equivalence is established by replacing the renormalized time τ in [138] by $1-T^2$.

In the case of a linearly amplifying fibre ($\sigma = -1$), in the limit of zero temperature ($n_{\text{th}} = 0$) and zero reflection ($R = 0$), the upper limit for the excess gain $g = T^2 - 1 \geq 0$ for which inseparability changes to separability is given by the squeezing parameter itself [S7],

$$g = q = \tanh\zeta \tag{5.36}$$

In particular, this means that entanglement cannot be created by amplifying the vacuum state. Moreover, there exists an overall upper bound on the gain for which inseparability can be retained. Since q is bounded from above by one, Eq. (5.36) says that for devices which more than double the intensity of an incoming signal, hence $g \geq 1$, or $T^2 \geq 2$, respectively, any TMSV state with arbitrarily high squeezing becomes separable.

It is worth noting that for a TMSV state the separability length l_{S} derived in Eq. (5.35) for absorbing fibres coincides with the transmission length after which all squeezing is lost [S14]. Indeed, applying the input-output relations (3.5), we obtain for the normally-ordered variance $:(\Delta F)^2:$ of the phase-sensitive quantity $F = F_1 e^{i\varphi_1}a_1 + F_2 e^{i\varphi_2}a_2 + \text{H.c.}$,

$$
\begin{aligned}
:(\Delta F)^2:_{\text{out}} &= 2F_1^2\left[T_1^2\sinh^2\zeta + n_{\text{th}1}\left(1-R_1^2-T_1^2\right)\right] \\
&\quad +2F_2^2\left[T_2^2\sinh^2\zeta + n_{\text{th}2}\left(1-R_2^2-T_2^2\right)\right] \\
&\quad -2F_1F_2T_1T_2\sinh 2\zeta\cos\left(\varphi_1+\varphi_2+\phi_{T_1}+\phi_{T_2}+\theta\right) \tag{5.37}
\end{aligned}
$$

$[T_i = T_i e^{i\phi_{T_i}}]$. For equal amplitudes $F_1 = F_2 = F$ and equal fibres the phase-dependent minimum is reached for $\cos(\varphi_1+\varphi_2+\phi_{T_1}+\phi_{T_2}+\theta) = 1$ such that

$$:(\Delta F)^2:_{\text{out}}^{\text{min}} = 4F^2\left[n_{\text{th}}\left(1-R^2-T^2\right)-\frac{1}{2}T^2\left(1-e^{-2\zeta}\right)\right] \tag{5.38}$$

from which we obtain that

$$:(\Delta F)^2:_{out}^{min} \geq 0 \Leftrightarrow n_{th} \geq \frac{T^2(1-e^{-2r})}{2(1-R^2-T^2)} \qquad (5.39)$$

The conditions for the TMSV losing all its squeezing [inequality (5.39)] and becoming separable [inequality (5.34)] after transmission through absorbing optical fibres ($\epsilon = +1$) are therefore equivalent.

5.3.2 Distance to the set of separable Gaussian states

If a TMSV state has been transmitted through absorbing optical fibres and one has checked for inseparability, the question arises how much entanglement is contained in the resulting mixed quantum state. The relative entropy (5.7) can be computed easily if we restrict ourselves to Gaussian states, both for the given density operator for which we want to compute its entanglement content, and for the separable states we compare the state with [S14]. If we denote the set of separable Gaussian states by $\mathcal{G}$, we define the distance to the set of separable Gaussian states as

$$E_G(\rho) = \min_{\mathcal{G}} \text{Tr}\left[\rho(\ln\rho - \ln\sigma)\right] \qquad (5.40)$$

With the definition of the entropy (5.4) and the representation of a Gaussian density operator

$$\sigma = \exp\left[-\frac{1}{2}\begin{pmatrix} a^+ \\ a \end{pmatrix} M \begin{pmatrix} a \\ a \end{pmatrix}\right] \qquad (5.41)$$

we can write Eq. (5.40) as

$$E_G(\rho) = -S(\rho) + \frac{1}{2}\min_{\mathcal{G}} \text{Tr}\left[M \begin{pmatrix} a^+ \\ a \end{pmatrix}\begin{pmatrix} a \\ a \end{pmatrix}\right] \qquad (5.42)$$

and furthermore, using the representation of the characteristic function corresponding to the density operator

$$\sigma(\xi) = \exp\left[-\frac{1}{2}\xi_+^+ V \xi_+\right] \qquad (5.43)$$

it follows that

$$E_G(\rho) = -S(\rho) + \frac{1}{2}\min_{\mathcal{G}} \text{Tr}\left[M V\right] \qquad (5.44)$$

The Gaussian separable states needed for the minimization are obtained by constructing their Wigner function according to the separability criterion for Gaussian quantum states [76, 77] described in Sec. 5.3.1. After transforming the variance matrix associated with

into the canonical form (5.27), minimization is done with respect to three real parameters. For example, given a triple of real numbers $(y\ z_1\ z_2)$ we can compute the fourth parameter x by using (5.28) as an equality.

The distance of a Gaussian state to the set of separable Gaussian states need not be an entanglement measure according to all requirements described in Sec. 5.1. In particular, it is not known whether the separable Gaussian states really provide the minimum distance over *all* quantum states. Although obviously being zero for separable states and being invariant under local unitary transformations, yet little is known about the behaviour of $E_G(\ )$ under local CP maps. Despite this, we believe that it is at least a good upper bound on the entanglement content of a Gaussian quantum state.

Let us apply this idea to the state (5.22). To this end, we need the variance matrix of the outgoing quantum state (5.30)   (5.33) and bring it to the generic form (5.27). This is done simply by neglecting the phases of the   bre transmission coe   cients and the squeezing parameter, hence setting $T_i\ \ \mathbb{R}$ and $= 0$, respectively. These operations are local and unitary, and do not change the entanglement content. Then, by Eq. (5.33), $Z_{12} = Z_{21} = 0$.
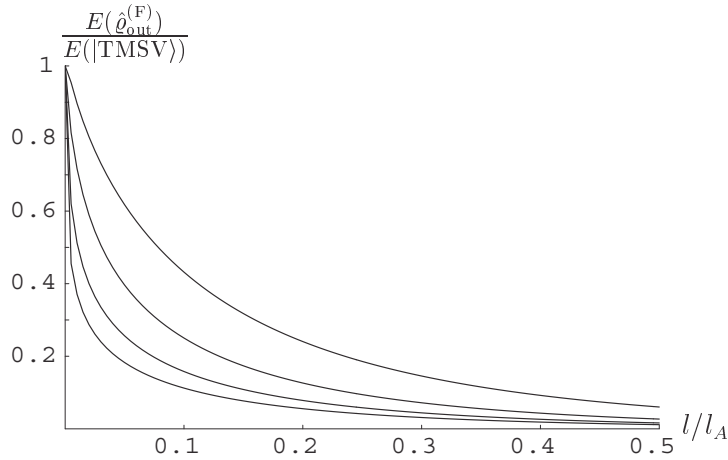

Figure 5.3: Entanglement content of a TMSV state transmitted through optical   bres with temperature zero as a function of the transmission length l measured in units of the absorption length l_A. The curves correspond to mean photon numbers in one mode of 1 (topmost curve), 10, 100, and 1000 (lowest curve) and are normalized with respect to the initial entanglement.

The result of the numerical calculation is depicted in Fig. 5.3. It shows the entanglement degradation of a TMSV transmitted through absorbing optical   bres with transmission coe   cients satisfying $T\ = e^{\ l\ l_A}$. Degradation becomes faster the higher the mean number of photons in the initial squeezed state was [the mean photon number in one mode is $n = \sinh^2\ $]. In the context of decoherence of n qubits during a quantum computation it has been noted that the decoherence time scales roughly exponentially with n [139]. This is

supported by our calculation, too.

Besides the degradation of entanglement with increasing bre length one can ask the question how much entanglement can be transmitted through bres of given length. This question becomes important when setting up real quantum communication systems based on continuous variables. It will eventually provide us with an answer about the ultimate limits for the performance of schemes that make use of quantum information. Figure 5.4 shows
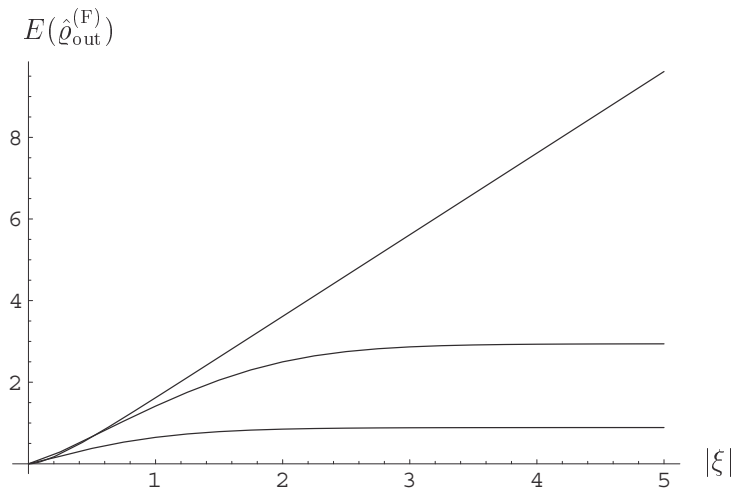

Figure 5.4: Entanglement content of a TMSV state transmitted through optical bres with temperature zero as a function of the initial squeezing strength   . The curves correspond to lossless bres (upper curve), and lossy bres with lengths $l = 0\ 01 l_A$ (middle curve) and $l = 0\ 1 l_A$ (lower curve), respectively.

the result of the numerical calculation. As expected, for lossless bres (upper curve) the transmitted entanglement is identical with the initial entanglement of the TMSV state

$$E(\text{ TMSV }) = \cosh^2 \quad \ln \cosh^2 \quad \sinh^2 \quad \ln \sinh^2 \quad {}^1 2 \qquad (5.45)$$

For absorbing bres, however, we observe a saturation e ect. Optical bres of given length are only capable for transmitting a nite amount of entanglement even in the limit of in nite initial squeezing. The reason for this remarkable saturation e ect can be understood in terms of the width of the Wigner function of two quadratures, say x_1 and x_2. For simplicity, we choose $= 0$. From the de nition of the Wigner function (5.23) in terms of the variance matrix **V** for the original TMSV state it follows that

$$W(x_1\ x_2) = \quad dp_1\ dp_2\, W(\ ) = \frac{1}{\ } \exp \quad \frac{1}{2}(x_1 + x_2)^2 e^2 \quad \frac{1}{2}(x_1 \quad x_2)^2 e^{\ 2}$$

$$(5.46)$$

For large squeezing, this Wigner function narrows and eventually turns into a sharply peaked line along the diagonal $x_1 + x_2 = 0$ with a width $e^{\ 2}$ that is zero for in nite squeezing.

Thus, x_1 and x_2 are perfectly correlated. After transmission through equal optical bres, choosing $R = n_{\text{th}} = 0$ and $T \in \mathbb{R}$ for simplicity, in the limit of in nite squeezing , the width of the Wigner function along the diagonal $x_1 + x_2 = 0$ becomes $1 - T^2$. That is, for $T < 1$ the width does not vanish and is determined by the bre material. In Fig. 5.5 we have plotted the Wigner function of two quadratures x_1 and x_2 of a TMSV state with $ = 3$. On the left, the initial Wigner function is shown, which broadens after transmission through the optical bres (right gure).

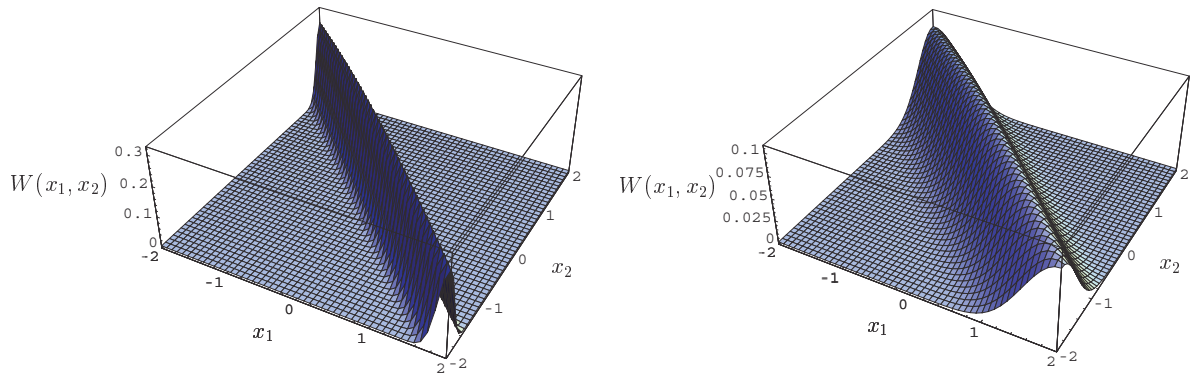Figure 5.5: Wigner function $W(x_1 \ x_2)$ for the quadratures x_1 and x_2 of a TMSV state with $ = 2$ and $ = 0$ before (left gure) and after transmission through equal optical bres with transmission coe cients $T_1 = T_2 = 0\,9$ (right gure).

We compare this saturation e ect with result of calculations of error probabilities in quantum dense coding. The scheme considered in [140] encodes a classical bit in a coherent displacement $D(\ )$ that is applied to one mode of a TMSV state. As in our case a symmetric noisy quantum channel is considered. In the limit of large mean photon numbers in the TMSV and the displacement their conclusion is that a quantum dense coding scheme is superior to a classical communication system only if the transmission coe cients do not drop below $T^2 = 0\,75$, that is, $l \ l_{\text{A}} \quad 0\,14$. From Fig. 5.4 we can estimate that the amount of transmitted entanglement is then just $E \quad 0\,7$. This is just the information that is needed to encode the classical bit. Smaller transmission coe cients only allow for transmitting less quantum information, and subsequently a classical coding scheme could perform better.

Concluding, the theory of quantum-state transformation developed in Chapter 4 is best suited to study entanglement degradation of bipartite quantum states in noisy environments. Based on the convexity of the relative entropy, upper bounds on the entanglement content after transmission through noisy quantum channels have been derived. For Gaussian states the distance to the set of separable Gaussian states (Sec. 5.3) provides a new tool to estimate their entanglement content. In particular, it has been shown that optical bres are only capable to transmit a nite amount of quantum information.

6 Quantum teleportation in noisy environments

The theory of quantum-state transformation developed in Sec. 4 and its consequences for entanglement transmission described in Sec. 5 is now applied to quantum teleportation which is a fundamental issue in quantum information processing. The idea behind it is to communicate an arbitrary quantum state between two spatially separated locations. In a classical setup one would measure all relevant parameters of the state and transmit them. In quantum mechanics, measuring the state would destroy it. However, quantum mechanics also provides us with a useful tool, the entangled states, for which communicating the information becomes possible without even fully knowing the state [120, 121]. The first experimental demonstration has been performed with polarization-entangled single-photon states [13, 14, 15]. Besides single-photon schemes teleportation of continuous quantum variables has been experimentally demonstrated [137], at least in principle. The basic idea of quantum teleportation is shortly summarized in Sec. 6.1. Entanglement degradation due to the interaction with a noisy environment spoils perfect teleportation which is discussed in Sec. 6.2. We then propose in Sec. 6.3 how to prepare an entangled state conditionally to increase the average teleportation fidelity [S15].

6.1 General scheme with Bell-basis states

Suppose a sender wants to communicate an arbitrary superposition of states $|0\rangle$ and $|1\rangle$,

$$|\psi\rangle_{\mathrm{in}} = a|0\rangle + b|1\rangle \qquad a, b \in \mathbb{C} \qquad |a|^2 + |b|^2 = 1 \tag{6.1}$$

which is also called a qubit, to a receiver without completely measuring it. The sender needs to create an additional entangled state (Fig. 6.1). The input state $|\psi\rangle_{\mathrm{in}}$ is mixed with one part of the entangled state. Then a single measurement in the Bell basis $|\Psi\rangle, |\Phi\rangle$ [see Eqs. (5.10) and (5.18) with $n = 1$ for their definition] is performed at the input state and the first part of the entangled state. Ideally, the second part of the entangled state now contains all information about the input state. The resulting two bits of classical information about the measurement outcome are communicated to the receiver who then performs, conditionally
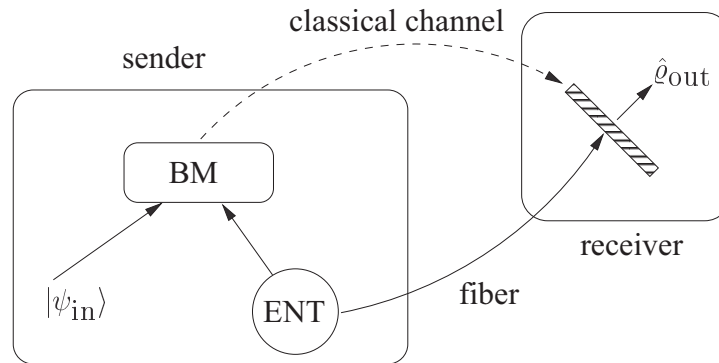
Figure 6.1: Standard scheme for quantum teleportation of qubits. One part of an entangled state (ENT) and the input state ψ_{in} are subject to a Bell measurement (BM). The result is classically communicated to the receiver who perform a conditional single-qubit rotation on the second part of the entangled state.

on the measurement result, one of the following rotations:

$$\mathbb{I} = |0\rangle\langle 0| + |1\rangle\langle 1| \qquad \text{measurement result } |\Phi^+\rangle \tag{6.2}$$

$$\sigma_x = |0\rangle\langle 1| + |1\rangle\langle 0| \qquad \text{measurement result } |\Psi^+\rangle \tag{6.3}$$

$$i\sigma_y = |0\rangle\langle 1| - |1\rangle\langle 0| \qquad \text{measurement result } |\Psi^-\rangle \tag{6.4}$$

$$\sigma_z = |1\rangle\langle 1| - |0\rangle\langle 0| \qquad \text{measurement result } |\Phi^-\rangle \tag{6.5}$$

where the σ_i are the usual spin-$\frac{1}{2}$ Pauli operators with the commutation rules

$$[\sigma_i, \sigma_j] = 2i\,\epsilon_{ijk}\,\sigma_k \qquad i,j,k = x,y,z \tag{6.6}$$

written in the qubit basis. The resulting state ϱ_{out} is then exactly the input state ψ_{in}.

A measure of successful teleportation is the fidelity which is defined as the overlap between the output state after the teleportation and the input state, $F = \langle\psi_{in}|\varrho_{out}|\psi_{in}\rangle^2$. Choosing a maximally entangled state as the entanglement resource, i.e. one of the four Bell states, the fidelity is always unity. For non-maximally entangled states it is less.

6.2 Absorbing optical fibres

From the general description of quantum teleportation one recognizes that maximal teleportation fidelity of unity is achieved only if the auxiliary quantum state is maximal entangled with respect to the Hilbert space of the input state. The situation described above is idealized in the sense that losses during the transmission of the entangled state from its source to sender and receiver have not been taken into account. The loss mechanism we are considering is such that it causes transitions from the state $|1\rangle$ to $|0\rangle$. Physical examples of

such transitions are spontaneous decay of two-level atoms (the qubit being encoded in the energy levels) or photon loss in optical bres (the qubit space is spanned by photon-number states). For de niteness we consider the latter case of optical qubits. As we have seen in Chapter 4, absorbing optical devices turn pure states into mixed states and, by the results in Chapter 5, decrease entanglement. Therefore, since the resulting auxiliary quantum state is not maximally entangled anymore, the teleportation delity is expected to decrease as well. We assume that the sender owns the source of the maximally entangled state and the communication line to the receiver can be modelled by an absorbing optical bre with transmission coe cient T_3. Then, before the Bell measurement, the tripartite object shared by sender and receiver is described by the mixed density operator

$$
\rho_{123} = \frac{1}{2}\left(1-|T_3|^2\right)\rho_{in}\langle in|\otimes|1_2\,0_3\rangle\langle 1_2\,0_3|
$$
$$
+\frac{1}{2}\rho_{in}\langle in|\otimes\left(|0_2\,0_3\rangle+T_3|1_2\,1_3\rangle\right)\left(\langle 0_2\,0_3|+T_3^*\langle 1_2\,1_3|\right) \tag{6.7}
$$

which follows immediately from the general quantum-state transformation formula (4.21) and the example (5.20). Performing the Bell measurement with the density matrix (6.7), the density matrix on the receiver s side is then one of the following:

measurement outcome	density operator at the receiver
+	$(1-|T_3|^2)\,|b|^2\,|0_3\rangle\langle 0_3| + [a|0_3\rangle + bT_3|1_3\rangle][a^*\langle 0_3| + b^*T_3^*\langle 1_3|]$
+	$(1-|T_3|^2)\,|a|^2\,|0_3\rangle\langle 0_3| + [aT_3|1_3\rangle + b|0_3\rangle][a^*T_3^*\langle 1_3| + b^*\langle 0_3|]$
	$(1-|T_3|^2)\,|a|^2\,|0_3\rangle\langle 0_3| + [aT_3|1_3\rangle - b|0_3\rangle][a^*T_3^*\langle 1_3| - b^*\langle 0_3|]$
	$(1-|T_3|^2)\,|b|^2\,|0_3\rangle\langle 0_3| + [a|0_3\rangle - bT_3|1_3\rangle][a^*\langle 0_3| - b^*T_3^*\langle 1_3|]$

The outcomes are equally likely with probabilities $p_i = 1\,4$, the index i labelling the four possible results. According to the standard teleportation scheme, the receiver now has to perform one of the single-qubit rotations $\mathbb{I},\ \sigma_x,\ i\sigma_y,\ \sigma_z$, leading to an output density operator $\rho_{out\,i}$. For a single teleportation event i, a delity

$$
F_i = \langle in|\rho_{out\,i}|in\rangle \tag{6.8}
$$

can be de ned. The F_i di er for di erent measurement outcomes in general. Therefore, we use a delity that is averaged over all possible results,

$$
F = \sum_i p_i F_i = \sum_i p_i \langle in|\rho_{out\,i}|in\rangle
$$
$$
= \frac{1}{2}\left[|a|^4 + \left(1-|a|^2\right)^2\left(1+|T_3|^2\right) + 2|a|^2\left(1-|a|^2\right)\left(|T_3|^2 + 2\mathrm{Re}\,T_3\right)\right] \tag{6.9}
$$

where we have used that $|a|^2 + |b|^2 = 1$. In contrast to perfect teleportation, the delity also depends on the input state. A state-independent average delity may thus be de ned

by integrating Eq. (6.9) over $|a|^2$ giving

$$F = \int_0^1 d|a|^2\, F = \frac{1}{2}\left(1 + \frac{1}{3}|T_3|^2 + 2\mathrm{Re}T_3\right) \tag{6.10}$$

The maximal (average) fidelity of one is achieved only if $T_3 = 1$, that is, when the communication line to the receiver is lossless. For all realistic systems that show absorption, the average teleportation fidelity (6.10) lies below 1. Moreover, the fidelity becomes phase-dependent, indicating that the standard teleportation scheme is not optimal for noisy channels, a fact that has also been noted in continuous-variable schemes [141, 142]. Optimization can be done by placing a phase shifter (a local unitary operation) on the receivers side that reverts the phase introduced by the fibre so that we can assume from now on that $T_3 \in \mathbb{R}$.

6.3 Conditional preparation of the entangled state

The average teleportation fidelity can be enhanced by modifying the standard teleportation scheme. We present two possible modifications based on conditional measurements, using a tripartite entangled state as the entanglement resource, and filtering.

Since Bell states, being maximally entangled bipartite states in the 2×2-dimensional qubit Hilbert space, are optimal only for ideal transmission ($T_3 = 1$) the question arises which states should be used for noisy communication instead. In the following we concentrate on the Greenberger–Horne–Zeilinger (GHZ) state [143]

$$|\mathrm{GHZ}\rangle = \frac{1}{\sqrt{2}}\left(|0_2\,0_3\,0_4\rangle + |1_2\,1_3\,1_4\rangle\right) \tag{6.11}$$

We assume that modes 2 and 3 are used for the teleportation process, whereas mode 4 is subject to a projection measurement. The situation is depicted in Fig. 6.2. The entangled state after transmission through the absorbing device is described by the density operator

$$\begin{aligned}
\rho_{234} &= \frac{1}{2}\left(1 - |T_3|^2\right)|1_2\,0_3\,1_4\rangle\langle 1_2\,0_3\,1_4| \\
&\quad + \frac{1}{2}\left(|0_2\,0_3\,0_4\rangle + T_3|1_2\,1_3\,1_4\rangle\right)\left(\langle 0_2\,0_3\,0_4| + T_3\langle 1_2\,1_3\,1_4|\right)
\end{aligned} \tag{6.12}$$

We now apply the projection operator

$$P_4 = \left(|0_4\rangle + \sqrt{1-\epsilon^2}\,|1_4\rangle\right)\left(\langle 0_4| + \sqrt{1-\epsilon^2}\,\langle 1_4|\right) \tag{6.13}$$

to the density operator (6.12) and obtain with a success probability $1/2$ the state

$$\begin{aligned}
\rho_{23} &= \left(1 - |T_3|^2\right)\left(1 - \epsilon^2\right)|1_2\,0_3\rangle\langle 1_2\,0_3| \\
&\quad + \left(|0_2\,0_3\rangle + T_3\sqrt{1-\epsilon^2}\,|1_2\,1_3\rangle\right)\left(\langle 0_2\,0_3| + T_3\sqrt{1-\epsilon^2}\,\langle 1_2\,1_3|\right)
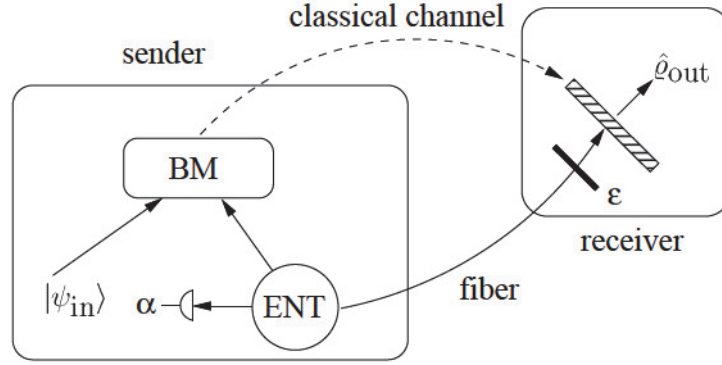\end{aligned} \tag{6.14}$$

Figure 6.2: Modified teleportation scheme using GHZ states and filtering.

The projection parameter α controls the weight of the separable contribution in (6.14). On the other hand, it also changes the entanglement of the residual pure state in a competitive way. We have checked numerically that the density operator (6.14), for appropriately chosen α, indeed contains more entanglement than the state (6.12) [S15]. The measurement probabilities p_i of the Bell measurement are now different,

$$p_{|\Phi^\pm\rangle} = \frac{1}{2}\left[\left(1 - |\alpha|^2\right)\left(1 - |a|^2\right) + |\alpha|^2|a|^2\right], \tag{6.15}$$

$$p_{|\Psi^\pm\rangle} = \frac{1}{2}\left[\left(1 - |\alpha|^2\right)|a|^2 + |\alpha|^2\left(1 - |a|^2\right)\right]. \tag{6.16}$$

This leads to an average fidelity

$$\bar{\bar{F}} = \frac{1}{3}\left\{\left(1 - |T_3|^2\right)\left(1 - |\alpha|^2\right) + 2\sqrt{1 - |\alpha|^2}\mathrm{Re}(\alpha T_3) + 2\left[|\alpha|^2 + |T_3|^2\left(1 - |\alpha|^2\right)\right]\right\}. \tag{6.17}$$

Depending on T_3, the average fidelity (6.17) can be optimized with respect to the projection parameter α. The maximum is obtained for (recall that we can assume $T_3 \in \mathbb{R}$)

$$|\alpha| = \frac{1}{\sqrt{1 + T_3^2}} \quad \Rightarrow \quad \bar{\bar{F}} = \frac{2 + 3T_3^2 + T_3^4}{3(1 + T_3^2)}. \tag{6.18}$$

That means again, that only for lossless devices with $T_3 = 1$ perfect teleportation is achieved. For all realistic devices we have $\bar{\bar{F}} < 1$ but the value of (6.18) is larger than (6.10).

Further improvement can be achieved if we use a filter [144] on the receiver's side. In the following, we consider the operation $|0_3\rangle \rightarrow \epsilon|0_3\rangle$, $|1_3\rangle \rightarrow |1_3\rangle$ with some $\epsilon < 1$, which is obviously non-unitary. In the case of photon-number states such a filter can be constructed by quantum-state engineering [145, 146]. The average teleportation fidelity is now ($T_3 \in \mathbb{R}$)

$$\bar{\bar{F}} = \frac{1}{3N}\left[\left(1 - T_3^2\right)\epsilon^2 + 2T_3\epsilon + 2\left(T_3^2 + \epsilon^2\right)\right] \tag{6.19}$$

with $N = 2\epsilon^2 + T_3^2\left(1 - \epsilon^2\right)$. The maximum is obtained for $\epsilon = T_3/(2 - T_3^2)$ at

$$\bar{\bar{F}} = \frac{2}{3} + \frac{1}{6 - 3T_3^2}. \tag{6.20}$$

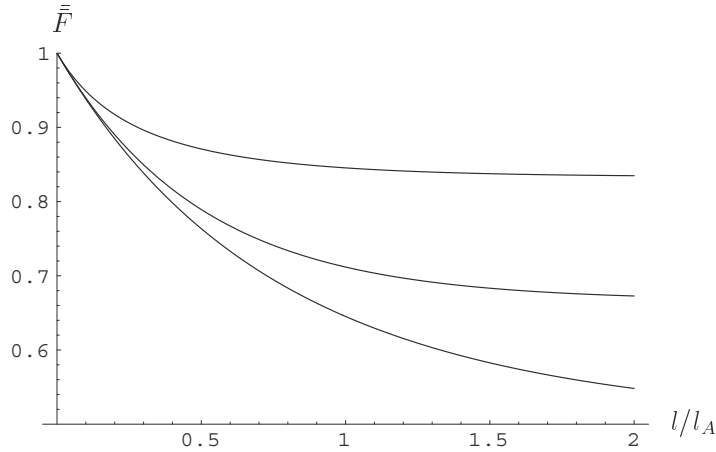Again for absorbing devices the average teleportation delity is always less than unity.

Figure 6.3: Average teleportation delity using Bell states (lowest curve), using the GHZ state (middle curve), and using a lter (topmost curve).

Figure 6.3 depicts the dependence of the average teleportation delities on the transmission length using $T_3 = e^{-l/l_A}$. The lowest curve corresponds to the standard teleportation scheme (Fig. 6.1) with the delity (6.10). The middle curve depicts the result of the scheme using GHZ states, Eq. (6.18). Even higher lies result obtained by ltering, Eq. (6.20). Combining both methods, using the GHZ state and subsequent ltering, may then su ce to achieve an average delity close to unity. The drawback is the success probability which is expected to decrease very fast with stronger ltering.

The increased delity in the modi ed schemes are due to the conditional process that selects a highly entangled state from the ensemble $_{23}$ shared between sender and receiver. By that, indeed more quantum information is transmitted compared to the standard scheme. On the other hand, the increased classical teleportation delity, which is obtained for $T_3 \to 0$, can be understood as follows. In the standard scheme the outcomes of the Bell measurement were all equally likely with probabilities $p_i = 1 \, 4$. The modi cations change these probabilities such that it becomes more likely that is measured. In turn, the receiver would more often perform $_x$ and $i \,_y$ that ip 0_3 and 1_3 .

To conclude, we have shown that the average teleportation delity, which drops below unity when using noisy communication channels, can be increased by choosing GHZ states as the entanglement source and ltering. These modi cations conditionally, with a certain probability, select higher entangled states from the ensemble shared between sender and receiver and therefore, on average, increase the delity.

7 Quantization of the electromagnetic field in the presence of atoms

So far we were interested in the properties of the electromagnetic field and the statistical implications on the quantum state of light coupled to a dielectric material with the emphasis on the electromagnetic field only. In this chapter a general theory of the interaction of the quantized electromagnetic field with additional atomic sources in the presence of dielectric bodies is developed [S9, S11]. The theory, which is a natural extension of the standard concept of mode decomposition, gives a unified approach to the atom-field interaction without restricting to a particular frequency range. In Sec. 7.1 minimal and multipolar coupling are discussed in the framework of source-quantity representation, and electric-dipole and rotating-wave approximations are described in Sec. 7.2.

7.1 Minimal coupling (vs. multipolar coupling)

There are essentially two different ways to describe the coupling of atoms to the electromagnetic field. In the minimal coupling scheme the atoms are described by point-like charged particles coupled to the potentials of the Maxwell field. On the other hand, the multipolar coupling scheme introduces atomic polarizations and magnetizations whose interactions with the electromagnetic field is described in terms of the field strengths. Both schemes are equivalent since they are related to each other by a unitary transformation.

7.1.1 Minimal coupling

Given an ensemble of point-like particles, where the αth particle having mass m_α and charge q_α is described by its position operator $\mathbf{r}_\alpha$ and canonical momentum operator $\mathbf{p}_\alpha$, their charge density

$$\rho_A(\mathbf{r}) = \sum_\alpha q_\alpha \delta(\mathbf{r} - \mathbf{r}_\alpha) \tag{7.1}$$

leads to a scalar potential

$$\varphi_A(\mathbf{r}) = \int d^3r' \frac{\rho_A(\mathbf{r}')}{4\pi\varepsilon_0 |\mathbf{r} - \mathbf{r}'|} \tag{7.2}$$

Therefore, the free Hamiltonian describing the motion of the particles reads as (the factor $1/2$ removes double counting)

$$H_A = \sum_\alpha \frac{\mathbf{p}_\alpha^2}{2m_\alpha} + \frac{1}{2} \int d^3r\, \rho_A(\mathbf{r}) \varphi_A(\mathbf{r}) \tag{7.3}$$

Together with the Hamiltonian of the dielectric medium-assisted electromagnetic field (2.48)

$$H_{\mathrm{F}} = \int d^3\mathbf{r} \int_0^\infty \hbar\omega\, \mathbf{f}^\dagger(\mathbf{r},\omega)\mathbf{f}(\mathbf{r},\omega) \tag{7.4}$$

and the interaction Hamiltonian of the charged particles with the electromagnetic field

$$H_{\mathrm{int}} = \sum \left[-\frac{q}{m}\, \mathbf{p}\cdot\mathbf{A}(\mathbf{r}) + \tfrac{1}{2}q\, \mathbf{A}(\mathbf{r})\cdot\mathbf{A}(\mathbf{r}) \right] + \int d^3\mathbf{r}\, \rho_{\mathrm{A}}(\mathbf{r})\varphi_{\mathrm{F}}(\mathbf{r}) \tag{7.5}$$

the total Hamiltonian of the system can be written in the form

$$
\begin{aligned}
H \;=\;& H_{\mathrm{F}} + H_{\mathrm{A}} + H_{\mathrm{int}} \\[4pt]
=\;& \int d^3\mathbf{r} \int_0^\infty \hbar\omega\, \mathbf{f}^\dagger(\mathbf{r},\omega)\mathbf{f}(\mathbf{r},\omega) + \sum \frac{1}{2m}\left[\mathbf{p} - q\,\mathbf{A}(\mathbf{r})\right]^2 \\[4pt]
&+ \tfrac{1}{2}\int d^3\mathbf{r}\, \rho_{\mathrm{A}}(\mathbf{r})\varphi_{\mathrm{A}}(\mathbf{r}) + \int d^3\mathbf{r}\, \rho_{\mathrm{A}}(\mathbf{r})\varphi_{\mathrm{F}}(\mathbf{r})
\end{aligned}
\tag{7.6}
$$

The scalar potential φ_{F} and the vector potential $\mathbf{A}$ associated with the medium-assisted field have to be thought of as being expressed in terms of the basic fields $\mathbf{f}(\mathbf{r},\omega)$ as in Eqs. (2.83) (2.85) [together with Eq. (2.50)].

The operators of the electric and displacement fields now contain contributions from the medium-assisted fields and contributions from the additional charges,

$$\mathbf{E}(\mathbf{r}) = \mathbf{E}_{\mathrm{F}}(\mathbf{r}) + \varphi_{\mathrm{A}}(\mathbf{r}) = \int_0^\infty d\omega\, \underline{\mathbf{E}}(\mathbf{r},\omega) + \mathrm{H.c.} + \varphi_{\mathrm{A}}(\mathbf{r}) \tag{7.7}$$

$$\mathbf{D}(\mathbf{r}) = \mathbf{D}_{\mathrm{F}}(\mathbf{r}) + \varepsilon_0\varphi_{\mathrm{A}}(\mathbf{r}) = \int_0^\infty d\omega\, \underline{\mathbf{D}}(\mathbf{r},\omega) + \mathrm{H.c.} + \varepsilon_0\varphi_{\mathrm{A}}(\mathbf{r}) \tag{7.8}$$

where $\underline{\mathbf{E}}(\mathbf{r},\omega)$ and $\underline{\mathbf{D}}(\mathbf{r},\omega)$ are the (frequency components of the) medium-assisted electric and displacement fields. Recall that the polarization $\mathbf{P}(\mathbf{r})$, which is related to the degrees of freedom of the matter, commutes with the radiation-field operators. Furthermode, quantities of the medium-assisted electromagnetic field commute with quantities of the additional charged particles. Thus, one can verify both the correct (equal-time) commutation relations between the electromagnetic field operators and the operator-valued Maxwell equations [S11]

$$\nabla\cdot\mathbf{B}(\mathbf{r}) = 0 \tag{7.9}$$

$$\nabla\times\mathbf{E}(\mathbf{r}) + \dot{\mathbf{B}}(\mathbf{r}) = 0 \tag{7.10}$$

$$\nabla\cdot\mathbf{D}(\mathbf{r}) = \rho_{\mathrm{A}}(\mathbf{r}) \tag{7.11}$$

$$\nabla\times\mathbf{H}(\mathbf{r}) - \dot{\mathbf{D}}(\mathbf{r}) = \mathbf{j}_{\mathrm{A}}(\mathbf{r}) \tag{7.12}$$

CHAPTER 7. FIELD QUANTIZATION IN THE PRESENCE OF ATOMS　　63

where the atomic current density is defined by

$$\mathbf{j}_A(\mathbf{r}) = \frac{1}{2}\sum_\alpha q_\alpha \left[\dot{\mathbf{r}}_\alpha\, \delta(\mathbf{r}-\mathbf{r}_\alpha) + \delta(\mathbf{r}-\mathbf{r}_\alpha)\dot{\mathbf{r}}_\alpha \right] \tag{7.13}$$

Here the velocity operator (actually the equation of motion of the atomic position operator) is given by the expression

$$\dot{\mathbf{r}}_\alpha = \frac{1}{m_\alpha}\left[\mathbf{p}_\alpha - q_\alpha \mathbf{A}(\mathbf{r}_\alpha) \right] \tag{7.14}$$

and the operator-valued Newtonian equations of motions read

$$m_\alpha \ddot{\mathbf{r}}_\alpha = q_\alpha \left\{ \mathbf{E}(\mathbf{r}_\alpha) + \frac{1}{2}\left[\dot{\mathbf{r}}_\alpha \times \mathbf{B}(\mathbf{r}_\alpha) - \mathbf{B}(\mathbf{r}_\alpha) \times \dot{\mathbf{r}}_\alpha \right] \right\} \tag{7.15}$$

7.1.2 Multipolar coupling

In the minimal-coupling scheme the interaction between the atomic system and the medium-assisted Maxwell field is expressed in terms of the potentials of the electromagnetic field. In most cases it is desirable to describe the interaction in terms of the electromagnetic field strengths and the polarization and magnetization of the atomic system. This can be achieved by a unitary transformation of the Hamiltonian (7.6) which is called the Power–Zienau–Woolley transformation [147, 148, 149, 150, 151].

The polarization of an atomic system at position $\mathbf{r}_A$ is introduced as [151]

$$\mathbf{P}_A(\mathbf{r}) = \sum_\alpha q_\alpha (\mathbf{r}_\alpha - \mathbf{r}_A) \int_0^1 d\lambda\, \delta[\mathbf{r} - \mathbf{r}_A - \lambda(\mathbf{r}_\alpha - \mathbf{r}_A)] \tag{7.16}$$

leading to a charge density

$$\rho_A(\mathbf{r}) = q_A\, \delta(\mathbf{r} - \mathbf{r}_A) - \nabla \cdot \mathbf{P}_A(\mathbf{r}) \tag{7.17}$$

with $q_A = \sum_\alpha q_\alpha$ being the total charge of the atomic system. The unitary operator that performs the transformation from minimal coupling to multipolar coupling is

$$U = \exp\left[\frac{i}{\hbar} \int d^3r\, \mathbf{P}_A(\mathbf{r})\mathbf{A}(\mathbf{r}) \right] \tag{7.18}$$

As U depends on the position operators $\mathbf{r}_\alpha$ [via the polarization $\mathbf{P}_A(\mathbf{r})$] and the vector potential $\mathbf{A}(\mathbf{r})$ only, the position operators are left unchanged,

$$\mathbf{r}_\alpha' = U\mathbf{r}_\alpha U^\dagger = \mathbf{r}_\alpha \tag{7.19}$$

whereas momentum operators $\mathbf{p}$ and basic fields are transformed by the rules:

$$\mathbf{p}' = U\mathbf{p}\,U^\dagger$$

$$= \mathbf{p} - q\,\mathbf{A}_{\mathrm{F}}(\mathbf{r}) - q\int_0^1 d\lambda\,(\mathbf{r}-\mathbf{r}_{\mathrm{A}})\times\mathbf{B}[\mathbf{r}_{\mathrm{A}}+\lambda(\mathbf{r}-\mathbf{r}_{\mathrm{A}})] \tag{7.20}$$

$$\mathbf{f}'(\mathbf{r}) = U\mathbf{f}(\mathbf{r})U^\dagger$$

$$= \mathbf{f}(\mathbf{r}) - \frac{i}{\hbar}\sqrt{\frac{\hbar}{\pi\varepsilon_0}}\frac{\omega}{c^2}\int d^3r'\,\mathbf{P}_{\mathrm{A}}(\mathbf{r}')\,\mathbf{G}(\mathbf{r},\mathbf{r}',\omega) \tag{7.21}$$

Expressing the Hamiltonian H in Eq. (7.6) in terms of the new variables (7.19)–(7.21) one obtains the multipolar Hamiltonian [S9]

$$H = \int d^3r\int_0^\infty d\omega\,\hbar\omega\,\mathbf{f}^\dagger(\mathbf{r},\omega)\,\mathbf{f}(\mathbf{r},\omega) + \sum\frac{1}{2m}\left[\mathbf{p}+\int d^3r\,\mathbf{n}(\mathbf{r})\times\mathbf{B}(\mathbf{r})\right]^2$$

$$+\frac{1}{2\varepsilon_0}\int d^3r\,\mathbf{P}_{\mathrm{A}}(\mathbf{r})\cdot\mathbf{P}_{\mathrm{A}}(\mathbf{r}) - \frac{1}{\varepsilon_0}\int d^3r\,\mathbf{P}_{\mathrm{A}}(\mathbf{r})\cdot\mathbf{D}'(\mathbf{r}) + \frac{1}{\varepsilon_0}\int d^3r\,\mathbf{P}_{\mathrm{A}}(\mathbf{r})\cdot\mathbf{P}_{\mathrm{F}}(\mathbf{r}) \tag{7.22}$$

where $\mathbf{D}'(\mathbf{r}) = \mathbf{D}(\mathbf{r}) + \mathbf{P}_{\mathrm{A}}(\mathbf{r})$ and

$$\mathbf{n}(\mathbf{r}) = q\,(\mathbf{r}-\mathbf{r}_{\mathrm{A}})\int_0^1 d\lambda\,\lambda\,\delta[\mathbf{r}-\mathbf{r}_{\mathrm{A}}-\lambda(\mathbf{r}-\mathbf{r}_{\mathrm{A}})] \tag{7.23}$$

7.2   Dipole and rotating-wave approximation

Let us assume that the (localized) atomic system is globally neutral, hence $\sum q = 0$. If in addition the spatial extent of the atomic systems is small compared to the spatial variations of the electromagnetic potentials, one can expand the latter in powers of the position operators $\mathbf{r}$ giving rise to multipole moments of the atomic system. Keeping only the lowest-order term in the expansion yields the electric-dipole approximation which can be expressed in terms of the atomic dipole operator

$$\mathbf{d}_{\mathrm{A}} = \sum q\,\mathbf{r} \tag{7.24}$$

The interaction Hamiltonian (7.5) between medium-assisted electromagnetic field and atomic system in minimal coupling can then be written, on neglecting the $\mathbf{A}^2$ term for optical fields that are weak compared to intra-atomic electric fields [152], as

$$H_{\mathrm{int}} = -\sum\frac{q}{m}\mathbf{p}\cdot\mathbf{A}(\mathbf{r}) + \int d^3r\,\rho_{\mathrm{A}}(\mathbf{r})\varphi_{\mathrm{F}}(\mathbf{r})$$

$$= -\frac{1}{i\hbar}\,\mathbf{d}_{\mathrm{A}}\cdot H_{\mathrm{A}}\,\mathbf{A}(\mathbf{r}_{\mathrm{A}}) + \int d^3r\,\rho_{\mathrm{A}}(\mathbf{r})\varphi_{\mathrm{F}}(\mathbf{r}) \tag{7.25}$$

with the atomic Hamiltonian H_A from Eq. (7.3). In electric-dipole approximation the function in the polarization (7.16) can be expanded in powers of $(\mathbf{r} - \mathbf{r}_A)$. Keeping only the lowest-order term and integrating over gives

$$\mathbf{P}_A(\mathbf{r}) = \mathbf{d}_A \delta(\mathbf{r} - \mathbf{r}_A) \tag{7.26}$$

Recalling that $\rho_A(\mathbf{r}) = -\nabla \mathbf{P}_A(\mathbf{r})$ for globally neutral systems [Eq. (7.17)] and $\mathbf{E}_F(\mathbf{r}) = \mathbf{E}_F(\mathbf{r})$ [Eq. (2.83)], partial integration in the second term on the rhs of Eq. (7.25) yields

$$H_{\text{int}} = \frac{1}{i\hbar} [\mathbf{d}_A, H_A] \mathbf{A}(\mathbf{r}_A) - \mathbf{d}_A \mathbf{E}_F(\mathbf{r}_A) \tag{7.27}$$

We may specify the atomic Hamiltonian H_A further by restricting to the case of a two-level atom with lower level l and upper level u. Thus,

$$H_A = \hbar\omega_u |u\rangle\langle u| + \hbar\omega_l |l\rangle\langle l| = \frac{1}{2}\hbar\omega_A \sigma_z + \text{const.} \tag{7.28}$$

where the operator $\sigma_z = |u\rangle\langle u| - |l\rangle\langle l|$ and the atomic transition frequency $\omega_A = \omega_u - \omega_l$ have been introduced. The additive constant is dropped. In the rotating-wave approximation, only those electromagnetic field components with frequency ω_A are taken into account. Thus, we have $i\omega_A \mathbf{A}^{(+)}(\mathbf{r}_A) \approx \mathbf{E}^{(+)}(\mathbf{r}_A)$ for the positive-frequency components of the transverse electric-field operator. Finally we obtain for the interaction Hamiltonian

$$\begin{aligned} H_{\text{int}} &= \frac{1}{i\hbar} [\mathbf{d}_A, H_A] \mathbf{A}(\mathbf{r}_A) - \mathbf{d}_A \mathbf{E}_F(\mathbf{r}_A) \\ &\approx -\mathbf{E}_F^{(+)}(\mathbf{r}_A)\mathbf{d}\sigma - \mathbf{E}_F^{(+)}(\mathbf{r}_A)\mathbf{d}\sigma^\dagger + \text{H.c.} \\ &= -\mathbf{E}_F^{(+)}(\mathbf{r}_A)\mathbf{d}\sigma + \text{H.c.} \end{aligned} \tag{7.29}$$

with the lowering operator defined by $\sigma = |l\rangle\langle u|$ and the dipole operator $\mathbf{d}_A = \mathbf{d}\sigma_x$ with real dipole moment $\mathbf{d}$. The operators $\sigma_x = \sigma + \sigma^\dagger$, $\sigma_y = i(\sigma - \sigma^\dagger)$, and σ_z form the well-known spin-1⁄2-algebra with the commutation rule (6.6). It is worth noting that the interaction Hamiltonian having the structure $-\mathbf{d}_A \mathbf{E}_F^{(\pm)}$ in electric-dipole approximation (7.29) contains the positive (respectively negative) frequency components of the full electric field strength operator $\mathbf{E}_F^{(\pm)}(\mathbf{r}_A)$, not only its transverse part. From Eqs. (7.25) and (7.27) it is clear that the longitudinal contribution is due to the scalar potential $\varphi_F(\mathbf{r})$ of the medium-assisted electromagnetic field which induces a Coulomb interaction with the charged particles.

Generally, equations of motion for atomic operators can be derived that are expressed in terms of the Green function and the fundamental basic fields. Besides spontaneous decay near dielectric bodies which is discussed in the following chapter, cavity QED provides a number of applications that can be treated with this general theory of the interaction of electromagnetic field and atoms in the presence of dielectric bodies [153, 154, 155].

8 Spontaneous decay of excited atoms in the presence of absorbing dielectrics

An important application of the quantization of the electromagnetic field interacting with atoms in the presence of dielectric bodies is the process of spontaneous decay. It represents the prime example of the action of ground-state fluctuations on physically measurable processes. It is well known since the work of Einstein [156] that, in order to obtain the correct Planck law of black-body radiation, a process as spontaneous emission must be included in the theory of atomic decay. Later it has been realized both theoretically [86, 157, 158, 159, 160, 161, 162, 163, 164, 165, 166, 167, 168, 169, 170] and experimentally [171, 172, 173, 174, 175, 176] that the ground state felt by an atom surrounded by dielectric matter changes, and the rate of spontaneous decay changes accordingly. Besides enhancement [80], the environment can be made such that spontaneous decay is inhibited [81, 82]. In the following chapter, we derive equations of motion of the atomic operators (Sec. 8.1) [S4] and apply the theory in Secs. 8.2 and 8.3 to spontaneous decay in absorbing media [S3, S4] as well as near planar interfaces [S5].

8.1 Equations of motions of atomic operators

Starting point is the interaction Hamiltonian (7.29) for a two-level atom in electric-dipole and rotating-wave approximations. The Heisenberg equations of motion for the basic fields $\mathbf{f}(\mathbf{r})$ describing the medium-assisted electromagnetic field and the Pauli spin operators σ_i for the atom follow from the general rule $\dot{O} = (i\hbar)^{-1}[O, H]$. From the commutation relations (6.6) of the Pauli spin operators, and Eqs. (2.46) and (2.47), respectively, the Heisenberg equations of motion read

$$\dot{\sigma}_z = \frac{2i}{\hbar}\,\mathbf{E}_F^{(+)}(\mathbf{r}_A)\mathbf{d} + \text{H.c.} \tag{8.1}$$

$$\dot{\sigma} = i\omega_A\sigma + \frac{i}{\hbar}\mathbf{E}_F^{(-)}(\mathbf{r}_A)\mathbf{d}\,\sigma_z \tag{8.2}$$

$$\dot{\mathbf{f}}(\mathbf{r}) = -i\omega\mathbf{f}(\mathbf{r}) + \frac{\omega^2}{c^2}\sqrt{\frac{\hbar\varepsilon_I(\mathbf{r})}{\pi\varepsilon_0}}\,\underline{G}^*(\mathbf{r},\mathbf{r}_A)\mathbf{d}\,\sigma \tag{8.3}$$

Equation (8.3) can be formally integrated and substituted into the expression for the electric-field operator (2.50) which yields, on using the integral relation (2.43) for the Green function,

for the positive frequency component of the electric field

$$\mathbf{E}_{F}^{(+)}(\mathbf{r}\ t) = \mathbf{E}_{F\,\text{free}}^{(+)}(\mathbf{r}\ t) + \frac{i}{\ _0}\int d\ \frac{\ ^2}{c^2}\,\text{Im}\,\boldsymbol{G}(\mathbf{r}\ \mathbf{r}_A\ \ )\mathbf{d}\int_{\ }^{t} d\ \ e^{\ i\ (t\ \ )}\ (\ ) \tag{8.4}$$

Substituting the formal solution (8.4) into the Heisenberg equations for the atomic quantities (8.1) and (8.2) leads to integro-differential equations for them. The solution to these integro-differential equations can be obtained numerically. However, there is a special case for which an analytical solution is known. When we assume that the time integral in Eq. (8.4) effectively runs only over a small correlation time interval $\ _c$, the lower limit in the integral can be extended to minus infinity. Moreover, if $\ _c$ is small compared to the time scale on which the atomic operators evolve, the slowly varying quantity $(\ )e^{i\ \ _A}$ can be taken at the time t and put in front of the integral. Thus, we have

$$\int_{\ }^{t} d\ \ e^{\ i\ (t\ \ )}\ (\ ) \qquad \int_{\ }^{t} d\ \ e^{\ i\ (t\ \ )}\ (\ )$$

$$(t)\int_{\ }^{t} d\ \ e^{\ i(\ \ _A)(t\ \ )} = \ (t)\ (\ _A\ \ ) \tag{8.5}$$

$[\ (x) = \ (x) + i\mathcal{P}x^{\ 1};\ \mathcal{P}:\ \text{principal value}]$. This is called the Markovian approximation saying that the atomic variables at time t have no "memory" about the variables at earlier times. Eq. (8.4) reads now

$$\mathbf{E}_{F}^{(+)}(\mathbf{r}\ t) = \mathbf{E}_{F\,\text{free}}^{(+)}(\mathbf{r}\ t) + \frac{i}{\ _0}\int d\ \frac{\ ^2}{c^2}\,\text{Im}\,\boldsymbol{G}(\mathbf{r}\ \mathbf{r}_A\ \ )\mathbf{d}\ (t)\ (\ _A\ \ ) \tag{8.6}$$

Substituting Eq. (8.6) into Eqs. (8.1) and (8.2) yields

$$\ _z = \ (1 + \ _z) + \frac{2i}{\hbar}\ \mathbf{E}_{F\,\text{free}}^{(+)}(\mathbf{r}_A)\mathbf{d} + \text{H.c.} \tag{8.7}$$

$$= \ i(\ _A\ \ )\ \ \frac{1}{2}\ + \frac{i}{\hbar}\mathbf{E}_{F\,\text{free}}^{(\ )}(\mathbf{r}_A)\mathbf{d}\ \ _z \tag{8.8}$$

where

$$\ = \frac{2\ _A^2 d_i d_j}{\hbar\ _o c^2}\,\text{Im}\,G_{ij}(\mathbf{r}_A\ \mathbf{r}_A\ \ _A) \tag{8.9}$$

is the rate of spontaneous decay of the upper state and

$$\ = \frac{d_i d_j}{\hbar\ _0}\mathcal{P}\int_0^{\ } d\ \frac{\ ^2}{c^2}\frac{\text{Im}\,G_{ij}(\mathbf{r}_A\ \mathbf{r}_A\ \ )}{\ \ _A} \tag{8.10}$$

is the contribution to the Lamb shift. It is worth noting that the rate formula (8.9) can equivalently be derived using expression (2.82) for the ground-state fluctuations of the electromagnetic field. Applying Fermi's Golden Rule (see for example [177]) then yields

$$\Gamma = \frac{2}{\hbar^2} d_i d_j \int_0^\infty d\tau \langle 0 | \underline{E}_i(\mathbf{r}_A, \tau) \underline{E}_j(\mathbf{r}_A, \omega_A) | 0 \rangle \tag{8.11}$$

Equations (8.9) and (8.10) for the spontaneous decay rate and the Lamb shift are most suitable for complicated geometries since only the Green function of the classical scattering problem is involved. It should be stressed, that the representation of the spontaneous decay rate in terms of the imaginary part of the Green function follows from the quantization scheme in absorbing media which is consistent with standard QED requirements and statistical physics. In particular, the dissipation-fluctuation theorem does not have to be invoked by hand [36, 159]. Moreover, usage of the imaginary part of the Green function is not restricted to real values of the permittivity [178], but it is valid for all frequencies and hence all possible complex values for the permittivity.

8.2 Spontaneous decay of an excited atom in absorbing dielectric media

Let us consider the situation where a single two-level atom with transition frequency ω_A is located inside an absorbing dielectric medium. The question arises how the spontaneous decay rate changes compared to its vacuum value

$$\Gamma_0 = \frac{\omega_A^3 d^2}{3\pi\hbar\epsilon_0 c^3} \tag{8.12}$$

where d is the dipole matrix element of the atomic transition. Arguments based on the change of the mode density due to the surrounding material suggested that the decay rate should be modified according to [179, 180, 181, 182]

$$\Gamma = n\Gamma_0 \tag{8.13}$$

where n is the real refractive index of the medium. Here it is assumed that the local field the atom interacts with is exactly the same as the electromagnetic field in the continuous medium. In reality the atom is in a small region of free space, and the local field is different from the field in the continuous medium. This has lead to the introduction of the so-called local-field correction factor ξ, and the decay rate is expected to be modified as
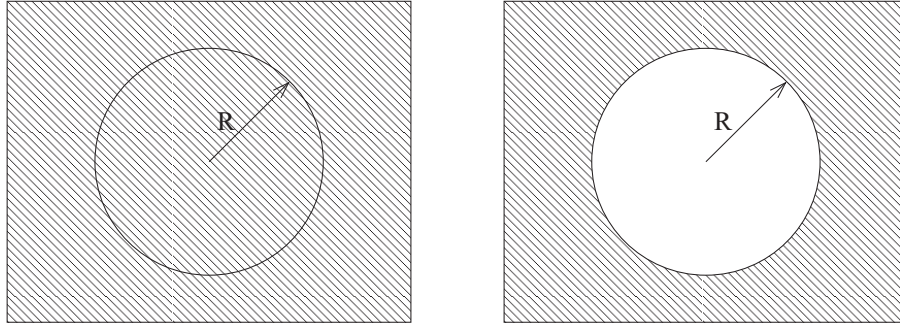
$$\Gamma = n\xi\Gamma_0 \tag{8.14}$$

Figure 8.1: Virtual-cavity model (left figure) and real-cavity model (right figure).

Different models have been proposed to calculate . The virtual-cavity model regards to the classical picture of an ensemble of dipoles in a (fictitious) ball of radius R in which depolarization effects change the electric-field strength of the continuous medium. On the other hand, the real-cavity model assumes that the radiating atom is sitting in an empty cavity of radius R surrounded by all other atoms (Fig. 8.1).

In the virtual-cavity model the local-field correction factor is given by [183]

$$
\text{VC} = \left(\frac{n^2 + 2}{3}\right)^2 \tag{8.15}
$$

whereas in the real-cavity model it is derived to be [28]

$$
\text{RC} = \left(\frac{3n^2}{2n^2 + 1}\right)^2 \tag{8.16}
$$

Experiments suggest that the latter model is a good candidate for describing substitutional guest atoms different from the host atoms [184, 185, 186], whereas the virtual-cavity model seems appropriate for describing interstitial guest atoms of the same kind as the host atoms [186]. For absorbing media, however, arguments based on real refractive index do not apply.

8.2.1 Virtual-cavity model

In the (Clausius Mosotti) virtual-cavity model it is assumed that the field outside the (fictitious) sphere is not modified by the small region inside the sphere, and the local electric field inside is [187]

$$
\underline{\mathbf{E}}(\mathbf{r}) = \underline{\mathbf{E}}(\mathbf{r}) + \frac{1}{3_0}\underline{\mathbf{P}}(\mathbf{r}) \tag{8.17}
$$

where $\underline{\mathbf{E}}(\mathbf{r})$ and $\underline{\mathbf{P}}(\mathbf{r})$ are the electric field and the polarization in the unperturbed medium. The factor $(3_0)^{-1}$ is the depolarization factor for an isotropic sphere (for more complicated inclusions, see for example [188, 189]). The polarization contains according to

the general theory also the noise contribution $\underline{\mathbf{P}}_N(\mathbf{r}\,\omega)$ which must not be omitted because it is part of the quantum vacuum.

The *ad hoc* introduction of the local electric field according to Eq. (8.17) is reminiscent of classical Maxwell theory and may not be fully consistent with quantum theory. For example, the correct (equal-time) commutation relations for the operators of local electric field and magnetic induction are only satisfied approximately. Indeed, the correct commutation rule is only recovered providing that the static permittivity is not too large [$\epsilon(\mathbf{r}\,0) \lesssim 10$] (for details, see [S3]). Moreover, it is not clear from first sight what kind of Green function should be applied. Instead of using the Green function, one proceeds with the definition of the local fields (8.17) and uses Fermi's Golden Rule (8.11) which in turn, by comparing with Eq. (8.9), allows in principle the definition of a local Green function.

Inserting Eq. (8.17) into Fermi's Golden Rule (8.11) and using the Green function $\mathbf{G}^{\mathrm{M}}(\mathbf{r}\,\mathbf{r}'\,\omega)$ of the (mean) field in the undisturbed medium with permittivity $\epsilon(\omega_A)$, we obtain [S3]

$$
\Gamma = \frac{2\omega_A^2 d_i d_j}{\hbar\,\epsilon_0 c^2}\left|\frac{\epsilon(\omega_A)+2}{3}\right|^2 \mathrm{Im}\,\overline{G_{ij}^{\mathrm{M}}(\mathbf{r}\,\mathbf{r}\,\omega_A)}
$$

$$
+\frac{4\omega_A^2 d_i d_j}{3\hbar\,\epsilon_0 c^2}\epsilon_I(\omega_A)\mathrm{Re}\left[\frac{\epsilon(\omega_A)+2}{3}\overline{G_{ij}^{\mathrm{M}}(\mathbf{r}\,\mathbf{r}\,\omega_A)}\right] + \frac{2 d_i d_j}{9\hbar\,\epsilon_0}\epsilon_I(\omega_A)\overline{\delta_{ij}(\mathbf{r}-\mathbf{r}')} \tag{8.18}
$$

For $\mathbf{r}\,\mathbf{r}' \to \mathbf{r}_A$ a singular behaviour in the terms on the second line of Eq. (8.18) is observed, hence regularization is required, for example averaging over the sphere. This singularity is associated with a diverging (Coulomb) energy of the radiating atom with the underlying continuous medium. Assuming a homogeneous background medium, the Green function $\mathbf{G}^{\mathrm{M}}(\mathbf{r}\,\mathbf{r}'\,\omega)$ may be identified with that for bulk material (see Appendix B). Averaging with respect to $\mathbf{r}$ and $\mathbf{r}'$ separately over the sphere, one obtains the decay rates associated with longitudinal and transverse fields, respectively, as

$$
\Gamma_\parallel = \Gamma_0 \frac{4\,\epsilon_I(\omega_A)}{27\,|\epsilon(\omega_A)|^2}\left(\frac{c}{\omega_R\,\omega_A}\right)^3 \tag{8.19}
$$

$$
\Gamma_\perp = \Gamma_0\left\{\mathrm{Re}[n(\omega_A)]\left|\frac{\epsilon(\omega_A)+2}{3}\right|^2\left[\frac{2\,\epsilon_I(\omega_A)^2}{9}+\frac{25\,\epsilon_I(\omega_A)}{54}\right]\left(\frac{c}{\omega_R\,\omega_A}\right)^3 \right.
$$

$$
\left. + \epsilon_I(\omega_A)[\epsilon_R(\omega_A)+2]\frac{8}{15}\frac{c}{\omega_R\,\omega_A}-\frac{2}{9}\epsilon_I(\omega_A)\right\} + \mathcal{O}(R) \tag{8.20}
$$

$[\omega_R \equiv n(\omega_A)\,\omega_A\,c^{-1} \ll 1]$, with Γ_0 being the free-space spontaneous emission rate (8.12). Inspection of Eqs. (8.19) and (8.20) reveals that, when absorption may be safely disregarded, i.e. $\epsilon_I(\omega_A) = 0$, then $\Gamma_\parallel = 0$, and $\Gamma_\perp$ exactly reproduces the spontaneous emission rate

(8.14) with the Lorenz Lorentz local- eld correction factor (8.15). For absorbing media both longitudinal and transverse decay rates show a strong dependence on the cavity radius R. In the near- eld zone the dominant terms are proportional to R^{-3} and correspond to nonradiative energy transfer. However, calculations of resonant energy transfer in a lattice of absorbing molecules [166] have shown that the total decay rate is purely transverse. The appearance of the longitudinal rate   may therefore be attributed to the quantum-mechanical inconsistency in de ning the local eld operators.

It should also be noted that di erent regularization methods can be applied leading to di erent numerical factors in Eqs. (8.19) and (8.20). Our results have been con rmed within a semi-microscopic approach [170] using a Schwinger Keldysh Green-function technique.

8.2.2   Real-cavity model

In contrast to the virtual-cavity model, in the (Glauber Lewenstein) real-cavity model the atom is placed in an empty (real) cavity of radius R, and the exact Green function for this geometry is used for computing the decay rate (8.9). That is, Maxwell s equations are solved inside and outside the cavity imposing appropriate boundary conditions at the cavity walls. By the general quantization scheme in Sec. 2.2, the fundamental (equal-time) commutation relations are satis ed exactly. Moreover, the Green function does not lead to a singular decay rate as in the virtual-cavity model.

According to Eq. (8.9) the decay rate is proportional to the imaginary part of the Green function in the coincidence limit, i.e. both spatial arguments taken at the position of the radiating atom. The Green function for an inhomogeneous problem of this type can always be written as the sum of the Green function $\boldsymbol{G}^{\mathrm{V}}(\mathbf{r}\ \mathbf{r}\quad)$ for a homogeneous problem of an atom located in vacuum and a Green function $\boldsymbol{R}(\mathbf{r}\ \mathbf{r}\quad)$ that ensures the correct boundary conditions at the cavity walls [89, 102] (see also the discussion on input-output coupling in Chapter 3). In fact, this decomposition of the Green function is valid in all situations in which the radiating atom is located in free space. By construction, the re ection term $\boldsymbol{R}(\mathbf{r}\ \mathbf{r}\quad)$ is purely transverse. Moreover, the imaginary part of the vacuum Green function $\boldsymbol{G}^{\mathrm{V}}(\mathbf{r}\ \mathbf{r}\quad)$ [Eq. (B.6)] does not contain a longitudinal part. Hence, we may write the rate formula (8.9) as

$$= \frac{2\ _{\mathrm{A}}^{2}d_{i}d_{j}}{\hbar\ _{0}c^{2}}\mathrm{Im}\,G_{ij}(\mathbf{r}_{\mathrm{A}}\ \mathbf{r}_{\mathrm{A}}\quad_{\mathrm{A}}) \tag{8.21}$$

That is, for atoms located in vacuum only transverse elds contribute to the decay rate. The longitudinal decay rate   that appeared in the virtual-cavity model is therefore an artifact.

The Green function for a spherical cavity, with the centre of the cavity as origin of

coordinates, and both spatial arguments inside the cavity, is therefore

$$G(\mathbf{r}, \mathbf{r}') = G^{\mathrm{V}}(\mathbf{r}, \mathbf{r}') + R(\mathbf{r}, \mathbf{r}') \tag{8.22}$$

where $G^{\mathrm{V}}(\mathbf{r}, \mathbf{r}')$ is the vacuum Green function given in Appendix B with $\varepsilon(\omega) = 1$, and $R(\mathbf{r}, \mathbf{r}')$ is the reflection term given in Appendix C.2. Since we are interested in the coincidence limit $\mathbf{r}, \mathbf{r}' \to 0$, we look at the asymptotics of the vector wave functions (C.6) and (C.7) for small r which is given by the corresponding asymptotics of the Bessel function $j_n(kr)$ in (C.8) [190]. We get

$$\mathbf{M}_{{}^e_o nm}(\mathbf{r}, k) \overset{kr \to 0}{\sim} (kr)^n \tag{8.23}$$

$$\mathbf{N}_{{}^e_o nm}(\mathbf{r}, k) \overset{kr \to 0}{\sim} (kr)^{n-1} \tag{8.24}$$

and thus, only the TM vector wave functions $\mathbf{N}_{{}^e_o 1m}(\mathbf{r}, k)$ contribute to $R(\mathbf{r}, \mathbf{r}')$ for which we find that

$$R_{ij}(\mathbf{r}, \mathbf{r}')\big|_{\mathbf{r}=0} = \frac{i}{6\pi c} C_1^N \, \delta_{ij} \tag{8.25}$$

with the generalized reflection coefficient

$$C_1^N(\omega) = \frac{[i + (n+1)\alpha - i\alpha^2 n - \alpha^3 n^2 (n+1)]e^{i\alpha}}{\sin\alpha - (\cos\alpha + in\sin\alpha) + i\alpha^2 n\cos\alpha - \alpha^3(\cos\alpha - in\sin\alpha)n^2 (n^2-1)} \tag{8.26}$$

$[n = \sqrt{\varepsilon(\omega)}; \alpha = R\omega c]$.

Inserting Eq. (8.25) and the imaginary part of the vacuum Green function (B.6) into Eq. (8.21) we obtain finally

$$\Gamma = \Gamma_0 \left[1 + \mathrm{Re}\, C_1^N(\omega_{\mathrm{A}}) \right] \tag{8.27}$$

with the free-space decay rate Γ_0 from Eq. (8.12). The result (8.27) is exact if the surrounding medium can be treated as a continuum, and it is valid for all transition frequencies ω_{A}. If the cavity radius R is small compared to the atomic transition wavelength, we can expand the generalized reflection coefficient $C_1^N(\omega_{\mathrm{A}})$ in powers of $\alpha = R\omega_{\mathrm{A}} c$ as [191, S4]

$$\Gamma = \Gamma_0 \left\{ \frac{9\varepsilon_I(\omega_{\mathrm{A}})}{|2\varepsilon(\omega_{\mathrm{A}})+1|^2} \left(\frac{c}{\omega_{\mathrm{A}} R}\right)^3 + \frac{9\varepsilon_I(\omega_{\mathrm{A}})[28\varepsilon(\omega_{\mathrm{A}})^2 + 16\varepsilon_R(\omega_{\mathrm{A}})+1]}{5|2\varepsilon(\omega_{\mathrm{A}})+1|^4} \frac{c}{\omega_{\mathrm{A}} R} \right.$$

$$+ \frac{9 n_R(\omega_{\mathrm{A}})}{|2\varepsilon(\omega_{\mathrm{A}})+1|^4} \left[4|\varepsilon(\omega_{\mathrm{A}})|^4 + 4\varepsilon_R(\omega_{\mathrm{A}})|\varepsilon(\omega_{\mathrm{A}})|^2 + \varepsilon_R^2(\omega_{\mathrm{A}}) - \varepsilon_I^2(\omega_{\mathrm{A}}) \right]$$

$$\left. \frac{9 n_I(\omega_{\mathrm{A}})\varepsilon_I(\omega_{\mathrm{A}})}{|2\varepsilon(\omega_{\mathrm{A}})+1|^4} \left[4|\varepsilon(\omega_{\mathrm{A}})|^2 + 2\varepsilon_R(\omega_{\mathrm{A}}) \right] + \mathcal{O}\left(\frac{R\omega_{\mathrm{A}}}{c}\right) \right\} \tag{8.28}$$

In frequency regions where absorption may be completely disregarded, i.e. $\varepsilon_I(\omega_{\mathrm{A}}) = 0$, only the term on the second line in Eq. (8.28) survives and reproduces exactly the spontaneous

emission rate including the familiar Glauber Lewenstein local- eld correction factor (8.16). For absorbing media terms with strong dependence on the cavity radius R appear. In particular, the R^{-3} term in Eq. (8.28) can be regarded as the dipole-dipole energy transfer term associated with nonradiative decay [162, 166]. The coupling between the decaying atom and the surrounding dielectric is mediated exclusively by transverse photons.
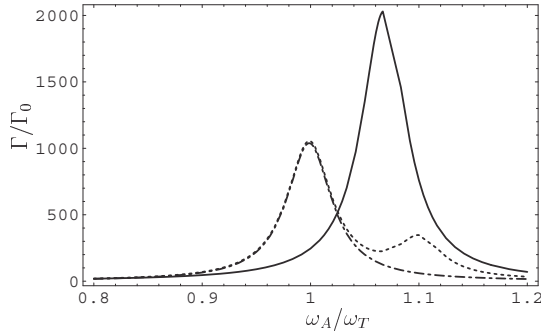

Figure 8.2: $= 0\,05$ $_T$, $R = 0\,02$ $_A$.
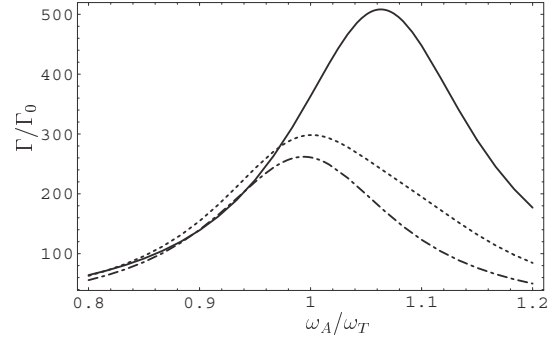
Figure 8.3: $= 0\,2$ $_T$, $R = 0\,02$ $_A$.
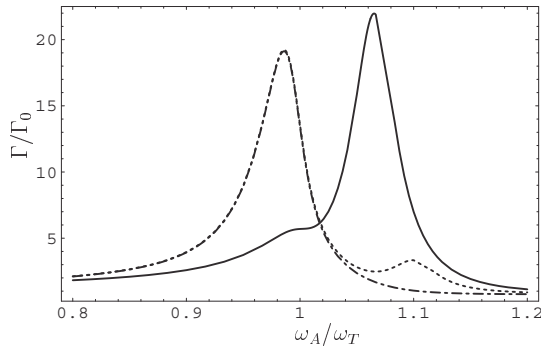
Figure 8.4: $= 0\,05$ $_T$, $R = 0\,1$ $_A$.
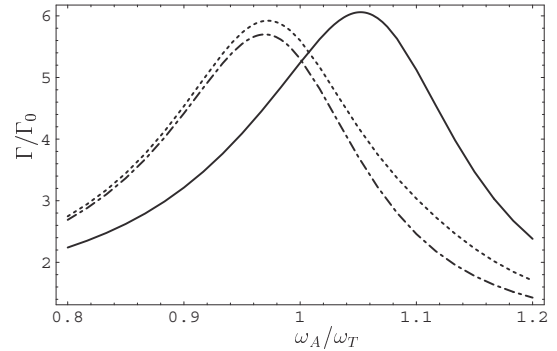
Figure 8.5: $= 0\,2$ $_T$, $R = 0\,1$ $_A$.

Spontaneous decay rates in the real-cavity model (solid lines) and in the virtual-cavity model (dotted lines, the dashed-dotted lines correspond to   only) for a single-resonance medium with permittivity (8.29).

In Figs. 8.2 8.5 the behaviour of the spontaneous decay of an atom in a spherical cavity with radius R surrounded by a dielectric medium with the single-resonance permittivity of Drude Lorentz type

$$(\ ) = 1 + \frac{\ _P^2}{\ _T^2 \quad ^2 \quad i\ }$$ (8.29)

[$_P$: Plasma frequency; $_T$: transverse resonance frequency] is shown. The solid lines correspond to the real-cavity model [Eq. (8.28)] and the dotted lines to the virtual-cavity model [Eqs. (8.19) and (8.20)], the dash-dotted lines indicating the transverse decay rate (8.20) alone. Around the absorption band, that is in the frequency region between the medium reso-

nance ω_T and the longitudinal frequency $\omega_L = \sqrt{\omega_T^2 + \omega_P^2}$ (here we have taken $\omega_P = 0\,46\,\omega_T$ giving $\omega_L = 1\,1\,\omega_T$) the two models differ considerably. In that region the permittivity (8.29) shows a gap, and the imaginary part $\varepsilon_I(\omega_A)$ is large. Thus, the leading contributions to the decay rate are the terms proportional to R^{-3} which appear with different weights. Comparing Fig. 8.2 with Fig. 8.4 (and Fig. 8.3 with Fig. 8.5), the effect of different values of R on the spontaneous decay rate is clearly seen. The smaller the cavity radius R gets, the larger becomes the contributions from dipole-dipole energy transfer to the surrounding dielectric.

In both models the value of R is undetermined from the outset. The virtual-cavity model assumes a "smearing" of the local electromagnetic field over a sphere with radius R. In the real-cavity model R is associated with a distance from the radiating atom at which the surrounding dielectric can be treated as a continuum. The continuum assumption is certainly not true when we consider the nearest neighbours to the radiating atom. Subsequent studies of microcavities filled with additional atoms are therefore necessary. Experiments measuring the decay rate of a single atom at different frequency could, in connection with Figs 8.2 8.5, provide a value of R that should be used in the models.

8.3   Spontaneous decay near planar interfaces

Finally we consider the spontaneous decay of an excited atom close to a planar dielectric surface. This configuration has been studied extensively in connection with Casimir and van der Waals forces (see, for example, [160, 163]). It may also serve as the basic configuration in scanning near-field optical microscopy [83].

Suppose the atom is located at a distance z from the surface of the absorbing dielectric. For a planar interface the Green function can again be decomposed into a sum of the vacuum Green function and the reflection term $\boldsymbol{R}(\mathbf{r}\,\mathbf{r}^\prime\,\omega)$ (see the discussion in Sec. 8.2.2). The reflection term can be expanded in terms of vector wave functions (see Appendix C.1) and in the coincidence limit can be given in the form [60, 103, 104, S5]

$$R_{xx}(z\,z\,\omega) = R_{yy}(z\,z\,\omega) = \frac{i}{8\pi}\int_0^\infty dk\,k^3\frac{e^{2i\beta z}}{\beta}r^s(k)\ \ \frac{i}{8\pi q^2}\int_0^\infty dk\,k\,\beta\,e^{2i\beta z}r^p(k) \quad (8.30)$$

$$R_{zz}(z\,z\,\omega) = \frac{i}{4\pi q^2}\int_0^\infty dk\,k^3\frac{e^{2i\beta z}}{\beta}r^p(k) \quad (8.31)$$

$[q = \omega\,c,\ \beta = \sqrt{q^2\ k^2}]$, where $r^p(k)$ and $r^s(k)$ are the usual Fresnel reflection coefficients for p- and s-polarized waves [187]. For a distance z of the atom to the dielectric interface that is much smaller than the transition wavelength $qz\ll 1$, one can evaluate the integrals

in Eqs. (8.30) and (8.31) asymptotically to

$$2R_{xx} = 2R_{yy} = R_{zz} = \frac{1}{16\ q^2 z^3} \frac{(\ )\ 1}{(\ )+1} + \mathcal{O}(z^{-1}) \tag{8.32}$$

which gives rise, after inserting into Eq. (8.9), to a leading term in the decay rate as $[\ =\ _A]$

$$= {}_0\frac{3}{8}\ 1+\frac{d_z^2}{d^2}\quad \frac{c}{{}_A R}^3 \frac{{}_I(\ {}_A)}{(\ {}_A)+1^2} + \mathcal{O}(z^{-1}) \tag{8.33}$$

It is worth noting that this result agrees with the one obtained in an involved microscopic approach [86] using explicitly the Huttner Barnett quantization procedure described in Sec. 2.1 for this speci c inhomogeneous problem.

   From the examples in Secs 8.2 and 8.3 it is clear that the inverse cubic dependence on the distance to the surface of an absorbing material is a general result for nonradiative decay associated with resonant energy transfer, with the numerical prefactors being of geometrical origin. For atoms in the extreme near- eld of an arbitrarily shaped dielectric surface, Eq. (8.33) represents the dominant contribution to the decay rate, because then the atom only feels the e ect of a planar surface.

   To conclude, the theory of the interaction of the electromagnetic eld with atoms in the presence of dielectric bodies enables us to calculate the rate of spontaneous decay of excited atoms in the near absorbing dielectric bodies. The rate formula (8.9), which expresses the dissipation- uctuation theorem, follows from the underlying quantization scheme and is not introduced by hand. When absorption is present, the decay rates are strongly distance-dependent and are dominated by a term R^{-3} that depends on the imaginary part ${}_I(\ )$ of the permittivity function.

9 Summary and Outlook

In this work it has been shown how the phenomenological Maxwell equations can be consistently quantized in the presence of causally and linearly responding dielectric media. The source-quantity representation of the electric-field operator with the Green function in terms of a bosonic vector field has been proved to be consistent with both the standard QED requirements as well as statistical physics (Chapter 2). An immediate consequence is that, specifying the Green function for a bounded dielectric object, three-dimensional input-output relations can be derived (Chapter 3), thereby generalizing the known one-dimensional result.

Based on the simpler one-dimensional input-output relations neglecting dependencies on polarization and incident angle the theory of quantum-state transformation by absorbing and amplifying dielectric four-port devices has been developed (Chapter 4). From there it was possible to derive closed formulas for the full density operator of the outgoing field leaving a dielectric device from the quantum state of the impinging field and the device properties. Applications to the transformation of coherent states and Fock states have been presented. Knowing the full density operator of the outgoing field, one can study decoherence and entanglement degradation of entangled states interacting with a noisy optical system such as a fibre. Upper bounds on the entanglement content have been derived using the convexity property of the relative entropy (Chapter 5). Moreover, for the first time an upper bound for Gaussian states has been derived that explicitly uses a particular separability criterion. The example of entanglement degradation of a two-mode squeezed vacuum state shows that decoherence becomes exponentially faster the more nonclassical the state becomes. Additionally, it could be shown that there exists an absolute upper limit on the amount of entanglement that can be transmitted through an optical fibre of given length.

Entanglement degradation inhibits perfect teleportation for which maximally entangled states would be necessary. Possible extensions of the standard teleportation scheme have been presented for qubits, i.e. two-level systems (Chapter 6). In particular, choosing multipartite entangled states and appropriate filtering has been shown to increase the average teleportation fidelity. The loss mechanism has been chosen such that it does not leave the Hilbert space within which teleportation is going to be performed. That means, the same mechanism is responsible for entanglement degradation in continuous-variable teleportation, too. It has been realized that even the choice of displacement and the location of the entanglement source play an important role in optimizing the fidelity of noisy teleportation [138, 141, 142].

Having developed the general theory of quantized light interacting with a dielectric surrounding, additional atomic sources were coupled to the medium-assisted Maxwell eld (Chapter 7). The dielectric surroundings have been shown to change the atomic dynamics. In particular, the equations of motion in the Heisenberg picture and Markovian approximation have been derived, and the important problem of modi ed spontaneous decay in absorbing dielectrics and near dielectric surfaces has been discussed (Chapter 8). For absorbing media the spontaneous decay rate strongly depends on the distance of the atom to the dielectric. The leading term which depends on the inverse cube distance can be regarded as corresponding to nonradiative decay. In principle, also the Schrodinger picture can be treated which leads to (integro-) di erential equations of c-number wave functions. This was successfully done in [153, 154, S11], where also the emitted radiation from the decaying atom near a dielectric microsphere and inside a spherical microcavity have been computed. Placing an excited atom and an atom in its ground state on opposite sides close to the surface of a dielectric microsphere, the spontaneous decay of the excited atom can generate entanglement by reabsorption of the emitted photon by the other atom [155].

The input-output coupling formalism is suitable not only for slab-like systems but also for more general geometries such as cavities. General group-theoretical considerations may help in the search for decoherence-free subspaces in dielectric systems [192]. They principally allow for entangling atoms in dissipative environments. This surprising e ect has its origin in monitoring the environment. Usually, the environment is not measured, but instead is traced over. This leads to the familiar phenomenon of entanglement degradation (Chapter 5). Because quantum states in identical Hilbert spaces can have very di erent decoherence properties, a detailed study of the operators associated with the generalized measurements will help classifying entangled states that are robust against decoherence.

In this work the emphasis is mostly on numerical calculation and derivation of upper bounds on the entanglement content measured by the quantum relative entropy. For quantum states in in nite-dimensional Hilbert spaces it is not even known how any entanglement measure could be computed at all. Moreover, quantifying entanglement is an even more conceptual problem since no unique measure has been found so far. It means that requirements on the measure [78, 79] are to be strengthened to narrow the class of candidate measures.

So far, the quantization of the electromagnetic eld in dielectrics primarily has been done in linear media at rest. In view of recent proposals for observing relativistic quantum e ects such as Hawking radiation in optical systems [193, 194], based on the existence of horizon-like singularities for light in moving media (for discussions on the horizon problem, see for example [195, 196]), a quantum theory of light in moving dielectric and magnetic media is desired. Relativistic quantum electrodynamics in dielectrics with real and frequency-

independent refractive index have already been discussed in [17, 18], and dispersion in the dielectric permittivity was into account in [35], but a fully causal response theory that necessarily includes absorption is still missing. Moreover, a consistent quantum theory of radiation in moving dielectrics may help to better understand the phenomenon of sonoluminescence [197, 198, 199].

Both Hawking radiation and sonoluminescence are particle (photon) production processes that can e ectively be described by input-output coupling connected with non-compact groups comparable to the quantum-state transformation by amplifying four-port devices derived in Sec. 4.3. Therefore, the input-output relations have to be extended to moving media as well. The input-output relations at arbitrarily shaped objects, for example air bubbles in water responsible for sonoluminescence, even for dielectric media at rest have not yet been fully understood. The general theory should hence be explored further, especially in connection with polarization e ects.

A   Integral relation for Green functions

The partial differential equation satisfied by the Green function of a medium which responds to both electric and magnetic fields reads

$$\nabla \times (\mu^{-1}(\mathbf{s}) \nabla \times) \, \boldsymbol{G}(\mathbf{s}, \mathbf{r}, \omega) - \frac{\omega^2}{c^2} \varepsilon(\mathbf{s}, \omega) \boldsymbol{G}(\mathbf{s}, \mathbf{r}, \omega) = \delta(\mathbf{s} - \mathbf{r}) \qquad (A.1)$$

where we restrict ourselves to isotropic media for simplicity. In cartesian coordinates, Eq. (A.1) reads (we drop the ω dependence to save notation)

$$\partial_k^s \mu^{-1}(\mathbf{s}) \partial_n^s G_{ki}(\mathbf{s}, \mathbf{r}) - \partial_k^s \mu^{-1}(\mathbf{s}) \partial_k^s G_{ni}(\mathbf{s}, \mathbf{r}) - \frac{\omega^2}{c^2} \varepsilon(\mathbf{s}) G_{ni}(\mathbf{s}, \mathbf{r}) = \delta_{ni} \delta(\mathbf{s} - \mathbf{r}) \qquad (A.2)$$

If we multiply Eq. (A.2) from the right by $G_{nj}(\mathbf{s}, \mathbf{r}')$ and integrate over $\mathbf{s}$, we obtain after partial integration

$$-\int d^3\mathbf{s} \, \frac{\omega^2}{c^2} \varepsilon(\mathbf{s}) G_{ni}(\mathbf{s}, \mathbf{r}) G_{nj}(\mathbf{s}, \mathbf{r}') + G_{ij}(\mathbf{r}, \mathbf{r}') =$$

$$\int d^3\mathbf{s} \, \mu(\mathbf{s}) \left[\partial_k^s G_{ni}(\mathbf{s}, \mathbf{r}) \right] \partial_k^s G_{nj}(\mathbf{s}, \mathbf{r}') - \int d^3\mathbf{s} \, \mu(\mathbf{s}) \left[\partial_n^s G_{ki}(\mathbf{s}, \mathbf{r}) \right] \partial_k^s G_{nj}(\mathbf{s}, \mathbf{r}') \qquad (A.3)$$

Taking the complex conjugate of Eq. (A.3), and interchanging $j \leftrightarrow i$ and $\mathbf{r} \leftrightarrow \mathbf{r}'$, we arrive at an analogous equation

$$-\int d^3\mathbf{s} \, \frac{\omega^2}{c^2} \varepsilon^*(\mathbf{s}) G_{ni}^*(\mathbf{s}, \mathbf{r}) G_{nj}(\mathbf{s}, \mathbf{r}') + G_{ji}^*(\mathbf{r}, \mathbf{r}') =$$

$$\int d^3\mathbf{s} \, \mu^*(\mathbf{s}) \left[\partial_k^s G_{ni}^*(\mathbf{s}, \mathbf{r}) \right] \partial_k^s G_{nj}(\mathbf{s}, \mathbf{r}') - \int d^3\mathbf{s} \, \mu^*(\mathbf{s}) \left[\partial_k^s G_{ni}^*(\mathbf{s}, \mathbf{r}) \right] \partial_n^s G_{kj}(\mathbf{s}, \mathbf{r}') \qquad (A.4)$$

Subtracting Eq. (A.4) from Eq. (A.3) yields, using Eq. (2.42),

$$\int d^3\mathbf{s} \, \frac{\omega^2}{c^2} \varepsilon_I(\mathbf{s}) G_{in}(\mathbf{r}, \mathbf{s}) G_{jn}^*(\mathbf{r}', \mathbf{s}) - \operatorname{Im} G_{ij}(\mathbf{r}, \mathbf{r}') =$$

$$\int d^3\mathbf{s} \, \mu_I(\mathbf{s}) \left[\partial_k^s G_{in}(\mathbf{r}, \mathbf{s}) \right] \partial_k^s G_{jn}^*(\mathbf{r}', \mathbf{s}) - \partial_n^s G_{jk}^*(\mathbf{r}', \mathbf{s}) \qquad (A.5)$$

For nonmagnetic matter, i.e. for $\mu(\mathbf{r}, \omega) = 1$, the integral relation (2.44) is recovered.

B Green function for isotropic bulk material

An important example is the dyadic Green function for a (homogeneous) bulk material of given permittivity $\varepsilon(\omega)$. The solution of the wave equation of the field of a point-like source

$$\nabla \times \nabla \times \boldsymbol{G}(\mathbf{r},\mathbf{r}') - q^2(\omega)\boldsymbol{G}(\mathbf{r},\mathbf{r}') = \boldsymbol{\delta}(\mathbf{r}-\mathbf{r}') \tag{B.1}$$

where

$$q(\omega) = \frac{\omega}{c}\sqrt{\varepsilon(\omega)} \qquad \sqrt{\varepsilon(\omega)} = \frac{\omega}{c}[n_R(\omega)+in_I(\omega)] \tag{B.2}$$

reads (see for example [89, 102])

$$\boldsymbol{G}(\mathbf{r},\mathbf{r}') = \left[\nabla_{\mathbf{r}}\nabla_{\mathbf{r}'} + \boldsymbol{I}q^2(\omega)\right]\frac{e^{iq(\omega)|\mathbf{r}-\mathbf{r}'|}}{4\pi q^2(\omega)|\mathbf{r}-\mathbf{r}'|} \tag{B.3}$$

It can be split up into a longitudinal and a transverse part ($\boldsymbol{\rho} = \mathbf{r}-\mathbf{r}'$) as [164]

$$\boldsymbol{G}^{\parallel}(\mathbf{r},\mathbf{r}') = -\frac{1}{4\pi q^2(\omega)}\left[\frac{4\pi}{3}\delta(\boldsymbol{\rho})\boldsymbol{I} + \left(\boldsymbol{I} - \frac{3\hat{\boldsymbol{\rho}}\hat{\boldsymbol{\rho}}}{\rho^2}\right)\frac{1}{\rho^3}\right] \tag{B.4}$$

and

$$
\begin{aligned}
\boldsymbol{G}^{\perp}(\mathbf{r},\mathbf{r}') =\ & \frac{1}{4\pi q^2(\omega)}\left[\left(\boldsymbol{I} - \frac{3\hat{\boldsymbol{\rho}}\hat{\boldsymbol{\rho}}}{\rho^2}\right)\frac{1}{\rho^3}\right.\\
& + q^3(\omega)\left[\left(-\frac{1}{q(\omega)\rho}+\frac{i}{[q(\omega)\rho]^2}-\frac{1}{[q(\omega)\rho]^3}\right)\boldsymbol{I}\right.\\
& \left.\left.+\left(\frac{1}{q(\omega)\rho}+\frac{3i}{[q(\omega)\rho]^2}-\frac{3}{[q(\omega)\rho]^3}\right)\frac{\hat{\boldsymbol{\rho}}\hat{\boldsymbol{\rho}}}{\rho^2}\right]e^{iq(\omega)\rho}\right]
\end{aligned}
\tag{B.5}
$$

From Eq. (B.5) is follows that the imaginary part of the transverse part of the Green function in the coincidence limit is given by

$$\operatorname{Im}\boldsymbol{G}^{\perp}(\mathbf{r},\mathbf{r}') = \lim_{\mathbf{r}\to\mathbf{r}'}\operatorname{Im}\boldsymbol{G}^{\perp}(\mathbf{r},\mathbf{r}') = \frac{\omega}{6\pi c}n_R(\omega)\boldsymbol{I} \tag{B.6}$$

For the longitudinal part we have

$$\operatorname{Im}\boldsymbol{G}^{\parallel}(\mathbf{r},\mathbf{r}') = \frac{\varepsilon_I(\omega)}{|\varepsilon(\omega)|^2}\frac{c^2}{4\omega^2}\left[\frac{4\pi}{3}\delta(\boldsymbol{\rho})\boldsymbol{I} + \left(\boldsymbol{I} - \frac{3\hat{\boldsymbol{\rho}}\hat{\boldsymbol{\rho}}}{\rho^2}\right)\frac{1}{\rho^3}\right] \tag{B.7}$$

which vanishes if $\varepsilon_I(\omega)=0$, for example in vacuum where $\varepsilon(\omega)\equiv 1$.

C   Green function for planar and spherical multilayers

C.1   Planar multilayers

In the notation of Sec. 3 the Green function for the electric field in region (layer) X in a planar multilayer dielectric is decomposed as

$$\boldsymbol{G}^{(X)}(\mathbf{r}\,\mathbf{s}\,) = \boldsymbol{G}^{(X0)}(\mathbf{r}\,\mathbf{s}\,)\,\delta_{Xs} + \boldsymbol{G}^{(Xs)}(\mathbf{r}\,\mathbf{s}\,) \tag{C.1}$$

where the subscript s denotes the spatial region (layer) in which the *source* point $\mathbf{s}$ is located. The first term describes the Green function for unbounded homogeneous space and the second term the scattering Green function accounting for the correct boundary conditions at the surfaces of discontinuity. The standard representation of the free Green function is presented in Appendix B. The scattering Green function can always be expanded in terms of its eigenfunctions [89, 102]. In particular, in cylindrical coordinates $(r\,\,z)$ the *even* and *odd* vector wave functions of angular momentum n are [103]

$$\mathbf{M}_{\substack{e\\o}n}(\mathbf{r}\,h) = \left[\frac{nJ_n(\,r)}{r}\,\frac{\sin}{\cos}\,n\,\mathbf{e}_r\,\,\frac{dJ_n(\,r)}{dr}\,\frac{\cos}{\sin}\,n\,\mathbf{e}\,\right]e^{ihz} \tag{C.2}$$

$$\mathbf{N}_{\substack{e\\o}n}(\mathbf{r}\,h) = \frac{1}{k}\left[\,ih\frac{dJ_n(\,r)}{dr}\,\frac{\cos}{\sin}\,n\,\mathbf{e}_r\,\,\frac{ihnJ_n(\,r)}{r}\,\frac{\sin}{\cos}\,n\,\mathbf{e}\,\right.$$
$$\left.+\,\,{}^2J_n(\,r)\,\frac{\cos}{\sin}\,n\,\mathbf{e}_z\,\right]e^{ihz} \tag{C.3}$$

$[J_n(\,r)$: Bessel function; $h^2 + \,{}^2 = k^2]$. The scattering Green function $\boldsymbol{G}^{(Xs)}(\mathbf{r}\,\mathbf{s}\,)$ can then be written in the form [103]

$$\boldsymbol{G}^{(Xs)}(\mathbf{r}\,\mathbf{s}\,) = \frac{i}{4}\,\int_0^{}d\,\sum_{n=0}^{}\frac{2\,\,_{0n}}{h_s}$$

$$(1\,\,_{X3})\mathbf{M}_{\substack{e\\o}n}(\mathbf{r}\,h_X)\,\left[(1\,\,_{s1})A_M^{Xs}\mathbf{M}_{\substack{e\\o}n}(\mathbf{s}\,\,h_s) + (1\,\,_{s3})B_M^{Xs}\mathbf{M}_{\substack{e\\o}n}(\mathbf{s}\,h_s)\right]$$

$$+(1\,\,_{X3})\mathbf{N}_{\substack{e\\o}n}(\mathbf{r}\,h_X)\,\left[(1\,\,_{s1})A_N^{Xs}\mathbf{N}_{\substack{e\\o}n}(\mathbf{s}\,\,h_s) + (1\,\,_{s3})B_N^{Xs}\mathbf{N}_{\substack{e\\o}n}(\mathbf{s}\,h_s)\right]$$

$$+(1\,\,_{X1})\mathbf{M}_{\substack{e\\o}n}(\mathbf{r}\,\,h_X)\,\left[(1\,\,_{s1})C_M^{Xs}\mathbf{M}_{\substack{e\\o}n}(\mathbf{s}\,\,h_s) + (1\,\,_{s3})D_M^{Xs}\mathbf{M}_{\substack{e\\o}n}(\mathbf{s}\,h_s)\right]$$

$$+(1\,\,_{X1})\mathbf{N}_{\substack{e\\o}n}(\mathbf{r}\,\,h_X)\,\left[(1\,\,_{s1})C_N^{Xs}\mathbf{N}_{\substack{e\\o}n}(\mathbf{s}\,\,h_s) + (1\,\,_{s3})D_N^{Xs}\mathbf{N}_{\substack{e\\o}n}(\mathbf{s}\,h_s)\right]$$

$$\tag{C.4}$$

where the scattering coefficients A^{Xs}_{MN}, B^{Xs}_{MN}, C^{Xs}_{MN}, and D^{Xs}_{MN} are determined by the boundary conditions at the interfaces between the layers and can be found in the literature [102, 103]. Note that the expansion (C.4) only involves vector wave functions of the same type. The TE(TM) vector wave functions are associated with $s(p)$-polarized waves. It means that different polarizations do not mix during the scattering process at a planar multilayer.

C.2   Spherical multilayers

Analogously, in the case of a spherical multilayer (here we need only two layers) we expand the reflection term $\boldsymbol{R}(\mathbf{r}, \mathbf{r}')$ in the full Green function (8.22) as [200, 201]

$$
\boldsymbol{R}(\mathbf{r}, \mathbf{r}') = \frac{i}{4\pi c} \sum_{e,o} \sum_{n=1}^{n} \sum_{m=0} \frac{2n+1}{n(n+1)} \frac{(n-m)!}{(n+m)!} (2 - \delta_{0m})
$$

$$
C^M_n(\omega) \mathbf{M}^e_{o\,nm}\left(\mathbf{r}, \frac{\omega}{c}\right) \mathbf{M}^e_{o\,nm}\left(\mathbf{r}', \frac{\omega}{c}\right)
$$

$$
+ C^N_n(\omega) \mathbf{N}^e_{o\,nm}\left(\mathbf{r}, \frac{\omega}{c}\right) \mathbf{N}^e_{o\,nm}\left(\mathbf{r}', \frac{\omega}{c}\right) \tag{C.5}
$$

The functions $\mathbf{M}^e_{o\,nm}(\mathbf{r}, k)$ and $\mathbf{N}^e_{o\,nm}(\mathbf{r}, k)$ in Eq. (C.5) are the (*even* and *odd*) TE and TM vector wave functions defined by

$$
\mathbf{M}^e_{o\,nm}(\mathbf{r}, k) = \nabla \times \psi^e_{o\,nm}(\mathbf{r}, k)\mathbf{r} \tag{C.6}
$$

$$
\mathbf{N}^e_{o\,nm}(\mathbf{r}, k) = \frac{1}{k} \nabla \times \nabla \times \psi^e_{o\,nm}(\mathbf{r}, k)\mathbf{r} \tag{C.7}
$$

with the generating function in spherical coordinates (r, θ, ϕ)

$$
\psi^e_{o\,nm}(\mathbf{r}, k) = j_n(kr) P^m_n(\cos\theta) \begin{matrix} \cos \\ \sin \end{matrix} (m\phi) \tag{C.8}
$$

[$j_n(kr)$: spherical Bessel function of the first kind; $P^m_n(\cos\theta)$: associated Legendre polynomial]. The functions $C^{M(N)}_n$ in Eqs. (C.6) and (C.7) are the generalized reflection coefficients whose lengthy expressions can be read off from [200, 201].

D   Derivation of the unitary matrix

With the definition (4.4) of $\mathbf{U}(\omega)$ and the relations (3.5) and (4.2) we write the sought (4×4)-matrix as

$$\mathbf{U}(\omega) = \begin{pmatrix} \mathbf{T}(\omega) & \mathbf{A}(\omega) \\ \mathbf{F}(\omega) & \mathbf{G}(\omega) \end{pmatrix} \tag{D.1}$$

where the transmission and absorption matrices $\mathbf{T}(\omega)$ and $\mathbf{A}(\omega)$ satisfy the relation (3.7). Accordingly, since we require also the operators $h_i(\omega)$ to be bosonic, we must also have

$$\mathbf{F}(\omega)\mathbf{F}^+(\omega) + \mathbf{G}(\omega)\mathbf{G}^+(\omega) = \mathbf{I} \tag{D.2}$$

Unitarity of $\mathbf{U}(\omega)$ leads to the additional constraint

$$\mathbf{F}(\omega)\mathbf{T}^+(\omega) + \mathbf{G}(\omega)\mathbf{A}^+(\omega) = \mathbf{0} \tag{D.3}$$

From Eq. (D.3) we find that

$$\mathbf{F}(\omega) = -\mathbf{G}(\omega)\mathbf{A}^+(\omega)\left[\mathbf{T}^+(\omega)\right]^{-1} \tag{D.4}$$

Substitution of Eq. (D.4) into Eq. (D.2) leads to

$$\mathbf{G}(\omega)\left[\mathbf{I} + \mathbf{A}^+(\omega)\left[\mathbf{T}(\omega)\mathbf{T}^+(\omega)\right]^{-1}\mathbf{A}(\omega)\right]\mathbf{G}^+(\omega) = \mathbf{I} \tag{D.5}$$

from which we obtain

$$\mathbf{I} + \mathbf{A}^+(\omega)\left[\mathbf{T}(\omega)\mathbf{T}^+(\omega)\right]^{-1}\mathbf{A}(\omega) = \left[\mathbf{G}^+(\omega)\mathbf{G}(\omega)\right]^{-1} \tag{D.6}$$

Using the relation $\mathbf{T}(\omega)\mathbf{T}^+(\omega) + \mathbf{A}(\omega)\mathbf{A}^+(\omega) = \mathbf{I}$ [Eq. (3.7)], we find that

$$\mathbf{G}^+(\omega)\mathbf{G}(\omega) = \mathbf{I} - \mathbf{A}(\omega)\mathbf{A}^+(\omega) \tag{D.7}$$

the general solution of which is

$$\mathbf{G}(\omega) = \mathbf{D}(\omega)\mathbf{C}(\omega)\mathbf{S}^{-1}(\omega)\mathbf{A}(\omega) \tag{D.8}$$

with the matrices $\mathbf{C}(\omega)$ and $\mathbf{S}(\omega)$ defined as [Eq. (4.6)]

$$\mathbf{C}(\omega) = \overline{\mathbf{T}(\omega)\mathbf{T}^+(\omega)} \qquad \mathbf{S}(\omega) = \overline{\mathbf{A}(\omega)\mathbf{A}^+(\omega)} \tag{D.9}$$

and $\mathbf{D}(\ )$ being a unitary, but otherwise arbitrary, $(2\ 2)$-matrix. Inserting the solution for $\mathbf{G}(\ )$ into Eq. (D.4), we obtain the general solution

$$\mathbf{F}(\ ) = \mathbf{D}(\ )\mathbf{S}(\ )\mathbf{C}^{1}(\ )\mathbf{T}(\ ) \tag{D.10}$$

Combining Eqs. (D.1), (D.9), and (D.10), we derive the general form of the unitary matrix $(\ )$ as

$$(\ ) = \begin{pmatrix} \mathbf{T}(\ ) & \mathbf{A}(\ ) \\ \mathbf{D}(\ )\mathbf{S}(\ )\mathbf{C}^{1}(\ )\mathbf{T}(\ ) & \mathbf{D}(\ )\mathbf{C}(\ )\mathbf{S}^{1}(\ )\mathbf{A}(\ ) \end{pmatrix} \tag{D.11}$$

Absorbing the matrix $\mathbf{D}(\ )$ into the additional device operators $h_i(\ )$, and absorbing a common phase $e^{i\ (\ )}$ into the input operators $a_i(\ )$ and $g_i(\ )$, the matrix $(\ )$ represents an element of the special unitary group SU(4).

E   Factorization of the U(4)-matrix

The matrix (4.5) [hence the general matrix (D.11) with $\mathbf{D}(\ ) = \mathbf{I}$] can be decomposed into the product

$$(\ ) = {}_2(\ )\ {}_1(\ ) \tag{E.1}$$

where

$$
{}_1(\ ) = \begin{pmatrix} \mathbf{C}^{-1}(\ )\mathbf{T}(\ ) & \mathbf{0} \\ \mathbf{0} & \mathbf{S}^{-1}(\ )\mathbf{A}(\ ) \end{pmatrix} \quad \text{and} \quad {}_2(\ ) = \begin{pmatrix} \mathbf{C}(\ ) & \mathbf{S}(\ ) \\ \mathbf{S}(\ ) & \mathbf{C}(\ ) \end{pmatrix} \tag{E.2}
$$

Whereas the matrix ${}_1(\ )$ is already in Jordan form, thus representing two lossless beam splitters acting on $a_i(\ )$ and $g_i(\ )$ alone, matrix ${}_2(\ )$ can be brought into quasidiagonal form ${}_2(\ )$ by the unitary transformation

$$
{}_2(\ ) = {}^+\ {}_2(\ ) \tag{E.3}
$$

with

$$
{}_2(\ ) = \begin{pmatrix} \mathbf{C}(\ ) & i\mathbf{S}(\ ) & \mathbf{0} \\ \mathbf{0} & \mathbf{C}(\ ) + i\mathbf{S}(\ ) \end{pmatrix} \quad \text{and} \quad = \frac{1}{\sqrt{2}} \begin{pmatrix} \mathbf{I} & i\mathbf{I} \\ i\mathbf{I} & \mathbf{I} \end{pmatrix} \tag{E.4}
$$

The decomposition (E.1), together with Eq. (E.3), corresponds to a decomposition into eight U(2) group transformations. Each of the matrices describes two U(2) transformations which can be seen as follows. Denoting by $\mathbf{Y}$ the (2×2)-matrix

$$
\mathbf{Y} = \frac{1}{\sqrt{2}} \begin{pmatrix} 1 & i \\ i & 1 \end{pmatrix} \tag{E.5}
$$

we can bring into Jordan form by formally exchanging the second and third row and the second and third column giving

$$
= \begin{pmatrix} \mathbf{Y} & \mathbf{0} \\ \mathbf{0} & \mathbf{Y} \end{pmatrix} \tag{E.6}
$$

Putting all matrices together and interchanging the correct rows and columns (input and output variables, respectively), the beam splitter network is readily obtained.

F Fock-state transformation by amplifying four-port devices

When the input field is prepared in a Fock state $|p\,q\rangle$ and the device in the ground state $|0\,0\rangle$, so that the overall input state is $|p\,q\,0\,0\rangle$, then the input Wigner function reads as

$$W_{\text{in}}(\boldsymbol{\alpha}) = \left(\frac{2}{\pi}\right)^4 (-1)^{p+q}\, e^{-2(|g_1|^2+|g_2|^2)} L_p(4|a_1|^2)\, L_q(4|a_2|^2)\, e^{-2(|a_1|^2+|a_2|^2)} \tag{F.1}$$

with $L_n(x)$ being the Laguerre polynomial. We now apply Eq. (4.57), making the substitutions according

$$\mathbf{a} \;\to\; \mathbf{T}^+\mathbf{a} - \mathbf{T}^+\mathbf{C}^{-1}\mathbf{S}\,\mathbf{g} \tag{F.2}$$

$$\mathbf{a}^* \;\to\; \mathbf{T}^T\mathbf{a}^* - \mathbf{T}^T(\mathbf{C}^T)^{-1}\mathbf{S}^T\mathbf{g}^* \tag{F.3}$$

$$\mathbf{g} \;\to\; \mathbf{A}^T\mathbf{a}^* + \mathbf{A}^T(\mathbf{S}^T)^{-1}\mathbf{C}^T\mathbf{g}^* \tag{F.4}$$

$$\mathbf{g}^* \;\to\; \mathbf{A}^+\mathbf{a} + \mathbf{A}^+\mathbf{S}^{-1}\mathbf{C}\,\mathbf{g} \tag{F.5}$$

Finally, we integrate over the device variables g_i to obtain the Wigner function of the outgoing field. Introducing the matrix $K_{ii} = \delta_{ii}\,k_i$ and employing the formula

$$4|a|^2 e^{-2|a|^2} = -\frac{\partial}{\partial k}\, e^{-2|a|^2+4k|a|^2}\Big|_{k=0} \tag{F.6}$$

we derive

$$W_{\text{out}}^{(F)}(\mathbf{a}\,\mathbf{a}^*) = \left(\frac{2}{\pi}\right)^2 \sum_{h=0}^{p}\sum_{l=0}^{q} \frac{(-1)^{h+p}}{h!}\binom{p}{h} \frac{(-1)^{l+q}}{l!}\binom{q}{l} \frac{\partial^h}{\partial k_1^h}\frac{\partial^l}{\partial k_2^l}$$

$$\times \left.\frac{\exp\left\{-2(\mathbf{a}^*)^T[\mathbf{N}-\mathbf{B}^T(\mathbf{D}^T)^{-1}\mathbf{B}]\mathbf{a}\right\}}{\det \mathbf{D}}\right|_{k_1=k_2=0} \tag{F.7}$$

where the abbreviations

$$\mathbf{N} \;=\; 2\mathbf{T}\mathbf{T}^+ - \mathbf{I} - 2\mathbf{T}\mathbf{K}\mathbf{T}^+ \tag{F.8}$$

$$\mathbf{B} \;=\; 2\mathbf{S}^T\mathbf{C}^T - 2\mathbf{S}\mathbf{C}^{-1}\mathbf{T}\mathbf{K}\mathbf{T}^T \tag{F.9}$$

$$\mathbf{D} \;=\; 2\mathbf{T}\mathbf{T}^T - \mathbf{I} - 2\mathbf{S}\mathbf{C}^{-1}\mathbf{T}\,\mathbf{K}\mathbf{T}^T\mathbf{C}^T\mathbf{S}^T \tag{F.10}$$

have been used. In order to calculate from the Wigner function the density operator, we make use of the relation [110]

$$\varrho_{\text{out}}^{(F)} = \pi^2 \int d^2\mathbf{a}\, W_{\text{out}}^{(F)}(\mathbf{a}\,\mathbf{a}^*)\,\delta(\mathbf{a}-\mathbf{a}^*) \tag{F.11}$$

where

$$\langle \mathbf{a} | \rho | \mathbf{a} \rangle = \frac{1}{\pi^4} \int d^2\mathbf{b}\, D(\mathbf{b})\, e^{\mathbf{a}^T\mathbf{b} - \mathbf{b}^T\mathbf{a}} \tag{F.12}$$

with $D(\mathbf{b})$ being the two-mode coherent displacement operator. For notational convenience we introduce the abbreviation notation

$$\mathcal{D}\begin{bmatrix} p & q \\ \\ h=0 \ l=0 \end{bmatrix} = \sum_{h=0}^{p}\sum_{l=0}^{q} \frac{(-1)^{h+p}}{h!}\binom{p}{h} \frac{(-1)^{l+q}}{l!}\binom{q}{l} \frac{\partial^h}{\partial k_1^h}\frac{\partial^l}{\partial k_2^l} \Bigg|_{k_1=k_2=0} \tag{F.13}$$

Substitution of Eq. (F.7) into Eq. (F.11) yields

$$\rho_{\text{out}}^{(F)} = \mathcal{D} \frac{4}{\pi^4 \det \mathbf{D}} \int d^2\mathbf{a}\, d^2\mathbf{b}\, D(\mathbf{b})\exp\left[2\mathbf{a}^+\mathbf{M}\mathbf{a} + \mathbf{a}^T\mathbf{b} - \mathbf{b}^T\mathbf{a}\right] \tag{F.14}$$

where $\mathbf{M} \equiv \mathbf{N} - \mathbf{B}^T(\mathbf{D}^T)^{-1}\mathbf{B}^+$. Using the Fock-state representation of the (single-mode) coherent displacement operator [110],

$$\langle m | D(b) | n \rangle = \sqrt{\frac{n!}{m!}} b^{m-n} e^{-|b|^2/2} L_n^{(m-n)}(|b|^2) \tag{F.15}$$

$[L_n^m(x)$, associated Laguerre polynomial], we can calculate the density matrix in the Fock basis. Performing the $\mathbf{a}$ integrals in Eq. (F.14), we derive

$$\langle m_1\, m_2 | \rho_{\text{out}}^{(F)} | n_1\, n_2 \rangle = \mathcal{D} \frac{1}{\pi^2 \det \mathbf{DM}}\bigg|_{n_1\, n_2\, m_1\, m_2} \sqrt{\frac{n_1! n_2!}{m_1! m_2!}} \int r_1 dr_1\, r_2 dr_2\, d\phi_1\, d\phi_2$$

$$\times \exp\left[\frac{1}{2}r_1^2\left(1+\frac{M_{22}}{\det \mathbf{M}}\right) - \frac{1}{2}r_2^2\left(1+\frac{M_{11}}{\det \mathbf{M}}\right) + \frac{|M_{12}|}{\det \mathbf{M}}r_1 r_2 \cos(\phi + \phi_2 - \phi_1)\right]$$

$$\times r_1^{m_1-n_1} r_2^{m_2-n_2} e^{i\phi_1(m_1-n_1)+i\phi_2(m_2-n_2)} L_{n_1}^{(m_1-n_1)}(r_1^2) L_{n_2}^{(m_2-n_2)}(r_2^2) \tag{F.16}$$

where we have used the notation $b_i = r_i e^{i\phi_i}$, and $M_{12} = |M_{12}| e^{i\phi}$. Recalling the definition of the modified Bessel functions, we perform the angular integrals to obtain

$$\langle m_1\, m_2 | \rho_{\text{out}}^{(F)} | n_1\, n_2 \rangle =$$

$$\mathcal{D} \frac{1}{\det \mathbf{DM}}\bigg|_{n_1\, n_2\, m_1\, m_2} \sqrt{\frac{n_1! n_2!}{m_1! m_2!}} e^{i\phi(m_2-n_2)} \delta_{m_1-n_1+m_2-n_2\, 0}$$

$$\times \int_0^\infty dx_1\, dx_2 \exp\left[\frac{1}{2}x_1\left(1+\frac{M_{22}}{\det \mathbf{M}}\right) - \frac{1}{2}x_2\left(1+\frac{M_{11}}{\det \mathbf{M}}\right)\right]$$

$$\times I_{m_2-n_2}\left(\frac{|M_{12}|}{\det \mathbf{M}}\sqrt{x_1 x_2}\right) x_1^{(m_1-n_1)/2} x_2^{(m_2-n_2)/2} L_{n_1}^{(m_1-n_1)}(x_1)\, L_{n_2}^{(m_2-n_2)}(x_2) \tag{F.17}$$

$(x_i = r_i^2)$. The x_2 integral is performed by means of the formula (2.19.12.6) in [202], which gives (for $m_2 \geq n_2$)

$$
\langle m_1\, m_2 |\, \hat{\varrho}_{\text{out}}^{(F)} \,| n_1\, n_2 \rangle =
$$

$$
\mathcal{D}\left(\frac{2}{\det \mathbf{D}}\right)_{n_1 n_2 m_1 m_2} \sqrt{\frac{n_1! n_2!}{m_1! m_2!}} (M_{12})^{m_2-n_2}\, \delta_{m_1-n_1+m_2-n_2,0}\, \frac{(M_{11}-\det \mathbf{M})^{n_2}}{(M_{11}+\det \mathbf{M})^{m_2+1}}
$$

$$
\int_0^\infty dx_1 \exp\left[-\frac{x_1}{2}\left(1+\frac{1+M_{22}}{M_{11}+\det \mathbf{M}}\right)\right] L_{n_1}^{(m_1-n_1)}(x_1)\, L_{n_2}^{(m_2-n_2)}\left(\frac{M_{12}^2}{M_{11}^2-(\det \mathbf{M})^2}x_1\right)
$$

$$
\tag{F.18}
$$

Finally, the x_1 integral is performed by expanding the associated Laguerre polynomials into power series [190]. The result is

$$
\langle m_1\, m_2 |\, \hat{\varrho}_{\text{out}}^{(F)} \,| n_1\, n_2 \rangle =
$$

$$
\mathcal{D}\left(\frac{2}{\det \mathbf{D}}\right)_{n_1 n_2 m_1 m_2} \sqrt{\frac{n_1! n_2!}{m_1! m_2!}}\, \delta_{m_1-n_1+m_2-n_2,0}\, \frac{(M_{11}-\det \mathbf{M})^{n_2}}{(M_{11}+\det \mathbf{M})^{m_2+1}} (M_{12})^{m_2-n_2} \binom{m_1}{n_1}
$$

$$
\sum_{k=0}^{n_2} \frac{c^k}{a^{k+1}} \binom{m_2}{n_2-k}\, {}_2F_1\left(k+1,-n_1; m_1-n_1+1; \frac{1}{a}\right)
\tag{F.19}
$$

where
$$
a = \frac{1+M_{11}+M_{22}+\det \mathbf{M}}{2(M_{11}+\det \mathbf{M})} \qquad c = \frac{M_{12}^2}{(\det \mathbf{M})^2 - M_{11}^2}
\tag{F.20}
$$

Integrating Eq. (F.7) over the phase space of one mode of the outgoing field yields the Wigner function of the quantum state of the other mode

$$
W_{\text{out}}^{(F)}(a_i, a_i^*) = \frac{2}{\pi}\sum_{h=0}^p \sum_{l=0}^q \frac{(-1)^{h+p}}{h!}\binom{p}{h}\frac{(-1)^{l+q}}{l!}\binom{q}{l}\frac{\partial^h}{\partial k_1^h}\frac{\partial^l}{\partial k_2^l}\frac{\det \mathbf{E}}{E_{ii}\det \mathbf{D}}\, e^{-2|a_i|^2 E_{ii}}\Big|_{k_1=k_2=0}
$$

$$
\tag{F.21}
$$

$(\mathbf{E} = \mathbf{M}^{-1})$. This Wigner function is equivalent to the density matrix in the Fock basis

$$
\langle \hat{\varrho}_{\text{out}\, i}^{(F)} \rangle = \sum_{n=0}^\infty \sum_{h=0}^p \sum_{l=0}^q \frac{(-1)^{h+l+p+q}}{h!l!}\binom{p}{h}\binom{q}{l}\frac{\partial^{h+l}}{\partial k_1^h \partial k_2^l}\frac{\det \mathbf{E}}{\det \mathbf{D}}\frac{2}{E_{ii}+1}\left(\frac{E_{ii}-1}{E_{ii}+1}\right)^n |n\rangle\langle n|\Big|_{k_1=k_2=0}
$$

$$
\tag{F.22}
$$

Bibliography

[1] B. Yurke, S. L. McCall, and J. R. Klauder, Phys. Rev. A **33**, 4033 (1986).

[2] S. Prasad, M. O. Scully, and W. Martienssen, Opt. Commun. **62**, 139 (1987).

[3] Z. Y. Ou, C. K. Hong, and L. Mandel, Opt. Commun. **63**, 118 (1987).

[4] H. Fearn and R. Loudon, Opt. Commun. **64**, 485 (1987).

[5] M. A. Campos, B. E. A. Saleh, and M. C. Teich, Phys. Rev. A **40**, 1371 (1989).

[6] U. Leonhardt, Phys. Rev. A **48**, 3265 (1993).

[7] C. H. Bennett, F. Bessette, G. Brassard, L. Salvail, and J. Smolin, J. Crypt. **5**, 3 (1992).

[8] P. D. Townsend, J. G. Rarity, and P. R. Tapster, Electronics Letters **29**, 1291 (1993).

[9] A. Muller, J. Breguet, and N. Gisin, Europhys. Lett. **23**, 383 (1993).

[10] T. Jennewein, C. Simon, G. Weihs, H. Weinfurter, and A. Zeilinger, Phys. Rev. Lett. **84**, 4729 (2000).

[11] D. S. Naik, C. G. Peterson, A. G. White, A. J. Berglund, and P. G. Kwiat, Phys. Rev. Lett. **84**, 4733 (2000).

[12] W. Tittel, J. Brendel, H. Zbinden, and N. Gisin, Phys. Rev. Lett. **84**, 4737 (2000).

[13] D. Bouwmeester, J. W. Pan, K. Mattle, M. Eibl, H. Weinfurter, and A. Zeilinger, Nature **390**, 575 (1997).

[14] D. Boschi, S. Branca, F. DeMartini, L. Hardy, and S. Popescu, Phys. Rev. Lett. **80**, 1121 (1998).

[15] D. Bouwmeester, K. Mattle, J. W. Pan, H. Weinfurter, A. Zeilinger, and M. Zukowski, Appl. Phys. B **67**, 749 (1998).

[16] J. S. Bell, Physics (Long Island City, NY) **1**, 194 (1964).

[17] J. M. Jauch and K. M. Watson, Phys. Rev. **74**, 950 (1948).

[18] J. M. Jauch and K. M. Watson, Phys. Rev. **74**, 1485 (1948).

[19] Y. R. Shen, Phys. Rev. **155**, 921 (1967).

[20] C. K. Carniglia and L. Mandel, Phys. Rev. D **3**, 280 (1971).

[21] I. Bialynicki-Birula and J. B. Brojan, Phys. Rev. D **5**, 485 (1972).

[22] I. Abram, Phys. Rev. A **35**, 4661 (1987).

[23] Z. Bialynicki-Birula and I. Bialynicki-Birula, J. Opt. Soc. Am. B **4**, 1621 (1987).

[24] L. Knoll, W. Vogel, and D.-G. Welsch, Phys. Rev. A **36**, 3803 (1987).

[25] T. A. B. Kennedy and E. M. Wright, Phys. Rev. A **38**, 212 (1988).

[26] H. Khosravi and R. Loudon, Proc. R. Soc. London Ser. A **433**, 337 (1991).

[27] H. Khosravi and R. Loudon, Proc. R. Soc. London Ser. A **436**, 373 (1992).

[28] R. J. Glauber and M. Lewenstein, Phys. Rev. A **43**, 467 (1991).

[29] L. Knoll and D.-G. Welsch, Prog. Quant. Electr. **16**, 135 (1992).

[30] W. Vogel, D.-G. Welsch, and S. Wallentowitz, *Quantum Optics, An Introduction* (Wiley-VCH, Berlin, 2001).

[31] B. J. Dalton, E. S. Guerra, and P. L. Knight, Phys. Rev. A **54**, 2292 (1996).

[32] M. Bordag, K. Kirsten, and D. V. Vassilevich, J. Phys. A: Math. Gen. **31**, 2381 (1998).

[33] B. J. Dalton, S. M. Barnett, and P. L. Knight, J. Mod. Opt. **46**, 1315 (1999).

[34] B. J. Dalton, S. M. Barnett, and P. L. Knight, J. Mod. Opt. **46**, 1495 (1999).

[35] K. M. Watson and J. M. Jauch, Phys. Rev. **75**, 1249 (1949).

[36] G. S. Agarwal, Phys. Rev. A **11**, 230 (1975).

[37] G. S. Agarwal, Phys. Rev. A **11**, 243 (1975).

[38] B. Huttner, J. J. Baumberg, and S. M. Barnett, Europhys. Lett. **16**, 177 (1991).

[39] P. D. Drummond, Phys. Rev. A **42**, 6845 (1990).

[40] P. W. Milonni, J. Mod. Opt. **42**, 1991 (1995).

[41] D. J. Santos and R. Loudon, Phys. Rev. A **52**, 1538 (1995).

[42] Z. Hradil, Phys. Rev. A **53**, 3687 (1996).

[43] P. D. Drummond and M. Hillery, Phys. Rev. A **59**, 691 (1999).

[44] M. Hillery and L. D. Mlodinow, Phys. Rev. A **30**, 1860 (1984).

[45] I. Abram and E. Cohen, Phys. Rev. A **44**, 500 (1991).

[46] L. G. Joneckis and J. H. Shapiro, J. Opt. Soc. Am. B **10**, 1102 (1993).

[47] L.-M. Duan and G.-C. Guo, Phys. Rev. A **56**, 925 (1997).

[48] E. M. Lifshitz, Sov. Phys. JETP **2**, 73 (1956).

[49] M. Fleischhauer and M. Schubert, J. Mod. Opt. **38**, 677 (1991).

[50] L. Knoll and U. Leonhardt, J. Mod. Opt. **39**, 1253 (1992).

[51] B. Huttner and S. M. Barnett, Europhys. Lett. **18**, 487 (1992).

[52] B. Huttner and S. M. Barnett, Phys. Rev. A **46**, 4306 (1992).

[53] S.-T. Ho and P. Kumar, J. Opt. Soc. Am. B **10**, 1620 (1993).

[54] R. Matloob, R. Loudon, S. M. Barnett, and J. Je ers, Phys. Rev. A **52**, 4823 (1995).

[55] S. M. Barnett, C. R. Gilson, B. Huttner, and N. Imoto, Phys. Rev. Lett. **77**, 1739 (1996).

[56] R. Matloob and R. Loudon, Phys. Rev. A **53**, 4567 (1996).

[57] J. R. Anglin and W. H. Zurek, Phys. Rev. D **53**, 7327 (1996).

[58] A. Tip, Phys. Rev. A **56**, 5022 (1997).

[59] A. Tip, Phys. Rev. A **57**, 4818 (1998).

[60] H. T. Dung, L. Knoll, and D.-G. Welsch, Phys. Rev. A **57**, 3931 (1998).

[61] A. Bechler, J. Mod. Opt. **46**, 901 (1999).

[62] R. Matloob, Phys. Rev. A **60**, 50 (1999).

[63] O. DiStefano, S. Savasta, and R. Girlanda, Phys. Rev. A **60**, 1614 (1999).

[64] O. DiStefano, S. Savasta, and R. Girlanda, Phys. Rev. A **61**, 023803 (2000).

[65] O. DiStefano, S. Savasta, and R. Girlanda, J. Mod. Opt. **48**, 67 (2001).

[66] J. J. Hopeld, Phys. Rev. **112**, 1555 (1958).

[67] K. Friedrichs, Commun. Pure Appl. Math. **1**, 361 (1948).

[68] U. Fano, Phys. Rev. **103**, 1202 (1956).

[69] T. Gruner and D.-G. Welsch, in *Third Workshop on Quantum Field Theory under the Inuence of External Conditions (Leipzig, 1995)*, edited by M. Bordag (Teubner, Stuttgart, Leipzig, 1996).

[70] T. Gruner and D.-G. Welsch, Phys. Rev. A **53**, 1818 (1996).

[71] T. Gruner and D.-G. Welsch, Phys. Rev. A **54**, 1661 (1996).

[72] T. Gruner and D.-G. Welsch, Opt. Commun. **134**, 447 (1997).

[73] S. M. Barnett, J. Jeers, A. Gatti, and R. Loudon, Phys. Rev. A **57**, 2134 (1998).

[74] A. Peres, Phys. Rev. Lett. **77**, 1413 (1996).

[75] P. Horodecki, Phys. Lett. A **232**, 333 (1997).

[76] L.-M. Duan, G. Giedke, J. I. Cirac, and P. Zoller, Phys. Rev. Lett. **84**, 2722 (2000).

[77] R. Simon, Phys. Rev. Lett. **84**, 2726 (2000).

[78] V. Vedral and M. B. Plenio, Phys. Rev. A **57**, 1619 (1998).

[79] M. Horodecki, P. Horodecki, and R. Horodecki, Phys. Rev. Lett. **84**, 2014 (2000).

[80] E. M. Purcell, Phys. Rev. **69**, 681 (1946).

[81] D. Kleppner, Phys. Rev. Lett. **47**, 233 (1981).

[82] E. Yablonovitch, Phys. Rev. Lett. **58**, 2059 (1987).

[83] C. Henkel and V. Sandoghdar, Opt. Commun. **158**, 250 (1998).

[84] O. W. Greenberg, Ann. Phys. **16**, 158 (1961).

[85] E. Schmidt, J. Je ers, S. M. Barnett, L. Knoll, and D.-G. Welsch, J. Mod. Opt. **45**, 377 (1998).

[86] M. S. Yeung and T. Gustafson, Phys. Rev. A **54**, 5227 (1996).

[87] L. D. Landau and E. M. Lifshitz, *Electrodynamics of continuous media* (Pergamon Press, Oxford, 1960).

[88] M. Altarelli, D. L. Dexter, H. M. Nussenzveig, and D. Y. Smith, Phys. Rev. B **6**, 4502 (1972).

[89] W. C. Chew, *Waves and elds in inhomogenous media* (IEEE Press, New York, 1995).

[90] P. A. Garabedian, *Partial Di erential Equations* (Chelsea, New York, 1964).

[91] R. G. Newton, *Scattering Theory of Waves and Particles* (Springer, Berlin, 1982).

[92] A. A. Abrikosov, L. P. Gorkov, and I. E. Dzyaloshinski, *Methods of Quantum Field Theory in Statistical Physics* (Dover, New York, 1975).

[93] C. M. Caves, Phys. Rev. D **26**, 1817 (1982).

[94] J. Je ers, N. Imoto, and R. Loudon, Phys. Rev. A **47**, 3346 (1993).

[95] J. Je ers, S. M. Barnett, R. Loudon, R. Matloob, and M. Artoni, Opt. Commun. **131**, 66 (1996).

[96] R. Matloob, R. Loudon, M. Artoni, S. M. Barnett, and J. Je ers, Phys. Rev. A **55**, 1623 (1997).

[97] M. Artoni and R. Loudon, Phys. Rev. A **57**, 622 (1998).

[98] E. Schmutzer, *Relativistische Physik* (B.G. Teubner, Leipzig, 1968).

[99] A. A. Maradudin and D. L. Mills, Phys. Rev. B **11**, 1392 (1975).

[100] D. L. Mills and A. A. Maradudin, Phys. Rev. B **12**, 2943 (1975).

[101] J.-J. Gre et, Phys. Rev. B **37**, 6436 (1988).

[102] C.-T. Tai, *Dyadic Green functions in electromagnetic theory* (IEEE Press, New York, 1994).

[103] L. W. Li, P. S. Kooi, M. S. Leong, and T. S. Yeo, J. of Electromagn. Waves and Appl. **8**, 663 (1994).

[104] M. S. Tomas, Phys. Rev. A **51**, 2545 (1995).

[105] M. Patra and C. W. J. Beenakker, Phys. Rev. A **61**, 063805 (2000).

[106] J. F. Cornwell, *Group theory in Physics* (Academic, London, 1984), Vol. 2.

[107] M. Reck, A. Zeilinger, H. J. Bernstein, and P. Bertani, Phys. Rev. Lett. **73**, 58 (1994).

[108] D. Giulini, E. Joos, C. Kiefer, J. Kupsch, I. O. Stamatescu, and H. Zeh, *Decoherence and the appearance of a classical world in quantum theory* (Springer, Heidelberg, 1996).

[109] G. Lindblad, Comm. Math. Phys. **33**, 305 (1973).

[110] K. E. Cahill and R. J. Glauber, Phys. Rev. **177**, 1857 (1969).

[111] K. E. Cahill and R. J. Glauber, Phys. Rev. **177**, 1882 (1969).

[112] W. Schleich, *Quantum Optics in phase space* (Wiley-VCH, Berlin, 2001).

[113] R. J. Glauber, Phys. Rev. Lett. **10**, 84 (1963).

[114] E. C. G. Sudarshan, Phys. Rev. Lett. **10**, 277 (1963).

[115] K. Husimi, Proc. Phys. Math. Soc. Jpn. **22**, 264 (1940).

[116] Y. Kano, J. Math. Phys. **6**, 1913 (1965).

[117] E. P. Wigner, Phys. Rev. **40**, 749 (1932).

[118] J. Perina, *Quantum Statistics of Linear and Nonlinear Optical Phenomena* (Reidel, Dordrecht, 1991).

[119] C. W. Gardiner, *Quantum Noise* (Springer, Berlin, 1991).

[120] C. H. Bennett, G. Brassard, C. Crepeau, R. Josza, A. Peres, and W. K. Wooters, Phys. Rev. Lett. **70**, 1895 (1993).

[121] L. Vaidman, PRA **49**, 1473 (1994).

[122] S. M. Barnett and S. J. D. Phoenix, Phys. Rev. A **40**, 2404 (1989).

[123] H. Araki and E. Lieb, Comm. Math. Phys. **18**, 160 (1970).

[124] C. H. Bennett, D. P. DiVincenzo, J. A. Smolin, and W. K. Wooters, Phys. Rev. A **54**, 3824 (1996).

[125] B. Schumacher and M. A. Nielsen, Phys. Rev. A **54**, 2629 (1996).

[126] V. Vedral, M. B. Plenio, M. A. Rippin, and P. L. Knight, Phys. Rev. Lett. **78**, 2275 (1997).

[127] S. Hill and W. K. Wooters, Phys. Rev. Lett. **78**, 5022 (1997).

[128] H. Barnum, M. A. Nielsen, and B. Schumacher, Phys. Rev. A **57**, 4153 (1998).

[129] M. Lewenstein and A. Sanpera, Phys. Rev. Lett. **80**, 2261 (1998).

[130] G. Lindblad, Comm. Math. Phys. **39**, 111 (1974).

[131] G. Lindblad, Comm. Math. Phys. **40**, 147 (1975).

[132] A. Wehrl, Rev. Mod. Phys. **50**, 221 (1978).

[133] T. M. Cover and J. A. Thomas, *Elements of information theory* (Wiley, New York, 1991).

[134] M. A. Neumark, C.R. Acad. Sci. USSR **41**, 359 (1943).

[135] K. Wodkiewicz and J. H. Eberly, J. Opt. Soc. Am. B **2**, 458 (1985).

[136] X. Ma and W. Rhodes, Phys. Rev. A **41**, 4625 (1990).

[137] S. L. Braunstein and H. J. Kimble, Phys. Rev. Lett. **80**, 869 (1998).

[138] J. Lee, M. S. Kim, and H. Jeong, Phys. Rev. A **62**, 032305 (2000).

[139] W. G. Unruh, Phys. Rev. A **51**, 992 (1995).

[140] M. Ban, J. Opt. B: Quantum Semiclass. Opt. **2**, 786 (2000).

[141] M. S. Kim and J. Lee, Phys. Rev. A **64**, 012309 (2001).

[142] A. V. Chizhov, L. Knoll, and D.-G. Welsch, submitted to Phys. Rev. A (unpublished).

[143] D. M. Greenberger, M. A. Horne, and A. Zeilinger, in *Bell s Theorem, Quantum Theory, and Conceptions of the Universe*, edited by M. Kafatos (Kluwer, Dordrecht, 1989).

[144] M. Horodecki, P. Horodecki, and R. Horodecki, Phys. Rev. Lett. **78**, 574 (1997).

[145] M. Dakna, J. Clausen, L. Knoll, and D.-G. Welsch, Phys. Rev. A **59**, 1658 (1999).

[146] J. Clausen, M. Dakna, L. Knoll, and D.-G. Welsch, J. Opt. B: Quantum Semiclass. Opt. **1**, 332 (1999).

[147] E. A. Power and S. Zienau, Phil. Trans. Roy. Soc. **A251**, 427 (1959).

[148] R. G. Woolley, Proc. Roy. Soc. Lond. **A321**, 557 (1971).

[149] D. P. Craig and T. Thirunamachandran, *Molecular Quantum Electrodynamics* (Academic Press, London, 1984).

[150] J. R. Ackerhalt and P. W. Milonni, J. Opt. Soc. Am. B **1**, 116 (1984).

[151] C. Cohen-Tannoudji, J. Dupont-Roc, and G. Grynberg, *Photons and Atoms, Introduction to Quantum Electrodynamics* (Wiley, New York, 1989).

[152] M. Schubert and B. Wilhelmi, *Nonlinear Optics and Quantum Electronics* (Wiley, New York, 1986).

[153] H. T. Dung, L. Knoll, and D.-G. Welsch, Phys. Rev. A **62**, 053804 (2000).

[154] H. T. Dung, L. Knoll, and D.-G. Welsch, Phys. Rev. A **64**, 013804 (2001).

[155] H. T. Dung, L. Knoll, and D.-G. Welsch, *Recent Research Developments in Optics* (Research Signpost, Trivandrum, 2001).

[156] A. Einstein, Z. Phys. **18**, 121 (1917).

[157] G. S. Agarwal, Phys. Rev. A **11**, 253 (1975).

[158] G. S. Agarwal, Phys. Rev. A **12**, 1475 (1975).

[159] J. M. Wylie and J. E. Sipe, Phys. Rev. A **30**, 1185 (1984).

[160] D. Meschede, W. Jhe, and E. A. Hinds, Phys. Rev. A **41**, 1587 (1990).

[161] S. M. Barnett, B. Huttner, and R. Loudon, Phys. Rev. Lett. **68**, 3698 (1992).

[162] G. Juzeliunas and D. L. Andrews, Phys. Rev. B **49**, 8751 (1994).

[163] M. Fichet, F. Schuller, D. Bloch, and M. Ducloy, Phys. Rev. A **51**, 1553 (1995).

[164] S. M. Barnett, B. Huttner, R. Loudon, and R. Matloob, J. Phys. B: At. Mol. Opt. Phys. **29**, 3763 (1996).

[165] K. Koshino and A. Shimizu, Phys. Rev. A **53**, 4468 (1996).

[166] G. Juzeliunas, Phys. Rev. A **55**, R4015 (1997).

[167] M. S. Tomas and Z. Lenac, Phys. Rev. A **56**, 4197 (1997).

[168] M. Fleischhauer and S. Yelin, Phys. Rev. A **59**, 2427 (1999).

[169] M. S. Tomas and Z. Lenac, Phys. Rev. A **60**, 2431 (1999).

[170] M. Fleischhauer, Phys. Rev. A **60**, 2534 (1999).

[171] K. H. Drexhage, Sci. Am. **222**, 108 (1970).

[172] K. H. Drexhage, in *Progress in Optics*, edited by E. Wolf (North-Holland, Amsterdam, 1974), Vol. 12.

[173] R. G. Hulet, E. S. Hilfer, and D. Kleppner, Phys. Rev. Lett. **55**, 2137 (1985).

[174] W. Jhe, A. Anderson, E. A. Hinds, D. Meschede, L. Moi, and S. Haroche, Phys. Rev. Lett. **58**, 666 (1987).

[175] F. DeMartini, G. Innocenti, G. R. Jacobovitz, and P. Mataloni, Phys. Rev. Lett. **59**, 2955 (1987).

[176] D. J. Heinzen, J. J. Childs, J. F. Thomas, and M. S. Feld, Phys. Rev. Lett. **58**, 1320 (1987).

[177] R. Loudon, *Quantum Theory of Light* (Oxford University Press, Oxford, 1983).

[178] V. V. Klimov, M. Ducloy, and V. S. Letokhov, J. Mod. Opt. **43**, 549 (1996).

[179] D. L. Dexter, Phys. Rev. **101**, 48 (1956).

[180] B. diBartolo, *Optical Interactions in Solids* (Wiley, New York, 1968).

[181] A. Yariv, *Quantum Electronics* (Wiley, New York, 1975).

[182] G. Nienhuis and C. T. J. Alkemade, Physica B+C **81**, 181 (1976).

[183] J. Knoester and S. Mukamel, Phys. Rev. A **40**, 7065 (1989).

[184] G. L. J. A. Rikken and Y. A. R. R. Kessener, Phys. Rev. Lett. **74**, 880 (1995).

[185] F. J. P. Schuurmans, D. T. N. de Lang, G. H. Wegdam, R. Sprik, and A. Lagendijk, Phys. Rev. Lett. **80**, 5077 (1998).

[186] P. de Vries and A. Lagendijk, Phys. Rev. Lett. **81**, 1381 (1998).

[187] M. Born and E. Wolf, *Principles of Optics* (Pergamon, Oxford, 1993).

[188] A. Lakhtakia and W. S. Weiglhofer, in *Proceedings of the 1996 Asia Paci c Microwave Conference*, edited by R. Gupta (New Delhi, 1996), p. 217.

[189] A. Lakhtakia, B. Michel, and W. S. Weiglhofer, J. Phys. D: Appl. Phys. **30**, 230 (1997).

[190] I. S. Gradstein and I. M. Ryshik, *Table of Integrals, Series, and Products* (Academic, San Diego, 1994).

[191] M. S. Tomas, Phys. Rev. A **63**, 053811 (2001).

[192] M. B. Plenio, S. F. Huelga, A. Beige, and P. L. Knight, Phys. Rev. A **59**, 2468 (1999).

[193] U. Leonhardt and P. Piwnicki, Phys. Rev. A **60**, 4301 (1999).

[194] U. Leonhardt and P. Piwnicki, Phys. Rev. Lett. **84**, 822 (2000).

[195] M. Visser, Phys. Rev. Lett. **85**, 5252 (2000).

[196] U. Leonhardt and P. Piwnicki, Phys. Rev. Lett. **85**, 5253 (2000).

[197] G. Barton and C. Eberlein, Ann. Phys. **227**, 222 (1993).

[198] C. Eberlein, Phys. Rev. Lett. **76**, 3842 (1996).

[199] C. Eberlein, Phys. Rev. A **53**, 2772 (1996).

[200] L. W. Li, P. S. Kooi, M. S. Leong, and T. S. Yeo, IEEE Trans. Microwave Theory Techn. **42**, 2302 (1994).

[201] L. W. Li, P. S. Kooi, M. S. Leong, and T. S. Yeo, IEEE Trans. on Antennas and Propagation **43**, 232 (1995).

[202] A. P. Prudnikov, Y. A. Brychkov, and O. I. Marichev, *Integrals and Series* (Gordon and Breach, Amsterdam, 1986), Vol. 2: Special functions.

List of publications

[S1] S. Scheel, L. Knoll, and D.-G. Welsch, *QED commutation relations for inhomogeneous Kramers Kronig dielectrics*. Phys. Rev. A **58**, 700 (1998).

[S2] L. Knoll, S. Scheel, E. Schmidt, D.-G. Welsch, and A.V. Chizhov, *Quantum-state transformation by dispersive and absorbing four-port devices*. Phys. Rev. A **59**, 4716 (1999).

[S3] S. Scheel, L. Knoll, D.-G. Welsch, and S.M. Barnett, *Quantum local- eld corrections and spontaneous decay*. Phys. Rev. A **60**, 1590 (1999).

[S4] S. Scheel, L. Knoll, and D.-G. Welsch, *Spontaneous decay of an excited atom in an absorbing dielectric*, Phys. Rev. A **60**, 4094 (1999); *ibid.*, **61**, 069901(E) (2000).

[S5] S. Scheel, L. Knoll, D.-G. Welsch, *Spontaneous decay in the presence of absorbing dielectric bodies*. Proceedings of the 6th Central-European Workshop on Quantum Optics, Chudobin, Czech Republic, Acta Phys. Slov. **49**, 155 (1999).

[S6] S. Scheel and D.-G. Welsch, *QED in the presence of Kramers-Kronig dielectric media*. Proceedings of the 6th International Conference on Squeezed States and Uncertainty Relations ICCSUR VI, Naples.

[S7] S. Scheel, L. Knoll, T. Opatrny, and D.-G. Welsch, *Entanglement transformation at absorbing and amplifying four-port devices*. Phys. Rev. A **61**, 043803 (2000).

[S8] S. Scheel, L. Knoll, T. Opatrny, and D.-G. Welsch, *Entanglement transformation at absorbing and amplifying dielectric four-port devices*. Proceedings of the 7th Central-European Workshop on Quantum Optics, Balatonfured, Acta Phys. Slov. **50**, 351 (2000).

[S9] S. Scheel and D.-G. Welsch, *Interaction of the quantized electromagnetic eld with atoms in the presence of dispersing and absorbing dielectric bodies*. Paper presented at the International Conference on Quantum Optics, Raubichi, Belarus, *arXiv: quant-ph/0006025*, to appear in Optics and Spectroscopy **91** (2001).

[S10] S. Scheel, T. Opatrny, and D.-G. Welsch, *Entanglement degradation of a two-mode squeezed vacuum in absorbing and amplifying optical bers*. Paper presented

at the International Conference on Quantum Optics, Raubichi, Belarus, *arXiv: quant-ph/0006026*, to appear in Optics and Spectroscopy **91** (2001).

[S11] L. Knoll, S. Scheel, and D.-G. Welsch, *QED in dispersing and absorbing media*, In *Coherence and Statistics of Photons and Atoms*, ed. J. Perina (Wiley, New York, 2001).

[S12] A. Tip, L. Knoll, S. Scheel, and D.-G. Welsch, *Equivalence of the Langevin and auxiliary eld quantization methods for absorbing dielectrics*. Phys. Rev. A **63**, 043806 (2001).

[S13] S. Scheel and D.-G. Welsch, *3D input-output relations of quantized light at dispersing and absorbing multilayer dielectric plates*. *arXiv: quant-ph/0102076*.

[S14] S. Scheel and D.-G. Welsch, *Entanglement generation and degradation by passive optical devices*. *arXiv: quant-ph/0103167*, submitted to Phys. Rev. A.

[S15] S. Scheel, D.-G. Welsch, and T. Opatrny, *Quantum teleportation in noisy environments*. Proceedings of the 8th Central-European Workshop on Quantum Optics, Prague, to be published in Acta Phys. Slov. **51** (2001).

Zusammenfassung

In der vorliegenden Arbeit wurde gezeigt, wie das elektromagnetische Feld in Anwesenheit kausaler und linearer dielektrischer Materialien konsistent quantisiert werden kann. Es wurde bewiesen, da die quellenma ige Darstellung der elektromagnetischen Feldoperatoren mit Hilfe der klassischen Greenschen Funktion und eines Kontinuums von bosonischen Feldoperatoren, welche die gemeinsamen Anregungen von Strahlungsfeld, Dielektrikum und Reservoir beschreiben, im Einklang mit Forderungen der Quantentheorie und der statistischen Physik ist (Kapitel 2). Die Tatsache, da die Schwankungen des elektrischen Feldes aus dem Imaginarteil der klassischen Greenschen Funktion gewonnen werden konnen, zeigt au erdem, da das Quantisierungsverfahren die klassische Kubo-Formel, Ausdruck des Fluktuations-Dissipations-Theorems, reproduziert. Eine direkte Anwendung des Quantisierungsverfahrens ist die Ableitung von Input-Output-Relationen an beliebig geformten dreidimensionalen Objekten. Die einlaufenden Felder wurden dort mit den auslaufenden Feldern uber Re exions-, Transmissions- und Absorptionskoe zienten (tatsachlich sind das Tensoren zweiter Stufe), die sich wiederum aus der klassischen Greenschen Funktion ergaben, verknupft (Kapitel 3).

Fur den Fall der eindimensionalen Ausbreitung linear polarisierten Lichts wurde die Theorie der Quantenzustandstransformation an absorbierenden bzw. verstarkenden dielektrischen Vierpolen, wie etwa Strahlteilern oder optischen Fasern, entwickelt (Kapitel 4). Dabei zeigte sich, da ein unitarer Operator, der die Operatoren einlaufender und auslaufender monochromatischer Felder miteinander verknupft, konstruiert werden konnte. Dieser Operator beschreibt eine unitare Transformation im Raum der Strahlungsfeld- und Geratoperatoren. Fur absorbierende Vierpole gehort zu jeder Frequenzkomponente der elektromagnetischen Strahlung eine SU(4)-Gruppentransformation, fur verstarkende Vierpole eine SU(2,2)-Transformation. Ausgehend von der unitaren Transformation der Operatoren wurde eine Transformationsvorschrift fur die Quantenzustande abgeleitet. Explizite Formeln fur transformierte Dichteoperatoren wurden fur ausgewahlte Beispiele wie Fockzustande und koharente Zustande angegeben.

Durch Anwendung der Quantenzustandstransformation steht der vollstandige Dichteoperator des auslaufenden Strahlungsfeldes an dielektrischen Vierpolen zur Verfugung, mit dem Dekoharenz und Verschrankungsdegradation studiert werden konnen. Verschrankte Mehrmoden-Quantenzustande des Strahlungsfeldes, dessen einzelne Moden durch separate Vierpole z.B. durch optische Fasern laufen, verlieren ihre Verschrankung aufgrund ihrer Wech-

selwirkung mit der verrauschten Umgebung. Die Quantenkorrelationen, die nach dem Durchgang durch optische Fasern noch vorhanden sind, lie en sich aus der Konvexitatseigenschaft der relativen Entropie nach oben abschatzen (Kapitel 5). Zum ersten Mal konnte auch ein Ma fur die Verschrankungsdegradation Gau scher Zweimodenzustande, das auf einem Separabilitatskriterium fur diese Klasse von Zustanden basiert, angegeben werden. Speziell fur das gequetschte Zweimodenvakuum wurden numerische Untersuchungen durchgefuhrt, die zeigten, da die Verschrankung umso schneller abklingt, je mehr davon anfanglich vorhanden war. Zudem existiert eine obere Schranke fur die Verschrankung, die durch optische Fasern gegebener Lange transportiert werden kann. Diese Schranke zeigt die ultimativen theoretischen Grenzen fur Quanteninformationsverarbeitung mit kontinuierlichen Variablen auf.

Verschrankungsdegradation ist auch die Ursache fur die Abnahme der Ubertragungsgute bei Quantenteleportation. Es wurden zwei Modi zierungen des Standardschemas vorgestellt, die die mittlere Teleportationsgute erhohen (Kapitel 6). Zum einen wurde die Verwendung eines verschrankten Dreimodenzustandes als Verschrankungsresource mit anschlie ender geeigneter Messung an der ungenutzten Feldmode untersucht, zum anderen wurde eine konditionale Filteroperation eingefuhrt.

Das eingangs erwahnte Quantisierungsverfahren wurde auf zusatzliche atomare Quellen ausgedehnt (Kapitel 7). Dabei wurden sowohl minimale als auch multipolare Kopplung betrachtet und elektrische Dipol- und rotating-wave-Naherung durchgefuhrt. Die Anwesenheit dielektrischer Materie beein u t die Zeitentwicklung der Atomoperatoren. Insbesondere die Modi kationen der spontanen Zerfallsrate eines einzelnen Zweiniveauatoms in einem absorbierenden Medium bzw. nahe einer dielektrischen Ober ache wurden eingehender untersucht (Kapitel 8). Aufgrund des konsistenten Quantisierungsverfahrens konnte nunmehr der spontane Zerfall fur alle atomaren Ubergangsfrequenzen, speziell auch in der Nahe von Resonanzen des dielektrischen Mediums, behandelt werden. Dabei zeigte sich, da die Anwesenheit absorbierender Materie zu einer starken Abhangigkeit der Zerfallsrate mit der inversen dritten Potenz des Abstand des Atoms zum Dielektrikum fuhrt, was auf nichtstrahlenden Zerfall uber resonanten Energietransfer hindeutet.

Ehrenwortliche Erklarung

Ich erklare hiermit ehrenwortlich, da ich die vorliegende Arbeit selbstandig, ohne unzulassige Hilfe Dritter und ohne Benutzung anderer als der angegebenen Hilfsmittel und Literatur angefertigt habe. Die aus anderen Quellen direkt oder indirekt ubernommenen Daten und Konzepte sind unter Angabe der Quelle gekennzeichnet.

Niemand hat von mir unmittelbar oder mittelbar geldwerte Leistungen fur Arbeiten erhalten, die im Zusammenhang mit dem Inhalt der vorgelegten Dissertation stehen. Insbesondere habe ich hierfur nicht die engeltliche Hilfe von Vermittlungs- bzw. Beratungsdiensten (Promotionsberater oder andere Personen) in Anspruch genommen.

Die Arbeit wurde bisher weder im Im- noch im Ausland in gleicher oder ahnlicher Form einer anderen Prufungsbehorde vorgelegt.

Die geltende Promotionsordnung der Physikalisch-Astronomischen Fakultat ist mir bekannt.

Ich versichere ehrenwortlich, da ich nach bestem Wissen die reine Wahrheit gesagt und nichts verschwiegen habe.

Jena, den 05.07.2001

Danksagung

Mein Dank gilt vor allem meinem Betreuer, Professor Welsch, der mich in vielfaltiger Weise bei der Anfertigung meiner Arbeit unterstutzte und dem ich zahlreiche Hinweise verdanke. Professor Knoll danke ich fur eine Vielzahl von Anregungen und ausgiebige Diskussionen. Besonderer Dank gilt Professor Barnett und Professor Fleischhauer, die sich bereiterklart haben, meine Arbeit zu begutachten.

Wahrend meiner Arbeitsaufenthalte in der Gruppe von Professor Audretsch an der Universitat Konstanz sowie in der Gruppe von Dr. Tip am FOM-Instituut voor Atoom- en Molecuulfysica in Amsterdam habe ich eine Reihe direkt verwandter Probleme kennengelernt. Beiden Gruppen danke ich fur die Gastfreundschaft, die mir dort zuteil wurde. Desweiteren danke ich dem Adam Haker-Fonds fur die freundliche nanzielle Unterstutzung einer Kongre reise.

Die Diskussionen mit Professor Martienssen, Professor Dultz und Professor Roskos an der Universitat Frankfurt fuhrten mich zu der intensiven Beschaftigung mit Verschrankungsma en. Viele anregende Hinweise verdanke ich au erdem Professor Barnett, Professor Fleischhauer, Dr. Chizhov, Dr. Ho und Dr. Opatrny sowie meinem langjahrigen Mitstreiter Eduard Schmidt. Allen Kollegen am Theoretisch-Physikalischen Institut danke ich fur die stimulierende Atmosphare. Spezieller Dank unserem Systemadministrator Dr. Wei .

Abschlie end danke ich meinen Eltern und meiner Freundin, Annett Klinder, ohne deren moralische Unterstutzung mir diese Arbeit nicht moglich gewesen ware.